

Seasonal Variation in Empirical and Modeled Periphyton at the Watershed Scale

A Thesis

Presented in Partial Fulfillment of the Requirements for the

Degree of Master of Science

with a

Major in Water Resources

in the

College of Graduate Studies

University of Idaho

by

Adrienne Zuckerman

Major Professor: Alexander K. Fremier, Ph.D.

Committee Members: Christopher C. Caudill, Ph.D, Cailin H. Orr, Ph.D

Department Chair: Jan Boll, Ph.D

June 2015

AUTHORIZATION TO SUBMIT THESIS

This thesis of Adrienne Zuckerman, submitted for the degree of Master of Science with a major in Water Resources and titled "Seasonal Variation in Empirical and Modeled Periphyton at the Watershed Scale," has been reviewed in final form. Permission, as indicated by the signatures and dates given below, is now granted to submit final copies to the College of Graduate Studies for approval.

Major Professor: _____ Date: _____
Alexander K. Fremier, Ph.D

Committee

Members: _____ Date: _____
Christopher C. Caudill, Ph.D

_____ Date: _____
Cailin Huyck Orr, Ph.D

Department

Administrator: _____ Date: _____
Jan Boll, Ph. D

ABSTRACT

The decline of Pacific salmon has fueled concerns about declining ecosystem productivity following the loss of salmon-supplied nutrient and material subsidies that supported primary and secondary production. Due to decreased salmon subsidies, freshwater ecosystems may be experiencing a bottom-up limitation of aquatic production, which can restrict current and future production. I used two contrasting approaches to understand the spatial and temporal patterns of basal resources in the form of periphyton biomass across a large temperate, mountainous watershed over one year. I examined the relationship between field collected periphyton biomass compared to physical, chemical, and biological environmental parameters to understand what parameters affected biomass. Specifically, I used empirical data collected monthly at 12 sites across a 5th order watershed for one year to investigate: the (1) spatial and temporal patterns of periphyton biomass across a watershed, evaluate (2) which environmental variables were the best predictors of biomass and if they (3) changed seasonally. As a second approach to understand basal resources, I tested the accuracy of a formalized mechanism-based model, the Aquatic Tropic Productivity Model (ATP Model), developed by Bellmore et al. (2014). I simulated periphyton biomass across the same sites as the empirical study and used the environmental parameter data collected in the field to parameterize the model. I (4) compared simulated biomass values to field collected biomass and examined how accurately a mechanism-based model performed in simulating biomass patterns compared to empirical patterns. Results of the empirical investigation indicate that drivers of periphyton shift seasonally. Nitrogen, solar access, and disturbance effects are important drivers throughout the year across the basin, though relative importance of each driver changes by season. The ATP model generated biomass estimates within the SE of observed values by site. Spatial patterns varied, however generally increased from up to downstream in the snowmelt-dominated watershed, the highest observed periphyton was observed in winter (January – March), whereas the ATP Model predicted the highest biomass in autumn, (from October-December). Observed periphyton was lowest in spring, and was predicted to be lowest by the ATP Model as well. The ATP Model could be used to predict aquatic basal resources in order to prioritize restoration locations and activities that support basal resource production that feed focal aquatic populations (such as Pacific salmon), though a few refinements are still needed.

ACKNOWLEDGMENTS

There have many phases of this graduate project, and I grateful to many people for support and encouragement. First and foremost, I appreciate Dr. Alex Fremier for taking chance on me as a student with a liberal arts background and a management-focused skill set. This has been an exciting and complex project with a lot of moving parts, and a lot to learn about science in practice. I am grateful for your mentorship and your approach. I am grateful to the thesis committee, Dr. Chris C. Caudill and Dr. Cailin H. Orr, who have been helpful at critical points and very patient in getting to this stage. I am grateful for your time, your questions, your early concerns about the scope of my ambitions, and your insights to improve drafts along the way. Francine H. Mejia, a colleague and collaborator extraordinaire, I am so grateful for your many conversations, detailed reviews, consistent questions, and general teamwork. It has been a pleasure working with you. Dr. J. Ryan Bellmore, you were instrumental in every phase, from periphyton study design, to model questions to help with model refinements and everything in between. Thanks for answering hundreds of questions and for thinking about what it was like to be a student within this project. Many thanks to the Fremier Lab – Dr. Kath Strickler, Aline Ortega, Francine Mejia, Rachel Hutchinson, Liza Mitchell, Cat Weichmann, Amanda Stahl, Laura Livingston, Joe Parzych, and John Jorgensen. You were full of good inquiry, listening ears, shared resources, and a cacophony of laughter. You have helped me turn each corner, and I am so grateful for your feedback. Thanks for help in the field as well, Aline, Joe, and Cat. Grace Watson of USGS (now Methow Salmon Recovery) in Twisp, was incredible in the field, highly skilled, detail oriented, and flat-out brave wading through winter. None of this analysis would have been possible with out your yearlong data collection expertise. Thank you for remembering every instrument and bottle, every single time. John Jorgensen (of Yakama Nation Fisheries) gets appreciation for always bringing the focus back to the fish. Frank Wilhelm was instrumental in helping me learn how to process Chlorophyll-*a*, and kindly answering my numerous questions and concerns. Frank Wilhelm and Brian Kennedy let me share their lab space for many months of sample processing. Mitchell Davis at the University of Idaho Statistics Consulting Center helped with numerous phases of statistical analysis. Tim Hatten at Invertebrate Ecology (Moscow) and Wade Hoiland processed and analyzed samples and mentored me as I assisted with the sorts. Clearwater Fly Casters (Pullman-Moscow) and Decagon Devices, Inc. (Pullman) provided financial and technical support. Interacting with Decagon staff and local fishers were memorable parts of the project and I'm grateful to both groups for help along the way.

This research was primarily supported by a grant from the Bureau of Reclamation, Portland, OR, Cooperative Agreement #R11 AC 17 061. Thanks to Michael Newsom for support of this work.

Last but not least, thank you to Sam Grimm, my fiancé and partner. Your belief in me and your help through each phase have been instrumental, and you have lightened my most stressful moments with your quick and quiet wit. I'm so grateful for you in my life. As I write this, you are flying to Maine to defend your own Master's in Forest Ecology. You will do very well, and we are almost there!

DEDICATION

This thesis is dedicated to you, Mom– thanks for your constant positivity and efforts to get us all outside! Those hikes started this journey.

TABLE OF CONTENTS

AUTHORIZATION TO SUBMIT THESIS.....	ii
ABSTRACT	iii
ACKNOWLEDGMENTS	iv
DEDICATION.....	vi
TABLE OF CONTENTS	vii
LIST OF TABLES.....	ix
LIST OF FIGURES	x
PREFACE: FROM PERIPHYTON TO SALMON	xii
INTRODUCTION.....	1
OBJECTIVES.....	4
METHODS	6
STUDY AREA.....	6
SAMPLING DESIGN AND SITE SELECTION	7
DATA COLLECTION	8
PERIPHYTON COLLECTION AND LAB PROCESSING METHODS	9
BIOMASS VERSUS PRODUCTION	9
INVERTEBRATE SAMPLING METHODS	10
METHODS FOR EVALUATING PERIPHYTON PATTERNS USING A MECHANISM BASED MODEL.....	11
STRUCTURE OF EARLY MECHANISM BASED PERIPHYTON MODELS.....	12
BASIS OF THE ATP MODEL’S FUNCTIONAL EQUATIONS.....	14
SIMULATING THE MECHANISM-BASED MODEL USING FIELD DATA.....	15
STATISTICAL ANALYSES.....	17
STATISTICAL ANALYSES IN THE FIELD COLLECTED PERIPHYTON AND ENVIRONMENTAL DATA	17
STATISTICAL PROCEDURES FOR COMPARING ATP MODEL OUTPUTS AND FIELD DATA	19
RESULTS.....	20
SPATIAL PATTERNS OF BIOMASS AND CORRELATION WITH ENVIRONMENTAL VARIABLES.....	20
HYPOTHESIS 1.....	20
HYPOTHESIS 2.....	21
HYPOTHESIS 3.....	21

HYPOTHESIS 4.....	22
HYPOTHESIS 5.....	22
RELATIVE IMPORTANCE OF ENVIRONMENTAL DRIVERS IN PREDICTING AFDM THROUGH SEASON.....	24
ATP MODEL ACCURACY: EVALUATING PREDICTED VS. OBSERVED BIOMASS BY SEASON.....	25
ATP MODEL ACCURACY: EVALUATING PREDICTED VS OBSERVED BIOMASS BY SITE	26
DISCUSSION.....	27
SPATIAL AND SEASONAL PATTERNS OF EMPIRICAL BIOMASS AND ENVIRONMENTAL DRIVERS	27
WINTER EFFECTS.....	28
SUMMER EFFECTS.....	29
CAVEATS.....	29
DISCUSSION OF ATP MODEL ACCURACY COMPARED TO EMPIRICAL DATA	30
ATP MODEL CAVEATS.....	31
OVERALL CONCLUSIONS AND POTENTIAL IMPLICATIONS FOR AQUATIC RESTORATION EFFORTS.....	33
REFERENCES.....	36
TABLES	42
APPENDIX A: RAW DATA	69
APPENDIX B: LABORATORY METHODS	97

LIST OF TABLES

Table 1. Summary of sample data at each site.....	42
Table 2: Sampling methods, frequency, and application.....	43
Table 3: Topographic measurements used in empirical mechanistic model analyses.....	44
Table 4: Principal components analysis (PCA) for the initial site selection.....	45
Table 5: Table 5: PCA of the field collected ancillary data.....	46
Table 6: Table 2 - Linear regression results for Periphyton AFDM and ChL a.....	47
Table 7: Table 7 Multiple Linear Regression results	48
Table 8: Showing intercept values of best models.....	50

LIST OF FIGURES

Figure 1: After data was collected in the field, it was used in two ways. Since the term “Model” is used with both approaches, I wanted to show how approaches differ. The Mechanistic Model is different from the statistical models evaluated in the Empirical Approach.	52
Figure 2: A conceptual map of the ATP Model (adapted from Bellmore, et al. 2014). Model parameters depict formal relationships between mechanistic environmental drivers and periphyton biomass and each component incorporates values from physical, biological and chemical drivers that represent actual dynamics known to occur in nature as closely as possible. See Table 1 for variables 1-7, and Table 2 for variables 8-10. Note: consumption by invertebrates was not evaluated in the model.	53
Figure 3: Site Map of Methow Basin	54
Figure 4: Testing H1-H4 with correlations between environmental drivers and AFDM using Simple Linear Regression. Annual AFDM data in are shown in Blue and Chl-a values are in red. Nitrogen has the strongest relationship on AFDM in the basin over the year. Nitrogen concentration has the strongest correlation with AFDM and Chl-a.....	57
Figure 5: Seasonal Dynamics of Beaver Creek (above) – a small, high biomass stream.....	58
Figure 7: Sampling periods and mainstem Methow Discharge.....	59
Figure 8: Field collected standing crop AFDM compared to Mechanistically Predicted AFDM and Chl-a by season. Model performance is best in worst in winter (Jan, Feb, Mar), and best in fall (Oct, Nov, Dec). Seasons were adjusted to group May and June together, when the seasonal high flows and annual disturbance occurs.	60
Figure 9: Field collected standing crop AFDM compared to mechanistically predicted AFDM over one year. The difference between the observed and predicted values is high in the early spring, but decreases though the summer and increases again in the fall. This pattern indicates model predictions are best in the summer and not as accurate in the early spring and early fall. The model was most accurate in November and December (fall).....	61
Figure 10: Site-wise comparison of field collected observed versus AFDM biomass predicted by the mechanistic ATP model	62

- Figure 11: Variation in nutrient levels shown by month and by site, the general pattern is higher N levels in winter. In the site comparison, BV is a consistent outlier due to adjacent.....63
- Figure 12: Biomass of invertebrates classified as part of the functional feeding group scappers at all sample sites over all dates in comparison with Chlorophyll-a values. The site with the highest invertebrate biomass (Middle Twisp) consistently had the lowest AFDM and Chl-a biomass in empirical samples. This graph indicates efficiency of invertebrates at MT.63
- Figure 13: There was a strong correlation between biomass and chlorophyll a. I used AFDM and Chl-a in simple linear regression evaluations and AFDM only in the multiple linear regression evaluations by season due to this strong correlation. Multiple R²: 0.7103, F-statistic: 306.4 on 1 and 125 DF, p-value: < 2.2e-1664
- Figure 14: Showing the non inear relationship between Drainage Area and Stream Power. The RCC predicts stream power will peak in mid-size streams, which was observed in this data. ((Label these points with the site name?))65
- Figure 15: Observed vs Predicted Biomass values, correlation = 0.475.....66
- Figure 16: Comparison between model accuracy at small streams vs large streams.....67
- Figure 17: Frequently, but not always, the mechanism-based model (diamonds) over predicts periphyton biomass compared to observed biomass (circles). Invertebrate consumption can help explain this over prediction. Though not all feeding types directly consume biomass, all invertebrates benefit from higher biomass (though filtering consumption or as predators feeding on direct consumers). This important finding demonstrates model the needs to be calibrated using modifiers that account for the affect of grazing.....68
- Figure 18: Example of ATP Model inputs organized for each study site in order to run the ATP Model in Stella software. Data includes channel topography from CHaMP surveys and daily or monthly environmental variables collected in the field (only a portion of the data are shown above).92
- Figure 19: Proportion of deciduous vs coniferous trees along riparian areas at 12 sites.....94

PREFACE: FROM PERIPHYTON TO SALMON

Low nutrient conditions and declining basal production in cold water streams have been attributed to the significant declines in the number of wild salmon migrating from the ocean to spawn, decay, and cycle back into the freshwater ecosystems over the past century (Gresh et al. 2000). The lack of nitrogen and phosphorus that were previously contributed by salmon carcasses has led to oligotrophication, or depressed nutrient conditions, leading to a bottom-up limitation in salmon-bearing ecosystems (Holtgrieve & Schindler, 2011, Stockner et al, 2003). Declining returns have created a negative feedback where low nutrient conditions decrease food availability so ecosystems can support fewer juveniles, which decreases the number of successful out-migrants and successful returning fish numbers (Wipfli et al, 2003, Cederholm, et al, 1999). Therefore, there has been great interest among entities that manage fisheries to better understand where and when, within a stream network, physical, chemical, and biological conditions contribute to basal food resources that support juvenile salmon (Beechie, et al, 2010, NRRSS). This study conducted below explored how the drivers of basal food resources (periphyton) vary seasonally and across a watershed. Efforts to restore aquatic communities increasingly aim to quantify basal resources and energy flows that feed aquatic organisms (Naiman et al. 2012). With a better understanding of the watershed and seasonal dynamics of periphyton, we will be better prepared to understand the complex landscape of aquatic production at scales important for the restoration of fish habitat. Restoration efforts to improve habitat conditions for endangered aquatic organisms, including *Oncorhynchus* species have been required by the Endangered Species Act was passed (1973) and has been implemented by Federal Agencies, primarily on public lands. However, restoration activities are not often aimed at restoring basal food webs, though this has started to change (Beechie et al, 2010, and see Minshall et al 2014, Hoyle et al 2014). Basal resources support tertiary consumers that feed on periphyton-eating aquatic invertebrates and feed herbivorous fish directly. Restoration efforts

frequently focus on increasing physical refugia (through substrate modifications and woody debris jams) that support historic planform conditions (Bernhardt et al. 2005, Polvi and Wohl, 2013, Roni et al, 2002, Doyle and Shields, 2012 and the NRRSS). In addition to restoring the physical structure, understanding food resource availability across a large network would benefit all aquatic organisms, including salmon species (Naiman et al., 2002, Ebel et al 2014, Marcarelli et al 2014). Restoration efforts located where food limitation can be addressed as part of other projects may be more successful in increasing aquatic production, and through trophic cascades, juvenile salmon populations (Naiman, 2012).

INTRODUCTION

Benthic stream periphyton is an important resource supporting lotic food webs (Minshall, 1978, 2014). Aquatic production in oligotrophic streams is a limiting factor for consumer organisms (Thorp and DeLong, 2002, Power et al. 2008, Beechie, 2010). However, despite considerable efforts to understand periphyton dynamics, there is limited knowledge about the seasonal patterns and drivers of periphyton production, especially at the watershed and multi-season scale (but see Power, 2008). Multiple, interacting, environmental variables control periphyton production and these variables change spatially and temporally (Stevenson et al, 1996, Lamberti et al, 1981). Limited emphasis has been placed on predicting periphyton patterns based on seasonality (but see Power et al., 2008) generally focusing instead on the spatial arrangement of primary productivity rather than the temporal patterns. The physical and chemical processes of rivers change in a downstream direction, which creates a longitudinal pattern in physical structure and associated biological communities (Vannote, et al 1980, Polis, 1997, Finlay, 2002). Numerous conceptual frameworks have been created in order to understand how lotic systems change from headwaters to mouth and how this affects productivity along the gradient. The River Continuum Concept (RCC) posits that a predictable pattern occurs along longitudinal gradient where production increases in a downstream direction, but does not make a network-scale prediction due to differences found in different stream types (Vannote et al. 1980). In contrast, the Network Dynamics Hypothesis predicts larger scale patterns are observed over entire catchments based on similar disturbances regimes (Benda et al. 2004). Poole evaluated the patch and hierarchical based-organization of stream and river ecosystems and the uniqueness found in each watershed (2002).

I evaluated spatial and temporal patterns in benthic periphyton production across a 5th order stream network over a full year at small tributary and mainstem sites.

In addition to physical structure, consumer–resource interactions are fundamental for understanding the direction and magnitude of food and energy flow in a stream network (Woodward, 2009). Past research indicates shifts in the food base between inputs from allochthonous or riparian sources to autochthonous-driven system primary production have a major effect on structure and function of lotic ecosystems (Odum, 1957, Cummins 1973, Hynes 1975, Minshall 1978, and Marcarelli et al., 2011). Because the environment is spatially structured by various energy inputs (Legendre and Fortin, 1989), improving the landscape for aquatic production is based on understanding the spatial and temporal patterns and drivers that generate food resources throughout the network.

Watershed-scale studies of periphyton dynamics generally use statistical approaches to infer which variables affect the system using empirical data (Gregory, 1987, Kiffney and Bull 2001). This approach was used in the evaluation of the field collected empirical data in his study. In addition, a process-based modeling approach was used to test formalized mechanistic relationships among environmental drivers to predict periphyton production. Researchers such as Lindeman (1942), Hagen (1992) and Golley (1993) developed mechanism-based models to explicitly link transfers of organic matter through food webs. McIntire (1973, 1978, 1996) built models to test the complex mechanistic interactions among environmental variables that affect periphyton growth. Mechanism-based models that formalize the relationship between environmental conditions and ecosystems responses enable users to test hypotheses about which environmental drivers will affect a unique catchment, and to what degree. A mechanism-based modeling approach can be used to develop and test hypotheses about what may occur if the environment changes (e.g., temperature change over time, or a one-time event like a landslide and subsequent sediment pulse)(IMW, Methow, 2013). Additionally, in future applications, this approach could be used to test predictions about effects that restoration-induced changes could have a particular site (based on a site’s particular topography, biotic, and

abiotic conditions). This predictive and hypothesis-driven approach is in contrast to the current approach of evaluating empirical data that reflects past conditions then altering a site for restoration purposes based on physical surveys (Doyle and Shields, 2012, Roni et al, 2002)

I tested a recently formalized mechanism based model of periphyton production (ATP Model, Bellmore et al. 2014) quantifying the spatial and temporal patterns of benthic periphyton within a stream network by comparing empirical biomass values to values predicted by the model. Since efforts to restore aquatic populations occur in diverse stream ecosystems (small/large, rain vs snow driven), a mechanism-based model can explore the environmental gradients that occur within a river basin (Chiarello et al., 1998). I evaluated spatial and temporal patterns of periphyton biomass and environmental drivers at the watershed scale since aquatic production in oligotrophic streams is considered a limiting factor for fish production in (Beechie, 2010). This study addresses gaps in knowledge about field collected periphyton biomass data using a novel spatial and temporal scale across heterogeneous sites (large mainstem sites and small tributaries) in a large network. In contrast, the majority of studies have used small laboratory streams, instead of large stream networks that include mainstem river sites (Labiod et al. 2007, Feminella and Hawkins 1995, Hildebrand and Kahlert, 2001, and Lamberti, et al. 1987). Additionally sampling in the majority of past studies may have occurred primarily in the summer field season, instead of year round (Rosemond et al., 1993; Lamberti et al 1987, Hildebrand and Kahlert, 2001, but see Power et al. 2008) due to logistical constraints, especially in colder climates.

Objectives

I applied two approaches to quantify and examine the relationship between the drivers of periphyton biomass in a montane stream network through a full year. I quantified spatial and temporal patterns in empirical benthic periphyton and evaluated the role of environmental variables on biomass across a 5th order watershed. I used two approaches: (1) correlation of observed periphyton data and environmental drivers and (2) predictions by a mechanism-based model against field measured data to see if empirical patterns of biomass could be accurately simulated across study sites (Figure 1).

Within the empirical conceptual approach, I tested hypotheses to learn about the spatial and temporal patterns of the study area. I hypothesized that: 1) periphyton biomass would be lower in headwaters with less sunlight and higher in downstream or mainstem reaches with greater solar access (Vannote et al. 1980) but there would be an asymptotic relationship (leveling off) in very large rivers. 2) Periphyton biomass would be higher in streams with greater nutrient levels (Fanta et al 2010). 3) Biomass would be higher in streams that had less disturbance power (smaller streams with less drainage area) and biomass would be lowest overall in the spring due to disturbance by high flows from snow melt 4) Biomass would be greater in streams that exhibit warmer average temperatures throughout the year (Poole and Berman, 2001). 5) Invertebrate biomass would be highest at sites and in seasons with the most abundant primary food resources. Though invertebrates that feed by scraping periphyton from rocks should have a negative relationship with algal biomass, periphyton biomass should also have a positive relationship with total invertebrate biomass since other feeding types also consume periphyton.

As a second approach (2), I tested a mechanism-based periphyton production model, the Aquatic Trophic Productivity (ATP) Model (Bellmore et al. 2014) to evaluate the accuracy of the

model in comparison with observed biomass values across the watershed over four seasons. I used field collected environmental data (collected daily or monthly) to code the model so the 12 sites were each represented with their variations over the entire year. Then, I compared the simulated periphyton biomass with the observed periphyton biomass to see how well the ATP Model predicted seasonal and temporal dynamics. I hypothesized that: 1) the ATP Model would predict the patterns of biomass (highs and lows) across sites, and 2) the ATP Model predictions would be within orders of magnitude of biomass at a given a location and season. I expected higher model accuracy during the low flow seasons (early fall and late winter). Finally, with these results, I discuss what the observed patterns and then what the observed vs modeled patterns mean as well as how the ATP could be used in an applied management sense, towards aquatic restoration efforts.

METHODS

Study Area

The Methow River Basin is a snowmelt dominated 5th order tributary of the Columbia River draining the east slope of the Cascade Mountain Range in north central Washington State (Figure 3). The basin is located upstream of nine mainstem Columbia River dams and 843 km from the mouth of the Columbia River. The Methow has diversions for agriculture in the summer but no major dams or impoundments. The Methow Basin has a catchment area of 4,462 km² and elevations that range from 2,700m in the Cascade Mountain Range to 240m at the confluence with the Columbia River in Pateros, WA (Konrad, 2003). The Cascade Range climate yields an average of 360 mm of precipitation annually with only 12% of annual precipitation falling between July and September. On average, the basin receives 180 cm of annual snowfall. Average temperatures range from -0.5C to 15.5C annually as measured (Western Regional Climate Center, Winthrop NOAA Cooperative Climate Station #49536, 2015).

The basin transitions dramatically from headwaters to mouth, from high alpine North Cascades ridgelines in the west to dry, shrub-steppe foothills from Twisp east to the Columbia River. The land cover is a mix of pine and fir forest, dry Columbia Plateau shrub-step, and irrigated agriculture (Konrad, 2003). Black cottonwood (*Populus trichocarpa*), alder (*Alnus incana*), maple (*Acer macrophyllum*), and Western Red Cedar (*Thuja plicata*), are abundant in riparian zones (personal observation). Wildfire is a catastrophic 100-300 year event in the forested west and an annual disturbance in the eastern part of the basin (Konrad, 2003).

Methow is considered a largely unimpaired basin (WA Dept. of Ecology, 1990) and supports six federally threatened and endangered species including: Upper Columbia River (UCR) spring Chinook salmon (*Oncorhynchus tshawytscha*), UCR steelhead (*Oncorhynchus mykiss*), Columbia River bull trout (*Salvelinus confluentus*) (Listed) and Pacific lamprey (*Entosphenus tridentatus*)

(NW Power & Conservation Council, 2004). The Methow supports annual returns of the above listed fish though there is variation in the number returning annually (USGS, 2014). As a result, agencies responsible for mitigating salmon losses due to human impacts invest in physical restoration projects in the Methow and nearby watersheds (\$95 million over 10 to 30 years, Washington State Salmon Recovery Funding Board – Upper Columbia River Basin). Restoration projects are designed to address physical limitations affecting juvenile life stage of salmon species. However physical restoration projects have demonstrated limited effectiveness (despite high costs) and aquatic production has been infrequently investigated as a component of these projects (Roni et al 2008, Beechie, 2010).

Sampling Design and Site Selection

To sample across the extant environmental variability related to stream production, my team selected sites from a list of 52 locations surveyed by the Columbia Habitat Monitoring Program (CHaMP, [CHaMPmonitoring.com]). Since 2011, CHaMP has been implementing a standard fish habitat monitoring protocol in 26 watersheds across the Columbia River Basin. CHaMP sites are selected to represent the heterogeneity in stream conditions found within each basin. CHaMP staff collect detailed topographic surveys during each visit and each site is re-surveyed either annually or every three years to capture topographic and geomorphic changes.

To select sites while still capturing the range of conditions throughout a large basin, I grouped characteristics of the 52 potential CHaMP Methow sites using Principal Components Analysis (PCA) of 17 environmental variables hypothesized to describe physical character of streams. Variables included drainage area, elevation, gradient, floodplain width, bankfull width, mean discharge, stream power, substrate size, canopy density, and solar radiation (among others) sourced from NetMap (terrainworks.com). From the site selection PCA, seven clusters of sites resulted across two axes, which explained 64% of the total variation (Table 4). The first axis

(PC1) corresponded generally to riparian cover, gradient, and elevation, and the second (PC2) to floodplain width and river size. Since the first two axes explained >60% of variation, PC3 was not included in the clustering step; however, PC3 corresponds to drainage area and disturbance regime. I selected 12 sites representing the range of variability in the basin, including a site located in each of the seven major sub-basins within the watershed, as well as small streams, substantial tributaries and large mainstem sites (Figure 3). I also considered wintertime access and coordination with other ongoing studies to decide on the final 12 study sites. Sites could not be considered fully independent because a few occurred within the same sub-watershed. While there were similarities between up and downstream sites in the same subwatershed, they were 5.6 km apart and represented both the unique characteristics of the site (solar access, riparian type, gradient, substrate size, temperature, nutrient levels) as well as characteristics of each sub-basin.

Data Collection

Between June 2013 and May 2014, my team made sampling visits to the 12 selected sites at least once per month for one year. We sampled periphyton biomass and environmental variables including sunlight, velocity and discharge, turbidity, substrate grain size and solar access. We also sampled inorganic nitrogen (N in mg/L), [from ammonia (NH₃), nitrate (NO₃), and nitrite (NO₂)] and Soluble Reactive Phosphorus (SRP in mg/L). Table 4 describes the sampling method and frequency of each environmental variable measured at each site. I extracted stream topography and geomorphology from the most recent CHaMP survey GPS points at each site (database access granted by ChampMonitoring.org). Methods for each topographic parameter are shown in Table 2.

Periphyton Collection and Lab Processing Methods

I collected periphyton biomass and Chlorophyll-*a* samples, using standard procedures described by Berkman and Canova (USGS, 2007). I randomly selected five rocks from the thalweg at 10 m intervals, starting from the downstream end of each site. Using a whole rock scrub method, I removed all periphyton from each rock with a small wire brush and rinsed both with a known amount of water. Samples were filtered onto pre-ashed glass fiber filters in the field, frozen, and processed for biomass as ash-free-dry-mass (AFDM) following standard methods (Hauer and Lamberti, 2006, Bechtold 2007). To extract Chlorophyll-*a* (Chl-*a*), I followed sample preparation methods by Ritchie (2006) and analyzed samples with a spectrophotometer following Standard Methods (APHA, 2000). From initial results reported in $\mu\text{g/L}$, I converted Chl-*a* values into mg/m^2 so I could compare biomass and Chl-*a*. I summarized biomass and Chl-*a* patterns by averaging the five samples collected at each site, however samples varied considerably, even when collected within 10 m of each other (40 m total), all from the thalweg, during each monthly sampling visit. I used the median value of Chl-*a* and AFDM of five samples from each month for analysis.

Biomass versus Production

Biomass measurements in this study represent the standing crop of benthic periphyton to describe all forms of autochthonous-produced aquatic macrophytes, bryophytes, benthic algae, biofilm and *Aufwuchs* (Hauer and Lamberti, 2006, p. 357). Grouping organisms in this way allowed comparisons across spatial and temporal scales at one point in time. Chlorophyll-*a* measures the photosynthetic pigments common to all types of algae, while periphyton processed into Ash Free Dry Mass (AFDM) captures carbon at the time of sampling. AFDM is a useful metric for comparing biomass quantities across different study areas, however AFDM is limited because it does not encompass the processes that generate or remove periphyton through the year or the periphyton productive capacity (Lamberti, et al, 1989). These

processes include grazing by invertebrates, density dependence, and disturbance by scour during high flows (Allan and Castillo, 2006, p. 117). While measuring biomass does not address the processes that generate and remove the standing crop, biomass samples were measured consistently and at the same intervals. Additionally, production estimates (Gross Primary Productivity and Respiration) were recorded simultaneously and are a component of another study that will provide a comparison to this study. Standing crop biomass was used to evaluate biomass at a novel spatial and temporal scale as well as to provide a comparison to simulated biomass values on a g/m^2 basis month by month using a mechanism-based modeling approach.

Invertebrate Sampling Methods

Extensive factors affect the standing crop biomass at any given time. Herbivory by aquatic invertebrates affects biomass as well as dislodgement rates (Rosemond, et al. 1993, Kiffney and Bull, 2000) through “bottom-up” and “top-down” controls (McQueen et al. 1986, Feminella and Hawkins, 1995). Despite removal of biomass through consumption, the presence of grazing invertebrates has positive feedbacks on algal turnover (Lamberti et al, 1981, Lamberti and Resh, 1983) as well as nutrient content via excretion (Hildebrand and Kahlert, 2001, Gende et al., 2002). Additionally, while a standing stock of biomass may decrease with herbivory, photosynthetic rates have been shown to increase, especially under intermediate levels of grazing pressure where benthic macroinvertebrates can achieve an ideal free distribution to follow resources (Allan and Castillo, 2009).

At six of 12 of the periphyton sampling sites (BV, BD, EW, MT, UC, and UM1), I collected drift and benthic invertebrates during four seasons (July, September, November, March). Drift samples were collected using a net of 250 μm mesh with a 25 cm x 45 cm rectangular opening and cod-end collection bucket. Nets were placed at the upper extent of the benthic sampling reach and deployed for approximately one hour. The net was placed so water flowing into the

net was not obscured by the net (to allow drifting insects unimpeded access). Flow (m^3/s) measurements in front of the net were used to calculate flow through the net for the collection time. The upstream net was placed at the upstream extent of the survey area, determined using a distance that measured 10 times the wetted width of the stream at the downstream extent (where continuous temperature was being recorded) and the first rock from the periphyton was collected each month (0 meters).

Benthic samples were collected by scraping each rock that lay within a surber sampling net collection frame of 0.096 m^2 using a net with $250 \mu\text{m}$ mesh and a cod end collection bucket. Any rocks that could be picked up were scraped around their entire surface, and rocks that were too large to pick up or were embedded were hand scrubbed in place. If the frame lay on a part of a rock, only the part within the frame was scraped. Each benthic sample was a bulk sample representing 10 sub-samples per site. Samples were collected in riffles, however samples collected during the summer period included samples collected in pool and side channel habitats until water depth required only riffle based samples. Invertebrates were classified into groups according to their feeding behavior (filtering collectors, gathering collectors, predators, scraping collectors, shredders and terrestrial invertebrates) (Benke and Wallace 1980, Benke and Huryn 2010). Invertebrate Ecology, Inc. (Moscow, ID), processed samples and calculated biomass ($\text{mg}/\text{sample area}/\text{sample date}$) using standard length-mass regression coefficients (Benke and Wallace 1980, Benke, Smock, and Wallace 1999, Benke and Huryn 2010).

Methods for Evaluating Periphyton Patterns using a Mechanism Based Model

I tested a mechanism-based periphyton production model (Aquatic Trophic Productivity Model; ATP, Figure 2, Bellmore et al. 2014) to evaluate accuracy of a model in simulating biomass patterns across diverse sites. Past models have performed well in small laboratory streams, but we wanted to evaluate model accuracy across a large watershed through four seasons. Early

periphyton models (McIntire, 1973 and 1996) and studies that form the basis of our understanding of lotic ecosystem (Feminella and Hawkins, 1995, Hildebrand and Kahlert, 2001, and Lamberti, et al. 1987) occurred in small laboratory streams, instead of large stream networks and mainstem-rivers. The interactions of biotic and abiotic drivers have been much more difficult to predict or model in natural environments comprised of larger river reaches. To address this limitation, the ATP Model (Figure 2) was based on the structure of early periphyton models (McIntire, 1973, 1996) and expanded the model to include a broad range of environmental variables known to alter the accrual and loss of periphyton biomass (Bellmore, et al, 2014). Environmental variables can be manipulated within the model to demonstrate how each variable mediates periphyton biomass, where: $Biomass_t =$

$$Biomass_{t-1} + Production_t - Respiration_t - Detachment$$

I used the field-collected environmental data as inputs to simulate the ATP Model at 12 sites using the daily or monthly values that had been collected in the field. I simulated biomass values (in AFDM g/m^2) at each location to get daily biomass and production estimates, and I ran the simulations for 2 years, using the same input data for year 2. I used the second year of simulated data for analysis the subsequent analysis to let the ATP Model adjust to lags or perturbations. Year 2 replicated simulations observed in Year 1 very closely. I compared the predicted periphyton biomass from the ATP Model results to the observed periphyton biomass to see how well the ATP Model predicted seasonal and temporal dynamics.

Structure of Early Mechanism Based Periphyton Models

Similar to other models, and based on McIntire's framework, the periphyton component of the ATP Model is centered around a stock of biomass that increases via production of new biomass and decreases via respiration and detachment (Figure 2). The model simulates interactions of biomass growth and loss at once, and generates predictions of daily periphyton biomass using a

detailed set of functional relationships and feedbacks derived from previous modeling research or other empirical studies. In an earlier paper using the ATP Model, a global sensitivity analysis demonstrated that biomass estimated by the ATP Model was most sensitive to gradient, substrate size, and shading (Bellmore et al., 2014).

Data from experiments in laboratory streams in Oregon form the basis of model parameter values and dictate the mathematical equations that control how periphyton affects light intensity, nutrient levels, current velocity, gradient, rainfall schedule, and other parameters (McIntire, 1973). Other factors in the early models account for the effect of temperature, light intensity, day length, concentration of total organic solids and turbidity that attenuate PAR reaching the benthos. The maximum rate of primary production (growth) from given periphyton biomass is identified using the equation:

$$P(max | A) = Umax \frac{a1}{a1A}$$

Where A is biomass and $a1$ is a constant (described in lab experiments by McIntire and Phinney 1965). The effects of nutrient concentration and temperature on the rate of primary production are found in the equations:

$$P_{(rmax | N)} = a_2N/1+a_2N \quad \text{and} \quad P_{(rmax | T)} = a_3T/1+a_3T$$

Where $P(rmax | N)$ and $P(rmax | T)$ are proportions of $P(rmax | A)$ $[(A=area)]$ allowable given a particular nutrient concentration (N) and temperature (T). McIntire estimated a_2 by fitting a hyperbolic curve to experimental data presented in McIntire and Phinney (1964). Carbon dioxide was included from experimental data and other background nutrients were modeled. The maximum rate of primary production given a particular biomass, nutrient concentration, temperature and current velocity is determined by the expression:

$$P_{(max | A, N, T, V)} = P_{(max|A)} P_{(rmax | N)} P_{(rmax | T)C}$$

Quantities of biomass and organic matter are expressed in grams per square meter and rates of consumption are expressed by differential equations (McIntire, 1973, Bellmore et al., 2014).

Basis of the ATP Model's Functional Equations

The ATP model incorporates more detailed mechanistic equations than earlier models, including both physiochemical and physical geomorphic factors affecting channel shape, stream chemistry, and seasonal impacts of solar inputs by leaf on / leaf off modifiers (Bellmore et al, 2014). Mechanism based expansions in the ATP Model resolve issues with earlier models because this version includes expanded relationships that control biomass growth and detachment and comparisons with the field study enable evaluation of real watershed conditions using values from large basin rather than a laboratory stream. The model is written in Stella 10.0.6 (ISEE Systems, Lebanon, NH, U.S.A.).

For some variables, equations forming the model were informed by reported rates, ratios, and values from other studies (Bellmore, et al. 2014). These calculations are intended to replicate the dynamic behavior occurring in natural stream systems. The approach was used because model simulations, though imperfect, can be valuable (Box and Draper, 1987). A model that predicts bioenergetic flows within expected ranges of variability can be used to make useful, interpretable statements about ecological processes in real stream conditions (Hobbs and Hilborn, 2006, McIntire, 1973).

Unlike earlier models, the ATP Model replicates biotic and abiotic interactions that are ongoing at any time in a stream network, including: light limitation on growth, temperature dependent growth rates, nutrient limitation, channel topography, and velocity limitation. As a specific example, temperature is one factor calculated within the model to predict periphyton. A temperature limitation factor occurs any time temperature values were above or below the optimum growth range (13-20°C). Temperature values used in the model were the field

collected temperature values for each site (daily average temperature based on readings collected every 10 minutes)(field methods and sampling intervals are described in Table 2). Temperature is only one of the many interactions that occur simultaneously. Numerous empirical factors go into calculating the hydraulic geometry (Table 3). Periphyton removal is controlled by respiration, discharge, gradient, friction velocity, critical substrate size, and as well as time factors that affect senescence of biomass based on age (See Bellmore et al., 2014).

Biomass is equal to production minus loss (which can be due to detachment, respiration, or consumption). However, each component incorporates values from physical, biological, and chemical drivers that represent actual dynamics known to occur in nature as closely as possible (Figure 2, Table 2). For example, the growth rate is based on (based on light, nutrient, velocity and temperature limitations) and the density of the population of biomass is based on density dependence divided by the physical channel dynamics (gradient, depths, discharge, floodplain area).

Simulating the Mechanism-Based Model using Field Data

Field collected data was used to parameterize and calibrate each ATP Model component. ATP mechanism-based model simulations generate daily estimates of periphyton biomass and production based on environmental data inputs. The majority of the effort associated with ATP Modeling effort in this study focused on learning the model, data preparation, and initial simulations. Using daily empirical data from the June 2013- May 2014 field study, I collected, summarized, and organized data from the yearlong empirical study to populate ancillary variable values used in the ATP Model (Figure 2). For each site, I organized daily measurements collected during the field effort and topographic characteristics from CHaMP surveys (Table 3). Using the ATP Model in Stella, I simulated daily biomass for 730 days (2 years) based on the empirical inputs and built-in functional equations.

Once initial simulations were completed, I evaluated results to determine if important mechanisms were missing and altered aspects of the model that could replicate real dynamics more accurately. Primary revisions focused on factors that affected the bank angle and therefore the channel geometry. I found that wetted depth was not being accurately depicted, so adjustments were made to calculate the wetted depth from CHaMP values (Table 3). Additionally, an important biological riparian aspect was missing from the function environment. I found that leaf out and leaf off period was not being replicated. Instead, the riparian canopy was static. Using riparian surveys from the basin and an understanding of system modeling, I worked with model creators to adjust the model so that the proportion of coniferous vs. deciduous trees considered in the model equations that depicted how much sunlight was reaching the benthos each month. This accounted for model revisions from version 10.3 to 10.4.

STATISTICAL ANALYSES

Statistical Analyses in the Field Collected Periphyton and Environmental Data

All analyses were run using R statistical software version 2.14.2 (R Development Team, <http://www.r-project.org/>) and significance was evaluated at $\alpha = 0.05$. Empirical data met tests of normality shown in histogram and QQ normality plots. I tested one-way ANOVAs to evaluate if mean AFDM, Chl-*a*, and environmental variables were significantly different by site or date.

To evaluate environmental variables and their effect on AFDM, I performed principal component analysis (PCA) on scaled and centered environmental drivers to examine the data and eliminate cross-correlated variables from subsequent analysis (Table 5). I found wetted width, bankfull width, floodplain width, and solar access to be cross-correlated, so I kept solar access in the majority of analyses. Discharge (cubic meters/second), and gradient were cross-correlated, so I maintained specific stream power = $\frac{(2 \text{ year peak flow} \times \text{gradient})}{\text{Bankfull width}}$.

Nutrients levels, measured as total inorganic nitrogen (N) and soluble reactive phosphorous (P), were independent and were maintained. Temperature and median substrate size (D50) were not cross-correlated and were maintained. Variables associated with the first three axes explained 68% percent of variation in the dataset. The first axis (PC1 = 28.5%) correlated with variables related to nutrients and velocity. The second axis (PC2 = 23.8%) correlated to variables related to discharge and velocity. The third axis (PC3 = 16.7%) correlated to drainage area and nutrients again, suggesting factors related to the sub-basin position (Table 5).

In order to evaluate the hypotheses: (H1) if biomass could be predicted based on drainage area nutrient levels (H2), disturbance regime (H3) temperature (H4) and if biomass could be predicted based on time period, I evaluated AFDM biomass versus single drivers using linear regression. I evaluated AFDM ~ drainage area, nitrogen, phosphorus, stream power,

temperature, percent solar access, and median substrate size (Table 6, average values are shown in Table 1). I also evaluated Chl-*a* against each of these drivers.

The significant predictor variables ($p=0.05$) in linear regression were kept in the global model and evaluated using multiple linear regression. I used multiple linear regression to evaluate the relative importance of environmental variables in predicting AFDM at the annual scale (1), and then by season (2). I started with the global model:

$$AFDM \sim Nitrogen + Phosphorus + D50 + Solar + Temp + Stream Power + Drainage Area$$

I evaluated the annual data set and then removed variables iteratively by least significant value until all variables in the model were significant ($<p=0.05$, usually $p=0.01$). To reduce the potential effect of temporal auto correlation, for example, where samples collected in September may have been representative of some of the effects environmental conditions at the site in August (Legende and Fortin, 1989), I grouped variable means by season (Winter, Spring, Summer, Fall). Seasons were defined as Winter (Jan – March), Spring (April – June), Summer, (July – September), and Fall (October – December) because snow melt occurs later in the year, so grouping spring runoff together in the spring season (April – June) accurately characterized the basin. September conditions were more closely matched to summer conditions than fall, so summer included September. Then I repeated the multiple linear regression model selection process starting with the global model in each season (Table 7 & 8).

I used Akaike Information Criterion (AIC) for statistic selection of the best performing candidate models using stepwise model selection. Model selection was based on AIC values to minimize the Kullback-Leibler distance between environmental parameters and AFDM (Burnham and Anderson, 2002). Best-fit models of drivers predicting AFDM were identified using AIC weights (w_i). Candidate models were considered if the difference between the best fit model and the competitor had a ΔAIC value of <1 (Table 7).

Statistical Procedures For Comparing ATP Model Outputs and Field Data

Statistical procedures to evaluate ATP Model performance were straightforward once parameterization and model updates were completed. I compared ATP Model simulated biomass values to field collected data using linear regression. Since simulated biomass did not meet the assumptions of normality, I used a Wilcoxon-Mann-Whitney rank sum test to evaluate if statistically significant differences existed between the predicted versus the empirical data by month, by site and by season.

RESULTS

Spatial Patterns of Biomass and Correlation with Environmental Variables

As expected from the site selection process, there was high variability in the dataset across the 4,500 km² study area. Biomass samples and other environmental variables show variation by site and season (Table 1). I used biomass values to evaluate hypotheses about environmental predictors of periphyton because I found that biomass (AFDM) and Chl-*a* data were highly correlated ($p < 0.01$, Pearson's r = correlation coefficient = 0.84, and $R^2 = 0.996$).

Annual average values and ranges for each site and season are shown in Tables 1 & 9. Biomass values peaked in February and March with another, smaller peak occurring in August, and another in November (Figure 9, Table 1). AFDM ranges with SE are shown by site (Figure 9) and by season (Figure 10).

I used a statistical approach to understand the effect of environmental parameters on AFDM, evaluating five hypotheses (predictions) in the empirical data set.

Hypothesis 1

H1 predicted that periphyton biomass would increase with stream size across a large watershed over a year, I hypothesized periphyton biomass would be lower in shaded, headwater streams and increase as stream size and stream order increased. The null hypothesis posited that there would be no difference in periphyton biomass based on stream size and solar access. The average annual data show that drainage area predicts AFDM, ($p < 0.0001$, $R^2 = 0.25$, $r = 0.49$). The highest biomass values were observed at the site with the second highest drainage area, 198 g/m² (annual total) at UM2 which had a Drainage Area of 1669 km² (Table 1, Figure 4) and average solar access of 85%. However the site with the largest drainage area overall (LM2) had less biomass than the site just upstream of it (UM2), where biomass decreased to 136 g/m² at LM2, DA = 1722 km²). As drainage area increased,

data confirmed the RCC prediction (H1) that productivity would peak (as shown in UM2 data) and then decrease at the largest site due to greater water depth and increased turbidity.

Notably, biomass values from Beaver Creek, a small tributary, were the second highest annual AFDM among 12 sites at 162 g/m² (annual sum, Table 1). Though BV has a small drainage area (179 km²), agricultural land use occurs throughout the area, and BV acts as a leverage point in the data set due to its very high biomass values resulting from elevated nutrient levels.

Hypothesis 2

Results support H2, that biomass would be higher in streams with greater nutrient concentrations. Results do not confirm the null hypothesis, that nutrient concentrations would not be highest at sites with the highest levels of nutrients (nitrogen and phosphorus). AFDM correlated to the increasing concentration of total inorganic nitrogen ($p < 0.0001$, $R^2 = 0.26$, $r = 0.51$). There was no relationship between phosphorus (Soluble Reactive Phosphorus) and AFDM ($p = 0.82$, $R^2 = 0.00042$, $r = -0.02$). One outlier site (BV) had the highest N and P concentrations at (N = 0.259 mg/L, 48% higher than the next highest site and P = .010 mg/L, 35% higher than the next highest site; see Table 1). There was no correlation between drainage area and N concentration ($r = 0.15$), indicating AFDM was highly sensitive to N at sites with high N values (impacted by local land use rather than through eroding sediment from underlying geological characteristics of each subbasin).

Hypothesis 3

For H3 that lower stream power would be correlated with higher biomass, the null hypothesis was supported. I thought biomass would be higher in streams with a smaller disturbance effect (lower stream power (SP)). However, I did not find that biomass was higher in streams that had a lower stream power (Table 1) ($P = 0.134$, $R^2 = 0.0178$, $r = 0.13$). Since specific stream power is an indicator of disturbance and detachment via erosion, this hypothesis is similar the

to the RCC prediction that periphyton decreases at a critical depth along the downstream gradient (H1), which was observed. Some of the smallest streams had the highest stream power due to naturally incised bank conditions combined with high gradients. The four sites with the highest stream power were LT, BD, EW, then BV (see Table 1, Figure 15). Lower Twisp had the highest SP value (0.056), 25% higher than the site with the next highest SP. Sampling occurred in a steep, constricted section of the lower Twisp River, a major tributary that contributes ~20% of the median annual flow to the Methow River. Boulder Creek a smaller tributary had the 2nd highest SP (0.0440), and is characterized by a very constricted, canyonized channel, though it has a relatively small drainage area.

Hypothesis 4

I hypothesized that biomass would be higher in locations with higher average stream temperatures. However I found the null hypothesis to be supported, relationship between biomass and temperature, predicting biomass would be greater in streams that exhibit warmer average temperatures throughout the year, was not statistically significant. Biomass and temperature did not correlate ($p = 0.15$, $R^2 = 0.01$, $r = -0.13$). There was a relationship between warmer sites and biomass, however it was not significant in the entire data set (p -value: 0.12), but was significant in summer (p -value: 0.01), and not fall (p -value: 0.17), winter (p -value: 0.37), or spring (p -value: 0.69). The coldest temperatures occurred in Early Winters Creek (EW, $\bar{x} = 4.9^\circ\text{C}$, Range = 11.8), which was not one of the sites with the lowest AFDM (Table 1).

Hypothesis 5

I hypothesized that periphyton biomass would be lower at sites with high levels of invertebrate biomass (particularly biomass of invertebrates that feed by scraping). The null hypothesis posited that periphyton biomass would not be affected by invertebrate biomass. I found H5 was supported since benthic invertebrate biomass had an effect on periphyton biomass. Benthic invertebrate biomass was correlated with AFDM ($r = 0.56$, $R^2 = 0.31$) comparing biomass values

of all invertebrate feeding types to AFDM. Invertebrates were classified into groups according to their feeding behavior (filtering collectors, gathering collectors, predators, scraping collectors, shredders and terrestrial invertebrates) (Benke and Wallace 1980, Benke and Huryn 2010). Correlations by each type of functional feeding group demonstrate scraper biomass was negatively correlated with AFDM ($r = -0.104$), since biomass is their main food source. Scraper biomass was not correlated with Chl-a ($r = 0.058$) (Table 10). Gatherer feeding type biomass was strongly correlated with AFDM ($r = 0.669$), and Chl-a (0.486) (Table 10). Predator biomass was strongly correlated with AFDM (0.607) and Chl-a (0.413) (Table 10, and Figure 16). Middle Twisp (MT) had the lowest periphyton AFDM values (annual total, 36 g/m^2) across all periphyton samples (Table 1) and MT also had the highest biomass of invertebrates classified as scrapers especially in the March (1637 mg/site) and November (933 mg/site) benthic samples (Figure 12). These results indicate that grazing pressure affected standing crop biomass. Chl-a values were (60 mg/m^2) and generally followed the pattern of biomass during the sampling period.

In summary, differences in environmental parameters measured at 12 sites were highly variable by month and by season. Biomass values peaked in February and March with another, smaller peak occurring in August, and another in November (Figure 9, Table 1). This pattern follows the high discharge events in early spring from spring snow melt (Figure 7), which annually disturb stream communities. Nitrogen and drainage area were significantly related to AFDM ($p < .001$). Phosphorus concentration, solar access, and median substrate were less significant ($p < 0.05$) in the Chl-a data (Table 4). A site to site (pairwise) comparison indicated that biomass values from Middle Twist (MT) were critically different (57.3 grams/m^2) different from 8 out of 12 sites (BV, EW, LC, LM1, LM2, UC, UM2, UT). Middle Twisp (MT) generally had the lowest biomass levels and nutrient concentrations each month and the

highest scraper invertebrate biomass. Invertebrates who feed by scraping periphyton off rocks may have an affect on observed biomass.

Relative Importance of Environmental Drivers in Predicting AFDM through Season

I used the biomass in the majority of analyses because grams of ash free dry mass (AFDM) and Chl-*a* were strongly correlated ($p < 0.01$, $R^2 = 0.996$, $r = 0.84$) (Figures 14 and 8). Chl-*a* was processed from the whole rock scrub slurry from each of the five rocks sampled at each site each month so Chl-*a* patterns closely follow biomass patterns. Differences in linear regression to predict the effect of environmental variables on AFDM or Chl-*a* are shown in Table 6, but were not different enough from AFDM to evaluate both response variables in the multivariate analysis, below and in (Figure 14). Additionally, the ATP Model generates simulations in terms of AFDM (g/m^2) (and not Chl-*a*), which is another reason I focused on AFDM in following series of analyses evaluating seasonal drivers and the comparison of empirical to simulated periphyton biomass.

I used multiple linear regression to evaluate the relative importance of environmental variables in predicting AFDM at the (1) annual scale and (2) by season. Results indicate the best model for drivers predicting AFDM at the annual scale were:

AFDM = Nitrogen + Temperature + D50 + Stream Power + Drainage Area (AICw = 0.07, Table 8).

Results indicate that drivers of AFDM were different in each season (adjusted R^2 range = 0.22-0.64) (Tables 8 and 9). Nitrogen was significantly correlated with AFDM at the $p < 0.01$ p-value in all seasons except for summer, as well as in the annual model (Table 8). Solar access and temperature correlate with AFDM in the summer months, unlike in the three other seasons.

In winter, which was the season where the highest biomass was observed, nitrogen and drainage area were correlated with AFDM in the best model at the $p > 0.01$ level with an adjusted R^2 of 0.48 (Table 8). Stream power correlated with AFDM in a slightly less robust

model, followed in the modeling iterations by solar access, again in a less robust model (AICw = 0.08). Finally, solar access, phosphorus, and temperature correlated with AFDM in a model with an AIC difference of less than 3 from the best model. In spring, the high flow season, N, P, D50 and Stream Power correlate with AFDM at the significance level of $p > 0.01$ (adj $R^2 = 0.35$) in contrast to the other seasons where P concentrations are not present in any other top models (Table 8). In fall N, solar, and SP were significant at the $p < 0.001$ level, however the effect of solar access was not included in the next best model and only correlated with AFDM when D50 correlated as well. Overall, AIC model selection results from multiple linear regression indicate the top models do confirm our hypotheses, significant drivers of periphyton biomass are light, total inorganic nitrogen, and discharge, however the important of each of these drivers changes seasonally. The correlation among drivers by season indicated that biomass is correlated with light and temperature in the summer but nitrogen and drainage area are stronger predictors of AFDM through fall, winter and spring. Additionally, periphyton biomass increased along the longitudinal gradient until decreasing slightly at the largest site, due to turbidity and water depth.

ATP Model Accuracy: Evaluating Predicted vs. Observed Biomass by Season

ATP Model simulations resulted in predictions of the daily biomass (summed to monthly and then seasonal averages). Overall, the model performed best in fall (July, August, September) and least accurately in winter (January, February, March). The mechanism-based model predicted lowest biomass quantities would occur in May and June, which mirrored the lowest quantity of biomass collected in the empirical dataset, and the disturbance mechanism). Predicted biomass values in winter differed most significantly (Figure 8) from observed biomass (-61% difference). Annual disturbance via high flows in May and June scoured biomass in both

datasets (difference = -40%). After June, model predicted biomass increased through summer and started to decline in the fall (Figure 9). Observed biomass also increased after the high flow events of early spring, but did not increase as much as predicted biomass (36% difference). Overall, the ATP model replicated the disturbance period, but growth rates in summer were predicted to be higher than were observed. For all predictions matched observed conditions most accurately (calculated difference between median biomass and model predictions = 6% difference). Winter conditions were predicted biomass least accurately (-61% difference) from observed AFDM.

ATP Model Accuracy: Evaluating Predicted vs Observed Biomass by Site

After the seasonal comparison, mean annual standing crop AFDM empirical values were compared to values predicted by the ATP Model at each of the 12 sites. I hypothesized that the model would be similar to the empirical spatial patterns of biomass at each site, and model predictions would be within orders of magnitude of biomass at a given a location. ATP Model performance followed relative abundances at each site (Figure 10), however quantities were significantly different (Wilcoxon rank sum test, p-value: 0.00647). In general, the ATP Model predicted biomass values at smaller streams more accurately than in larger streams (based on drainage area) (Figure 17). The smallest, high productivity site (BV) was predicted most accurately among 12 sites (BV, difference = 11%). The least accurate site was UM1 (difference = 128%, however, samples could not be collected for four months due to a completely frozen stream). I was not able to find a consistent pattern where the ATP Model over predicted or under predicted biomass at each site, and the range in predictions was high (range in under predictions = -37% to -80%, range in over predictions = 11% to 127%, Figure 16).

A global sensitivity analysis (GSA) of the ATP Model demonstrated the sensitivity of model-predicted AFDM quantity to substratum grain size, gradient, and shading (Bellmore, et al 2014).

I also found bank angle to be sensitive to slight adjustments, since the bank angle function in the model controls stream width, shading, as well as water depth, which are represented by the specific stream power variable. Despite variation, the ATP Model simulates biomass on a site-by-site basis within the standard error of samples collected at that site (Figure 16).

DISCUSSION

A discussion of spatial and seasonal patterns of biomass from the empirical study is addressed below, with a focus on findings about biomass quantities and driving variables changing by season. The empirical discussion is followed by a discussion about the ATP Model's performance in simulating biomass and why the model may have under or over predicted in certain cases. Finally, there is discussion of the overall implications of the study and the utility of the ATP Model in restoration applications.

Spatial and Seasonal Patterns of Empirical Biomass and Environmental Drivers

Periphyton assemblages exhibited strong seasonal shifts between seasons, and changes were especially apparent in measurements before and after spring runoff (April, May, June). For the majority of sites, biomass values peaked in February and March with another, smaller peak occurring in August, and another in November (Figure 7). This pattern matches the high discharge events over the year. The lowest biomass levels occurred in May when high flows scoured biomass off the substrate (Figure 7).

In summer, as solar access and temperature increased, AFDM increased as well (Table 9).

Temperature and solar access were the two variables in the top summer multiple linear regression model. This observation confirmed expectations that higher temperatures would yield higher growth (only in summer). In a less robust regression model, nutrients also influenced AFDM during summer, implying that these systems are light limited in summer and N limited in all other seasons. In the fall, daylight hours decrease, so nitrogen levels, and

specific stream power (2yr Peak Flow * gradient)/Bankfull width) become important predictors of biomass. Ecologically, the sites would experience the first rains after a pattern of dry, hot summer weather and dislodgement of biomass may occur after precipitation events. Nitrogen could enter streams from livestock or agricultural land uses adjacent to streams during fall and early winter rain, from excess nutrients used in domestic lawns and gardens, or from initial leaf fall in areas with alder (*alnus*) species in the riparian area. *Alnus* spp provide a labile organic matter and nitrogen input that has found to be important for invertebrates (Wipfli and Musselwhite, 2004).

Overall, AIC model selection results indicate that the top models in the empirical dataset confirm the empirical hypotheses (H1-H3, H5). Significant drivers of periphyton biomass are light, total inorganic nitrogen, and discharge. Periphyton biomass increased along the longitudinal gradient. However the relationship with temperature is only significant in summertime samples.

Winter effects

The highest biomass values were recorded in winter (Figure 10). Since temperature was not a significant driver of periphyton biomass, the fourth hypothesis, that temperature would have an important effect on the quantity of observed biomass (Table 1, Figure 4), was not supported. This was surprising considering low light at 48°N as well as the season-long periods of below freezing temperatures in the basin. However, psychrophilic algae adapted to cold temperatures form the base of autotrophic energy production in cold environments across the planet (Morgan-Kiss et al., 2006), so adaptations of the algal community to extended periods of annual low temperatures and low light can explain this observation. Co-limitation was likely occurring as well, since high flow events in May and June are the annual disturbance in this basin. Additionally, since precipitation fell as snow and stayed in place until the melt occurred, the

lowest flows were observed during winter across all 12 sites. Biomass values in February and March had the longest time to develop before another spring disturbance occurred, so as long as community competition was not limiting, periphyton growth could be exponential through fall and winter. Low-flow conditions also would have decreased the removal of biomass via scouring that occurred during the other precipitation events throughout the year. Finally, flows were so low at the majority of sites during winter that the effect of solar attenuation by water depth or turbidity may have decreased due to very shallow water. This may have resulted in higher rates of photosynthesis for cold-adapted species during winter.

Summer effects

In the summer, results demonstrated that solar access and temperature were the best predictors of periphyton biomass. However, in every other season, nitrogen concentrations and stream disturbance were the best predictors of biomass using a multiple linear regression approach. To explain the divergence between observed and simulated biomass values, the most critical factor was the effect of season (winter vs. summer). The majority of our understanding about factors that affect stream periphyton come from studies that have been conducted during summer (Rosemond et al., 1993, Hillebrand and Kalhert, 2001). Few studies of periphyton production have been completed in non-summer month because of logistical constraints (though this is changing).

Caveats

I was not able to collect data at a few sites due to high flows (in May) or snow and ice (February) one site (UM1), may have had lower biomass estimates during the sampling year than if there had been water at the site year round. The site was completely frozen and the streambed was completely dry under a 4-6 cm layer of ice between December and March. Additionally, I captured the variability and the overall patterns with the sampling design in the

invertebrate data set, but I sampled six of the 12 sites due to logistical needs of sampling during the school year, and therefore six sites do not have invertebrate data to compare to results.

Discussion of ATP Model Accuracy Compared to Empirical Data

I found that the ATP model predicted periphyton dynamics under real conditions compared to empirical results within the standard error of empirical variability (see comparison in Figure 12). There was large spatial variation in the empirical dataset (AFDM ranged from 36 to 198 g/m²), and variability in model predicted biomass (18 to 199 g/m²) varied as well. There was seasonal variation as well. Model simulations predicted that the highest biomass would occur late fall, when observed biomass levels were highest in late winter (Figure 9). Additionally, the ATP Model under predicted biomass at seven of 12 sites, and these sites demonstrated similar patterns. Generally, smaller sites were predicted more accurately than large sites (Figure 17) perhaps due to the original functional equations that the ATP Model is based on where conducted in small streams. Additionally, sites where the ATP Model generally under-predicted exhibited a pattern: these sites had populations of didymo (*Didymosphenia geminata*) an invasive and prolific diatom observed through the year. I focused on measuring and evaluating the seasonal and temporal patterns of periphyton in a novel dataset instead of evaluating the periphyton community composition therefore, I don't know the proportion of didymo found in biomass samples (in particular, in the winter samples). While quantitative values for the proportion of didymo at each site during each month were not evaluated, this species was present and noticeable during the majority of sampling periods, but varied in density at each site. Previously, didymo was primarily thought to colonize low nutrient, cold ecosystem streams though its range is expanding (Spaulding and Elwell, 2007). Didymo was abundant at sites where the model under predicted biomass.

The mechanism-based model's divergence from observed conditions was an expected outcome to some degree, since productive modeling occurs when model performance is continually evaluated against reality and adjusted to better reflect real conditions (Ford, 2010, pg. 346). Differences between model predictions and empirical data still represent progress in modeling the seasonal and temporal periphyton dynamics in a large watershed. This initial validation effort will be used to adjust and formally calibrate the model. After the ATP model is adjusted in the validation stage (BOR Integrated Watershed Management Report, 2013, pg. 9) to meet the final goal of using the model to generate and test formal hypotheses (Wiens and Milne, 1989). Since the objective at this stage was to understand periphyton patterns at the network scale, model performance meets the overall objective. In model calibration efforts, the performance (even failure) of the model is critical for learning about the dynamic of the system. Validation will consist of multiple refinements to model equations to replicate the interactions occurring in each season more accurately.

ATP Model Caveats

Areas of improvement include comparison with the production dataset, since the ATP Model also predicts daily production. I found the calculations that govern channel topography in the model, particularly the "bank angle" calculations to be sensitive to slight adjustments. The bank angle function in the model controls stream width, (correlated with the shading measured at the site), as well as water depth, which affect the empirical AFDM in the results presented here. Further evaluation of the bank angle and turbidity values could help refine model estimates as well.

The other biological aspect not represented in the model is the role of grazing by invertebrates. Grazing is not represented in the model tests, however grazing represents a significant component of the functional environment and may help explain over predictions in the model

compared to the empirical data (Power, 1992, Feminella et al. 1987, Lamberti, 1987, Rosemond et al., 1993). Alternatively, a lack of invertebrate production in the model may account for ATP Model over predictions, since a positive feedback may be generated by nutrient contributions from invertebrate waste (Grimm, 1988) or waste from invertebrate predators (fish, birds, amphibians) tracking the invertebrate food source into areas where invertebrates are high. Additionally, high densities of predators may influence local nitrogen and phosphorous concentrations (Grimm, 1988).

I evaluated if invertebrate biomass could explain over predictions by the ATP Model (where the model predicted higher biomass than was observed in the field collected data). The ATP Model generally over predicted biomass at the sites where invertebrates were measured, except for at MT. MT was also where the highest biomass levels of scraper feeding invertebrates were observed.

Invertebrates were classified into groups according to their feeding behavior and benthic invertebrate biomass was negatively related to AFDM and Chl-a, an expected result since scrapers feed on periphyton (Table 10). Notably, Middle Twisp (MT) had the lowest biomass values across all periphyton samples, and model predictions consistently over predict biomass values except at MT (Figure 13). MT also had the highest biomass of invertebrates classified as scrapers (mg/site per sample date) especially in the November and March benthic samples (Figure 12), evidence that grazing may impact on the accuracy of model results and that grazing should be calculated in future versions of the model. Beaver Creek (Figure 16) had a high proportion of predator invertebrates, indicating an overall high proportion of biomass resources to support all invertebrate feeding types.

Overall, investigating the invertebrate data helps explain model over predictions compared to the empirical periphyton data (Figure 17). This is not a seamless explanation, since the

proportion of invertebrates observed does exactly match the over prediction, but this is a notable finding.

Notably, ATP Model equations predicting biomass growth were based on studies that took place in summer, in small laboratory streams. Based on these findings, I recommend refinements that address temperature limitation and carrying capacity, since very low temperatures did not negatively affect late winter biomass, decreased solar access due on latitude in winter, or constrained by density dependence.

Overall Conclusions and Potential Implications for Aquatic Restoration Efforts

Selecting specific sites for restoration projects could be coupled with an assessment of the inherent biological productivity and potential food resources using a mechanistic model as an evaluation tool. Using ATP Model when selecting sites could help prioritize restoration activities at locations that have the highest potential for helping meet energetic demands of aquatic organisms. This approach could link a critical oversight in the current methodology, which is often opportunistic or based on addressing geomorphic limiting factors resulting from anthropomorphic use. Understanding the drivers of periphyton could lead to more informed assessment about how physical changes to habitat could be located for the best impacts on food resources that benefit support focal aquatic organisms. Additionally, the ATP Model could help foreshadow what might occur under different scenarios ahead of physical changes so combinations of projects or different levels of changes could be evaluated before more costly steps are taken. Since 19 other Columbia River sub-basins have been evaluated using the CHaMP protocol, “scaling up” to generate model predictions in each of these basins is feasible with a few additional data points: a USGS gaging station recording discharge, turbidity, and temperature. Solar access could be attained remotely as can proportion of deciduous vs coniferous riparian cover to estimate winter solar access. Additionally nutrient levels values in

other basins would be a critical aspect of data collection order to scale up and apply this method in other basins. These additional data gathering steps though not insignificant, could be an important aspect of selecting restoration locations in a river network that have a high probability of generating food resources to support salmon or the aquatic organisms of focus. Additionally, results indicating that nitrogen concentrations were not limiting in the summer have important implications for restoration aimed at restoring aquatic food webs. Nutrient enrichment-focused restoration projects may be less effective during summer since nitrogen limitation on AFDM biomass occurs in all seasons except summer. The effectiveness of nutrient enrichment projects could be increased if nutrients were added when natural levels were lowest, or when they could stay in place the longest and benefit the system for a long period. In this basin, the fall is the season when the majority of spawning salmon return, and the start of the low flow season.

Using a mechanism model calibrated on field collected conditions like the ATP Model represents an important advance for ecosystem management and fisheries research, but the model needs further calibration using production estimates. This study is one component of a larger project that measured whole stream metabolism (Gross Primary Production [GPP]/Respiration[R]) at the same study sites during the same period. Understanding the production rate is a more robust metric for understanding ecosystem productivity and will be coupled with biomass values to evaluate both data sets in comparison with model predictions. Additionally, findings during wintertime in this study present an opportunity for a critical adjustment to the ATP. Since biomass was highest in winter, (across all sites), model under predictions during winter could be revised in the model with equations that predict low biomass at low temperatures. Comparing data by season, the model over predicts in summer and under predicts in winter.

Overall, I found drainage area, nutrient levels, and disturbance to be significant predictors of periphyton biomass. Notably, different combinations of drivers predicted biomass in each season, confirming other studies that suggest there are multiple interacting factors synergistically affecting biomass through the year (Rosa et al., 2012).

Temperature was not a significant driver of AFDM or Chl-*a* in this basin and winter biomass was highest over all seasons. Periphyton communities may be exhibiting adaptation to cold environments (Morgan-Kiss 2006, Ward 1994). Alternatively, the explanation for high winter biomass may be that winter is the longest time period since disturbing stream flows, and population growth during low flow increases until the system resets in late spring (Poff and Ward, 1988). Performance simulating empirical conditions with the mechanism-based ATP Model predicted biomass values within the SE of empirically collected biomass samples, however the model still needs adjustment to replicate observations more accurately (especially during winter).

REFERENCES

- Azim, M. E., Verdegem, M.C.J., van Dam, A. A., Beveridge, M.C.M., eds. 2005. *Periphyton: Ecology, Exploitation, and Management*. CABI Publishing, Cambridge, MA.
- Bernhardt, E. S., M. A. Palmer, J. D. Allan, G. Alexander, K. Barnas, S. Brooks, J. Carr, S. Clayton, C. Dahm, J. Follstad-Shah, D. Galat, S. Gloss, P. Goodwin, D. Hart, B. Hassett, R. Jenkinson, S. Katz, G. M. Kondolf, P. S. Lake, R. Lave, J. L. Meyer, T. K. O'Donnell, L. Pagano, B. Powell, and E. Sudduth. 2005. Synthesizing U.S. river restoration efforts. *Science* 308:636-637.
- Bellmore, JR, Fremier, AK, Mejia, FH, Newsome, MA. 2014. The response of stream periphyton to Pacific salmon: using a model to understand the role of environmental context. *Freshwater Biology* 59:1437-1451
- Bellmore, JR and Baxter, CV. 2013. Effects of geomorphic process domains on river ecosystems: a comparison of floodplain and confined valley segments. *River Research and Applications* 30: 617-630.
- Benke, AC, Huryn, AD, Smock, LA, and Wallace, JB. 1999. Length-mass relationships for freshwater macroinvertebrates in North America with particular reference to the southeastern United States. *Journal of the North American Benthological Society* 18(3): 308-343.
- Benke, AC and Huryn, AD. 2007. Secondary production of macroinvertebrates. Pages 691-710 in F.R. Hauer and G.A. Lamberti, editors, *Methods in Stream Ecology*. Academic Press, Burlington, MA.
- Bergey EA, Getty GM. 2006. A review of methods for measuring the surface area of stream substrates. *Hydrobiologia* 556: 7-16.
- Box, GEP, and Draper, NR. 1987. *Empirical Model-Building and Response Surfaces*. Wiley & Sons, New York, New York, USA.
- Burnham, KP, and Anderson, DR. 2002. *Model selection and multi-model inference: a practical information-theoretic approach*. Springer-Verlag, New York, New York, USA.
- Chiarello E, Amoros C, Pautou, G and Jolion JM. 1998. Succession modeling of river floodplain landscapes. *Environmental Modelling and Software*, 13: 75-85.

- Doyle, MW & Shields MF. 2012. Compensatory Mitigation for Streams Under the Clean Water Act: Reassessing Science and Redirecting Policy. *JAWRA Journal of the American Water Resources Association* 48, 494–509.
- Ebel JD, Marcarelli AM, Kohler AK. 2014. Biofilm nutrient limitation, standing crop, and metabolism responses to experimental application of salmon carcass analog in Idaho streams. *Canadian Journal of Fisheries and Aquatic Sciences* 71:1796-1804.
- Feminella, JW, Power, ME and Resh, VH. 1989. Periphyton responses to invertebrate grazing and riparian canopy in three northern California coastal streams. *Freshwater Biology*. 22: 445-457.
- Feminella, JW and Hawkins, CP. 1995. Interactions Between Stream Herbivores And Periphyton: A Quantitative Analysis Of Past Experiments. *Journal of the North American Benthological Society*, 14: 465-509.
- Finlay, JC, Khandwala, S, and Power, ME. 2002. Spatial scales of carbon flow in a river food web. *Ecology* 83:1845-1859.
- Fremier, AK, Seo, JI, Nakamura, F. 2010. Watershed controls on the export of large wood from stream corridors . *Geomorphology*, 117: 33–43
- Gende, S. M., E. D. Edwards, M. F. Willson, and M. S. Wipfli. 2002. Pacific salmon in aquatic and terrestrial ecosystems. *BioScience* 52:917-928.
- Gregory, SV. 1980. *Effects Of Light, Nutrients, and Grazers On Periphyton Communities In Streams*. (Doctoral Dissertation). Retrieved from Oregon State University. Corvallis, OR
- Gresh, T, Lichatowich, J, and Schoonmaker, P. 2000. An estimation of historic and current levels of salmon production in the Northeast Pacific ecosystem: evidence of a nutrient deficit in the freshwater systems of the Pacific Northwest. *Fisheries* 25:15–21.
- Grimm, Nancy, B. 1988. Role Of Macroinvertebrates In Nitrogen Dynamics Of A Desert Stream. *Ecology*, 69: 1884-1893
- Hambrook-Berkman, JA and Canova, MG. 2007. Algal Biomass Indicators. USGS Field Manual.
- Holtgrieve, GW. 2011. Marine-derived nutrients, bioturbation, and ecosystem metabolism: reconsidering the role of salmon in streams. *Ecology*, 92: 373–385

- Hoffmann, JP. Simultaneous Inductive and Deductive Modeling of Ecological Systems via Evolutionary Computation and Information Theory. *Simulation*, Vol. 82, Issue 7. 439-450
- Hoyle, GM, Holderman, C, Anders, PJ, Shafii, B, Ashley, KI. 2014. Water quality, chlorophyll, and periphyton responses to nutrient addition in the Kootenai River, Idaho. *Freshwater Science*, 33: 1024-1029.
- Huryn, AD, Wallace, JB, and Anderson, NH. 2008. Habitat, life history, secondary production, and behavioral adaptations of aquatic insects. Pp. 55-103 in: Merritt, R.W., K.W. Cummins, and M.B. Berg editors, *An introduction to the aquatic insects of North America*. Kendall Hunt Publishing Company, Dubuque, IA.
- Hynes, HB. 1975. The stream and its valley. *Verhandlungen der Internationale Vereinigung Theoretische und Angewandte Limnologie* 19:1-15.
- Kondolf, GM. 1995. Five Elements for Effective Evaluation of Stream Restoration. *Restoration Ecology* 3, 133-136.
- Konrad, CP, Drost, BW, and Wagner, RJ, 2003, Hydrogeology of the unconsolidated sediments, water quality, and ground-water/surface-water exchanges in the Methow River Basin, Okanogan County, Washington: U.S. Geological Survey Water-Resources Investigations Report 03-4244
- Labioda, C., Godillotb, R., Caussadea, B. 2007. The relationship between stream periphyton dynamics and near-bed turbulence in rough open-channel flow. *Ecological Modelling*, 209:78-96.
- Lamberti, GA, Gregory, SV, Askenas, LR, Steinman, AD, McIntire, CD. 1989. Productive capacity of periphyton as a determinant of plant-herbivore Interactions in streams. *Ecology*, 70:1840-1856.
- Lamberti, GA, and Resh, VH. 1983. Stream periphyton and insect herbivores: an experimental study of grazing by a caddisfly population. *Ecology* 64, 1124-1135.
- Lindeman, R. 1942. The Tropic Dynamic Aspect of Ecology. *Ecology* 23: 399-417.
- Marcarelli AM, Baxter CV, Wipfli MS. 2014. Nutrient additions to mitigate for loss of Pacific salmon: consequences for stream biofilm and nutrient dynamics. *Ecosphere* 5:69.

- Marcarelli AM, Baxter CV, Mineau MM & Hall RO. 2011. Quantity and quality: unifying food web and ecosystem perspectives on the role of resource subsidies in freshwaters. *Ecology* 92:1215-1225.
- McCormick, PV, Shuford III, RBE, Backus, JG, Kennedy, WC. 1997. Spatial and seasonal patterns of periphyton biomass and productivity in the northern Everglades, Florida, U.S.A. *Hydrobiologia* 362: 185-210.
- McIntire, David. 1973. Periphyton dynamics in laboratory streams: A simulation model and implications. *Ecological Monographs* 43: 399-420.
- Minshall, G.W, 1978, Autotrophy in stream ecosystems. *BioScience* 28:767-771
- Minshall, G.W., Shafii, B, Price, WJ, Holderman, C, Anders, PJ, Lester, G, Barrett, P. 2014. Effects of nutrient replacement on benthic macroinvertebrates in an ultraoligotrophic reach of the Kootenai River, 2003-2010. *Freshwater Science*: 33, 1009-1023
- Montgomery DR. 1999. Process domains and the river continuum. *Journal of the American Water Resources Association* 35: 397-410.
- Montgomery DR, Abbe TB, Buffington JM, Peterson NP, Schmidt KM, Stock JD. 1996. Distribution of bedrock and alluvial channels in forested mountain drainage basins. *Nature* 381: 587-589.
- Montgomery DR, Buffington JM. 1997. Channel-reach morphology in mountain drainage basins. *Geological Society of America Bulletin* 109: 596-611
- Morgan-Kiss, RM, Priscu, JC, Pocock, T, Gudynaite-Savitch, L, & Huner, NPA. 2006. Adaptation and Acclimation of Photosynthetic Microorganisms to Permanently Cold Environments. *Microbiology and Molecular Biology Reviews*, 70: 222-252.
- Naiman, RJ, Bilby, RE, Schindler DE, and Helfield, JM. 2002. Pacific salmon, nutrients, and the dynamics of freshwater and riparian ecosystems. *Ecosystems*, 5: 399-417.
- NW Power & Conservation Council, 2004. "Methow River Subbasin Plan." Columbia River Basin Fish and Wildlife Program. Portland, OR.
- Poole, GC, and Berman, CH. 2001. An ecological perspective on in-stream temperature: natural heat dynamics and mechanisms of human-caused thermal degradation. *Environmental Management*, 27: 787-802.

Poole, GC. 2002. Fluvial landscape ecology: addressing uniqueness within the river continuum. *Freshwater Biology* 47:641-660.

Poff, NL, Ward, JV. 1988. Implications of streamflow variability and predictability for lotic community structure: A regional analysis of streamflow patterns.

Power, ME, Parker, MS, Dietrich, WE. 2008. Seasonal reassembly of a river food web: Floods, droughts, and impacts of fish. *Ecological Monographs*, 78: 263–282.

Polvi, LE, and Wohl, E. 2013. Biotic Drivers of Stream Planform: Implications for Understanding the Past and Restoring the Future. *BioScience* 63: 439–452

Rosa, J, Ferreira, V, Canhoto, C, Graça, MAS. 2012. Combined effects of water temperature and nutrients concentration on periphyton respiration – implications of global change. *International Review of Hydrobiology*, 98: 14-23.

Rosemond, A., Mulholland, P., Ellwood, J. 1993. Top down and bottom up control of stream periphyton: Effects of nutrients and herbivory. *Ecology* (74)4, 1264-1280.

Spaulding, SA, and Elwell, L, 2007, Increase in nuisance blooms and geographic expansion of the freshwater diatom *Didymosphenia geminata*: U.S. Geological Survey Open-File Report 2007-1425, 38, pg. 35

Steinman AD, Lamberti GA, Leavitt PR. 2006. Biomass and Pigments of Benthic Algae. In *Methods in Stream Ecology*, Hauer FR, Lamberti GA (eds). Academic Press: San Diego; 357–380.

Stevenson, RJ, Bothwell, M, Lowe, RL, editors. 1996. *Algal Ecology: Freshwater Benthic Ecosystems*. Academic Press, San Diego, CA

Stockner, JG, editor. 2003. *Nutrients in salmonid ecosystems: sustaining production and biodiversity*. American Fisheries Society, Bethesda, Maryland, USA.

Swanson FJ, Johnson LS, Gregory SV, Acker SA. 1998. Flood disturbance in a forested mountain landscape. *Bioscience* 48: 681–689.

Thorp, JH, and DeLong MD. 2002. Dominance of Autochthonous Autotrophic Carbon in Food Webs of Heterotrophic Rivers. *Oikos* 96: 543-550.

U.S. Environmental Protection Agency. 2001. AQUATOX: A modular fate and effects model for aquatic ecosystems. Office of Water Programs online at: (<http://www2.epa.gov/exposure-assessment-models/aquatox>) Accessed 28 April 2015.

U.S. Fish and Wildlife Service. 2001. Endangered Species Act Basics Fact Sheet. (<http://www.fs.fed.us/biology/resources/pubs/tes/esa20basics.pdf>) Accessed 25 May 2015.

Vannote RL, Minshall GW, Cummins KW, Sedell JR, Cushing CE. 1980. The river continuum concept. *Canadian Journal of Fisheries and Aquatic Sciences* 37: 130–137.

Wallace, JB, Eggert, SL, Meyer, JL, and Webster, J.R. 1997. Multiple trophic levels of a forest stream linked to terrestrial litter inputs. *Science* 277:102–104.

Ward, JV. Ecology of alpine streams. 1994. *Freshwater Biology*, 32: 277–294

Wipfli, MS, and J. Musslewhite, 2004. Density of Red Alder (*Alnus rubra*) in Headwaters Influences Invertebrate and Detritus Subsidies to Downstream Fish Habitats in Alaska. *Hydrobiologia* 520:153-163.

Wolman, M. Gordon. 1954. A method of sampling coarse river-bed material. *Transactions, American Geophysical Union*, 35: 951-956.

Woodward G. 2009. Biodiversity, ecosystem functioning and food webs in fresh waters: assembling the jigsaw puzzle. *Freshwater Biology* 54: 2171–2187.

TABLES

Table 1. Summary of field collected data at each site, arranged by drainage area at each site from left (smallest) to right.

Site Name	UT	BD	EW	BV	MT	LT	UM1	UC	LM1	LC	UM2	LM2
Drainage Area (km ²)	125	128	129	179	211	394	438	536	666	843	1669	1722
<i>Response</i>												
Total Benthic AFDM (g m ⁻²)	38.5	56.1	42.6	161.8	36.1	101.7	27.2	78.9	47.9	99.9	197.6	136.0
AFDM 12 month average (n=60)	3.2	4.7	3.5	13.5	3.0	8.5	2.3	6.6	4.0	8.3	16.5	11.3
Total Chl-a (mg m ⁻²)	71.2	127.6	91.6	1135.1	59.6	253.5	39.8	215.4	103.0	258.8	741.8	432.4
Chl-a 12 month average (n=60)	3.0	5.3	3.8	47.3	2.5	10.6	2.8	9.0	4.3	10.4	30.9	18.0
Annual Average GPP	0.19	0.06	0.13	0.77	0.33	1.41	0.18	1.30	0.94	1.24	4.83	4.82
<i>Stream Flow</i>												
Average Annual discharge (m ³ /s)	1.9	1.1	3.4	0.8	5.3	7.4	18.0	3.6	34.7	14.4	37.6	44.3
2 Year Peak flow (Bankfull discharge) (m ³ /s)	26.5	9.1	35.1	9.1	35.7	53.8	66.0	36.2	93.4	47.6	204.7	217.2
Specific Stream Power (2yr Pk Q*Gradient)/Bankfull width)	0.0074	0.0440	0.0276	0.0210	0.0108	0.0565	0.0075	0.0053	0.0054	0.0091	0.0190	0.0206
<i>Water Quality</i>												
Average Water Temp (°C)	5.3	6.7	4.9	5.9	5.7	6.4	6.1	6.5	7.0	7.6	7.6	7.7
Temp Range (°C)	9.3	14.5	11.9	14.8	11.6	14.0	11.6	15.6	9.0	16.2	12.9	13.6
Turbidity (NTU)	5.8	8.1	5.8	8.7	6.0	7.1	4.5	6.4	6.0	7.2	6.4	6.3
Average Total N mg/L (n=12)	0.068	0.040	0.058	0.259	0.063	0.073	0.051	0.029	0.046	0.055	0.095	0.159
Average Total P mg/L (n=12)	0.007	0.007	0.001	0.010	0.001	0.001	0.003	0.003	0.002	0.002	0.002	0.002
<i>Solar input</i>												
Solar Access %	62	37	44	68	55	61	70	59	80	60	85	86

Table 2: Sampling methods, frequency, and whether the method was applied in the empirical analysis or in ATP Mechanistic Model evaluation.

Measurement Name	Description	Sample Collection Frequency at 12 sites	Reference or Model No.	Used in Empirical Analysis or Mechanistic Model?
Light Limitation				
Photosynthetically active radiation (PAR)	Measured near Twisp, WA (central location to all the sites), at an unshaded site (Figure 1). Measured in ($\mu\text{mol}/\text{m}^2/\text{day}^1$)	Measured every 10 minutes, summed by day.	Hobo PAR	Mechanistic Model
Solar access	Measured at the center of the channel in at least three locations and averaged by site. Tool estimates daily solar access based on GPS coordinates.	Once, August 2013.	Solmetric SunEye 210	Both
Turbidity	Calculated the portion of the water body where light is sufficient for photosynthesis (euphotic depth)	Collected monthly	Hydrolab Quanta	Mechanistic Model
Nutrient Limitation				
Total inorganic nitrogen: NH ₃ , NO ₃ ⁻ , NO ₂ ⁻	Collected in sterile, acid washed bottles, and kept frozen until processed by IEH Aquatic Research Laboratory & Consulting Services (Seattle, WA).	Collected every month from channel thalweg	EPA methods	Both
Soluble reactive phosphorous (SRP)	Collected in sterile, acid washed bottles, and kept frozen until processed by IEH Aquatic Research Laboratory & Consulting Services (Seattle, WA).	Collected and filtered every month from channel thalweg	EPA methods	Both
Physical Limitation				
Substrate grain size - Wolman	Randomly sampled 100 particles across the entire stream reach. I calculated median (D50) grain size.	Once, August 2013	Wolman, 1954	Both
Temperature and Dissolved Oxygen	High flows occasionally displaced the sondes for short periods. I estimated missing data by using linear interpolation between known values. Deployed June 2013 - May 2014.	Measurements recorded every 10 min, calculated daily mean	USGS	Both
Discharge	Empirical measurements were taken during monthly sampling at each site	Collected monthly discharge based on channel cross section	Sontek Flowtracker	Both for some sites where gage data wasn't available.
Discharge	Gathered data from USGS gauge station network using StreamStats (http://waterdata.usgs.gov/wa/) to generate an estimate of daily discharge by tracing the watershed boundary. The USGS compares traced watershed to the downstream gage or a similar gaged watershed and adjusts flow estimates based on flow per unit area values.	Daily values	USGS	Mechanistic Model
Specific Stream Power (2 year peak flow * gradient /Bankfull width)	Disturbance effect: 2 year peak flows for each site were estimated using USGS Stream Stats regressions of estimate flow by drainage area and subbasin and were checked against empirically collected Q data.	Once	USGS	Empirical

Table 3: Topographic measurements from CHaMP and field effort used in empirical analyses and the mechanistic model

Topographic Measurements			UT	BD	EW	BV	MT	LT	UM1	UC	LM1	LC	UM2	LM2
Name	Description	Method												
Drainage Area (km ²)		USGS Pour-point in StreamStats	125	128	129	179	211	394	438	536	666	843	1669	1722
Reach Length (m)	Linear distance of the thalweg of the survey area.	CHaMP Protocol, 2014	511	202	372	214	326	297	649	634	642	656	612	601
Gradient (m/m)	Water surface slope for the reach (meters/ meters).		0.009	0.04	0.019	0.017	0.009	0.016	0.005	0.005	0.003	0.006	0.004	0.005
Bankfull width (m)	Average width of the bankfull polygon for a site (measured in GIS).		35	9	25	7	32	16	51	35	64	32	50	53
Floodplain Terrace Width (m)	Average (n=5) bankfull width (x2)	USFS Rapid Habitat Survey Protocol for Region 6, 2012	71	18	50	15	64	32	103	69	128	65	99	106
D50 (m)	Calculated from Wolman Pebble Counts	Wolman, 1954	0.08	0.13	0.13	0.06	0.07	0.10	0.12	0.06	0.12	0.11	0.11	0.10

Table 4: Principal components analysis (PCA) for the initial site selection process. The first two axes explain 64.35 % of the variation across 52 CHaMP sites in the basin. To select study sites, we clustered sites by PC1, which represented elevation, gradient, and canopy, roughly correlating to stream order (high gradient, high canopy sites occur in low stream order headwaters locations). PC2 represented the size of stream and its interaction with the hyporheic zone. Since >60% of variation was explained by the first two axes, PC3 was not fully evaluated, however PC3 corresponds to valley width, drainage area, and disturbance regime.

<i>Variables</i>	<i>PC1</i>	<i>PC2</i>	<i>PC3</i>
Disturba	-0.1108	-0.0001	0.1152
Areasqkm	-0.3009	-0.0755	-0.0038
Azimth_d	-0.022	-0.0605	0.0787
Order	-0.1157	0.0886	-0.0658
Elev_m	0.1034	0.0709	-0.0144
Mean_gra	0.0832	-0.0852	-0.0349
Acw_m	-0.2861	0.0561	-0.0427
Vwi_floo	0.0432	-0.0216	0.1208
Mnanprc_	0.0142	0.1228	-0.0781
Mean_annc	-0.3503	-0.0109	-0.0302
Strm_pow	-0.1408	-0.0353	-0.0408
Valley_widt	-0.0924	0.0864	0.1375
Bfw_m	-0.2562	-0.0178	0.064
Fpw_m	-0.0375	0.0524	0.119
Exchange	-0.0772	0.2819	0.0069
Canopy	0.2735	0.0701	0.0461
Solar_rad	-0.0201	-0.0185	0.0522
<i>Eigenvalue</i>	0.518	0.145	0.092
<i>Variance %</i>	50.282	14.068	8.978
<i>Cumulative %</i>	50.282	64.35	73.327

Table 5: PCA of the field collected environmental data. Three PCA axes explain 68.97% of the variation in the ancillary dataset. The first axis (PC1 = 28.5%) correlated with variables related to nutrients and velocity. The second axis (PC2 = 23.8%) correlated to discharge and velocity. The third axis (PC3 = 16.7%) correlated to drainage area and nutrients, suggesting factors related to the sub-basin position.

<i>Variables</i>	<i>PC1</i>	<i>PC2</i>	<i>PC3</i>
Nitrogen	0.2181839	-0.4880733	0.3148948
PhosphorusSRP	0.3772819	-0.33156212	-0.4478908
Solar	-0.5544208	-0.33563513	-0.1711442
Temp	-0.4717688	-0.08228059	-0.6082158
DrainageArea	-0.4708216	-0.1439415	0.509352
SpecificStreamPower	0.1435065	0.38849276	-0.1898066
<i>Eigenvalue</i>	1.412	1.291	1.081
<i>Variability %</i>	28.47	23.81	16.7
<i>Cumulative %</i>	28.47	52.27	68.97

Table 6: Linear regression results for Periphyton AFDM and Chl-a

Explanatory Variables in the Annual Dataset (n=720)		Coefficient		p - value	R2
		Estimate	Standard Error		
Nitrogen	AFDM	41.5	6.32	1.18e-09 ****	0.2571
	CHLA	276.626	28.848	<2e-16 ****	0.4238
Phosphorus	AFDM	N	N	N	
	CHLA	1815.334	838.113	0.0322 **	0.0036
% Solar Access	AFDM	N	N	N	
	CHLA	0.1995	0.12	0.099 *	0.0216
Drainage Area	AFDM	0.0059063	0.0009168	2.30e-09 ****	0.2492
	CHLA	0.017492	0.005257	0.001152 ***	0.0813
D50	AFDM	N	N	N	
	CHLA	-333.3	117.59	0.00536 ***	0.0562
Temperature	AFDM			N	
	CHLA			N	
Specific Stream Power	AFDM			N	
	CHLA			N	
Turbidity	AFDM			N	
	CHLA			N	
Significance codes: p-value for coefficients: * <0.01, **<0.05. ***<0.001, ****<0.0001					

Table 7: Table 7 Multiple Linear Regression results showing potential models for predicting AFDM in the annual data and through seasonal changes. Seasonal shifts in the Methow Basin have strong contrasts.

Model	AIC	R ²	Adj R ²	P-value
Annual Dataset				
N + T + D50 + SP + DA	403.95	0.4928	0.4718	<0.0001
N + T + Solar + D50 + SP + DA	405.51	0.4946	0.4693	<0.0001
Winter				
N + DA	119.44	0.5213	0.4871	<0.0001
N + SP + DA	120.37	0.5374	0.486	<0.0001
N + Solar + SP + DA	121.51	0.55	0.4808	<0.0001
N + P + Solar + T + SP + DA	122.25	0.5882	0.5059	<0.0001
Spring				
N + P + D50 + SP	77.97	0.4291	0.3252	0.01202
N + P + Solar + D50 + SP	79.01	0.449	0.3179	0.0203
Summer				
Solar + T	114.28	0.26	0.22	0.007
P + Solar + T	116.01	0.27	0.199	0.0173
N + P + Solar + T	117.54	0.2805	0.1606	0.0659
Fall				
N + Solar + SP	83.09	0.675	0.6413	<0.0001
N + SP	84.66	0.638	0.6136	<0.0001
N + D50 + Solar + SP	84.75	0.678	0.632	<0.0001

Table 8: AIC and AIC weights

Model	n	k	AIC	AICc	$\Delta AICc$	$\exp(-0.5 \cdot \Delta AICc)$	AICw
Annual Dataset							
N + T + D50 + SP + DA	127	5	403.95	424.0	0.0	1.00	0.07
N + T + Solar + D50 + SP + DA	127	6	405.51	429.2	5.2	0.07	0.00
Winter							
N + DA	127	2	119.44	122.3	0.0	1.00	0.65
N + SP + DA	127	3	120.37	124.3	2.0	0.38	0.25
N + Solar + SP + DA	127	4	121.51	126.5	4.2	0.12	0.08
N + P + Solar + T + SP + DA	127	6	122.25	129.4	7.1	0.03	0.02
Spring							
N + P + D50 + SP	127	4	77.97	81.2	0.0	1.00	0.71
N + P + Solar + D50 + SP	127	5	79.01	82.9	1.8	0.41	0.29
Summer							
Solar + T	127	2	114.28	117.0	0.0	1.00	0.75
P + Solar + T	127	3	116.01	119.8	2.7	0.25	0.19
N + P + Solar + T	127	4	117.54	122.4	5.3	0.07	0.05
Fall							
N + Solar + SP	127	3	83.09	85.8	0.0	1.00	0.52
N + SP	127	2	84.66	86.7	0.9	0.63	0.33
N + D50 + Solar + SP	127	4	84.75	88.2	2.4	0.30	0.15

Table 9: Intercept values of best models and significant of each variable

Best Fit Models Predicting AFDM ~	Variable	Coefficient	P-value
Annual			
~ (intercept) + N**** + D50** + T + SP**** + DA ****			< 2.2e-16
	N	26.27	0.000
	intercept	5.342	x
	D50	43.21	0.050
	T	15.95	x
	SP	111.3	0.000
	DA	620.9	0.000
Summer			
~ (intercept)*+ Solar** + Temp**			0.007
	Solar	0.13	0.050
	intercept	-9.86	x
	T	0.55	0.050
Fall			
~ (intercept) + N**** + Solar* + SP			0.000
	N	48.55	0.000
	int	0.78	x
	Solar	0.05	0.050
	SP	73.24	0.010
Winter			
~ (intercept) + N*** + DA****			0.000
	N	40.99	0.001
	int	0.525	x
	DA	0.008	0.000
Spring			
~ (intercept)*+ N** + P + D50* + SP**			0.012
	N	35.8	0.050
	int	7.08	0.010
	P	-298	x
	D50	-63	0.010
	SP	181	0.050

Significance codes: p-value for coefficients: * <0.01,
 <0.05. *<0.001, ****0

Best fit models from annual and seasonal data sets. Best models have AIC have values of >1.0 difference from other models. N = Total Inorganic Nitrogen (mgL-1), SP = Specific Stream Power, P = Soluble Reactive Phosphorus (mgL-1), DA = Drainage Area (km^2), T = Temperature, D50 = Median B-axis of substrate at each site

Table 10: Invertebrate Feeding Type and Pearson's Correlation ($r = \frac{n(\Sigma xy) - (\Sigma x)(\Sigma y)}{\sqrt{[n(\Sigma x^2) - (\Sigma x)^2][n(\Sigma y^2) - (\Sigma y)^2]}}$), with biomass and Chl-a values (total invertebrate dataset).

Invertebrate Type	Benthic Data		Drift	
	AFDM	CHLA	AFDM	CHLA
Scrapers	-0.10	0.06	0.30	0.60
Filterers	0.54	0.58	0.47	0.45
Gatherers	0.67	0.49	0.49	0.50
Predators	0.61	0.41	0.48	0.31
Shredders	-0.17	-0.10	0.10	-0.01
Terrestrial	0.00	0.00	0.04	0.05
TOTAL BIOMASS	0.56	0.46	0.52	0.46

FIGURES

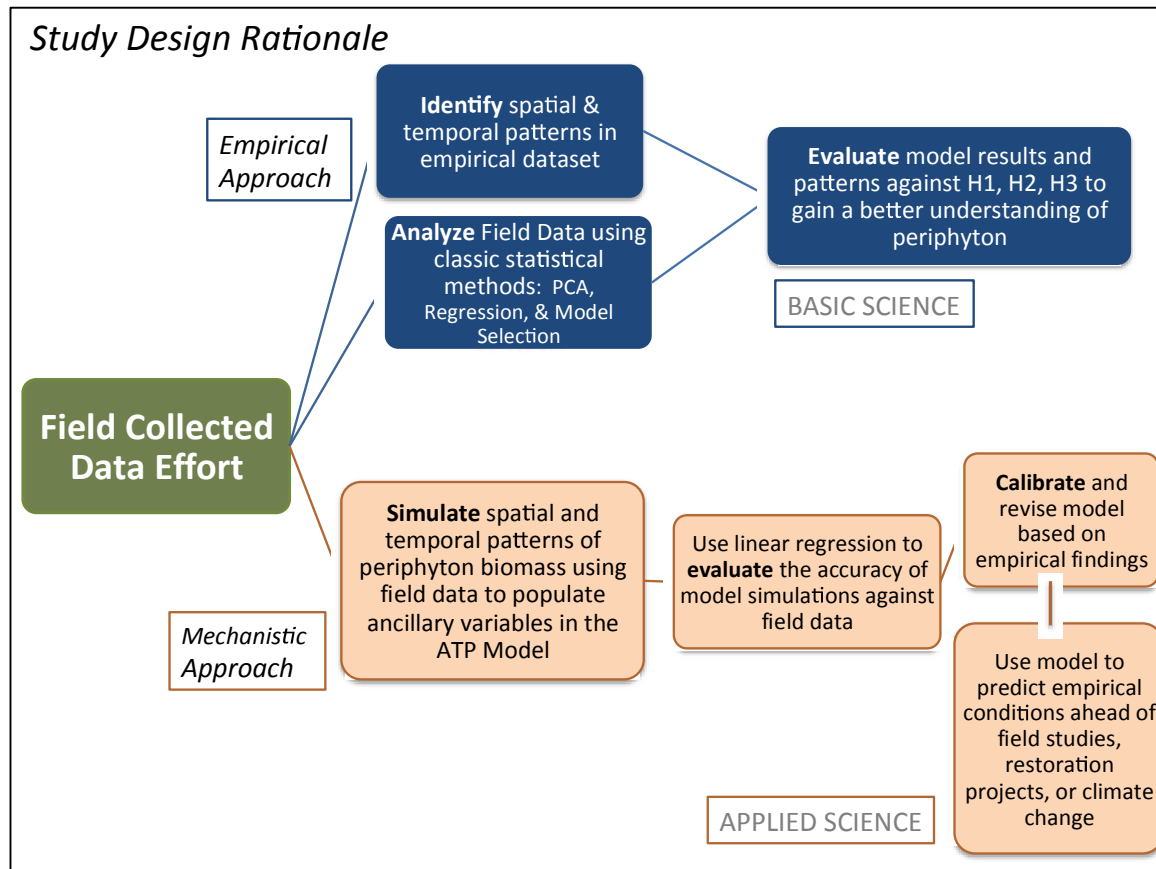


Figure 1: After data was collected in the field, it was used in two ways. Since the term “Model” is used with both approaches, I wanted to show how approaches differ. The Mechanistic Model is different from the statistical models evaluated in the Empirical Approach.

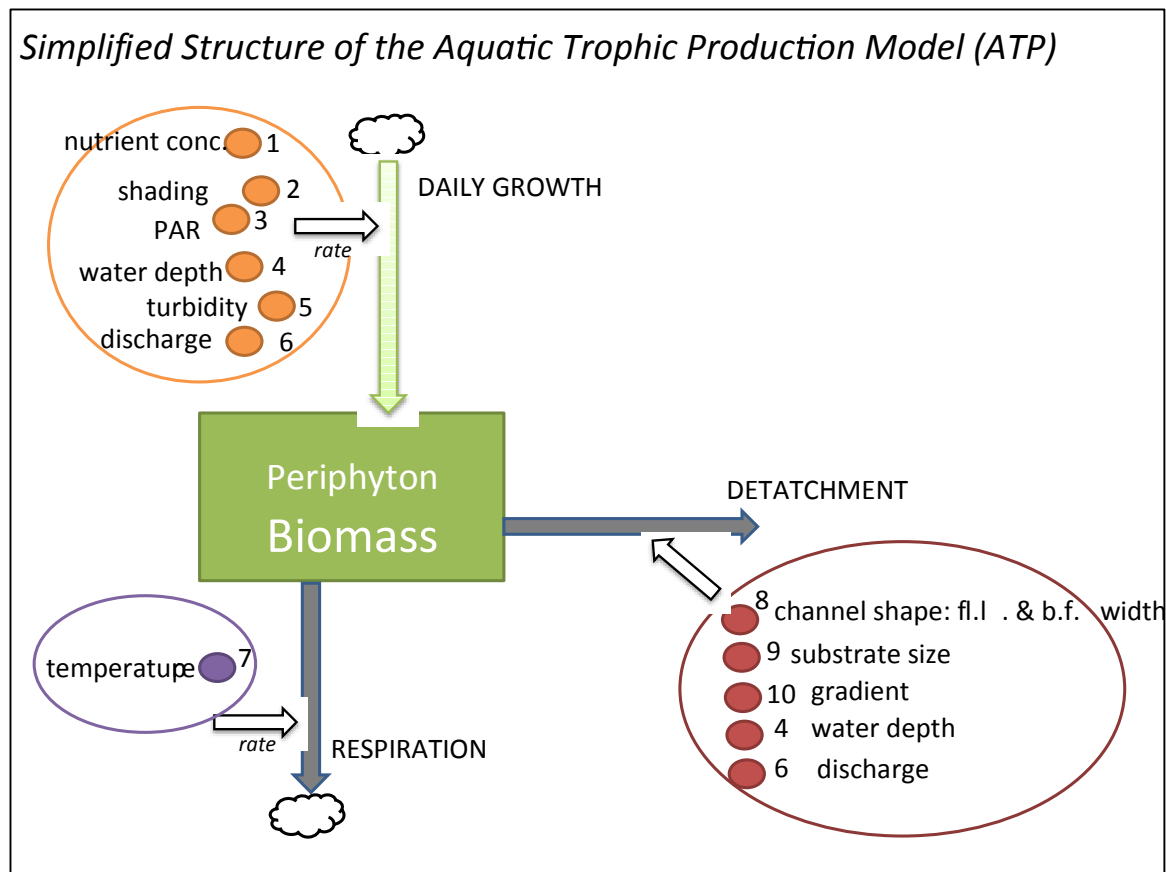


Figure 2: A conceptual map of the ATP Model (adapted from Bellmore, et al. 2014). Model parameters depict formal relationships between mechanistic environmental drivers and periphyton biomass and each component incorporates values from physical, biological and chemical drivers that represent actual dynamics known to occur in nature as closely as possible. See Table 1 for variables 1-7, and Table 2 for variables 8-10. Note: consumption by invertebrates was not evaluated in the model.

Methow River Basin Study Sites

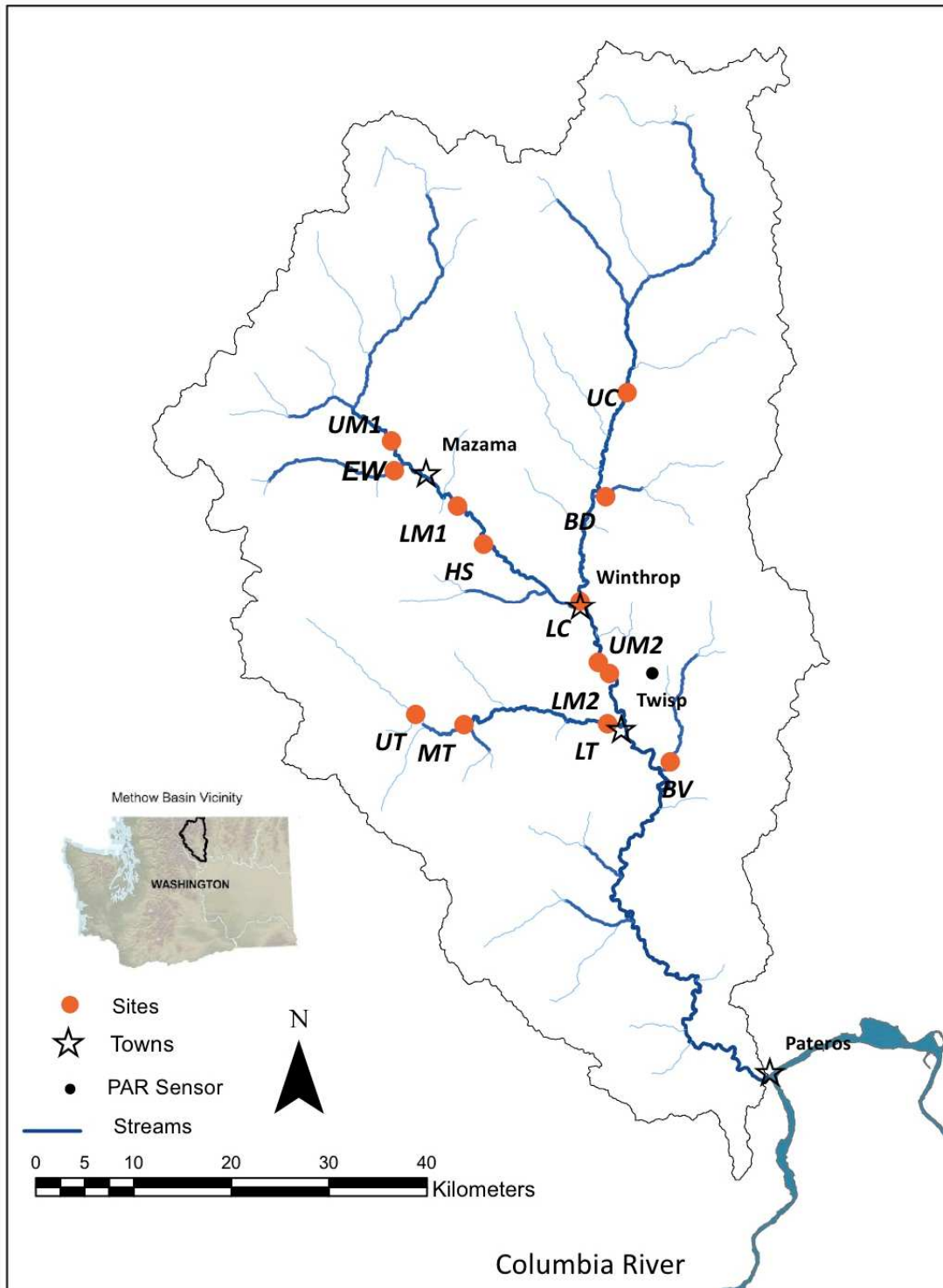
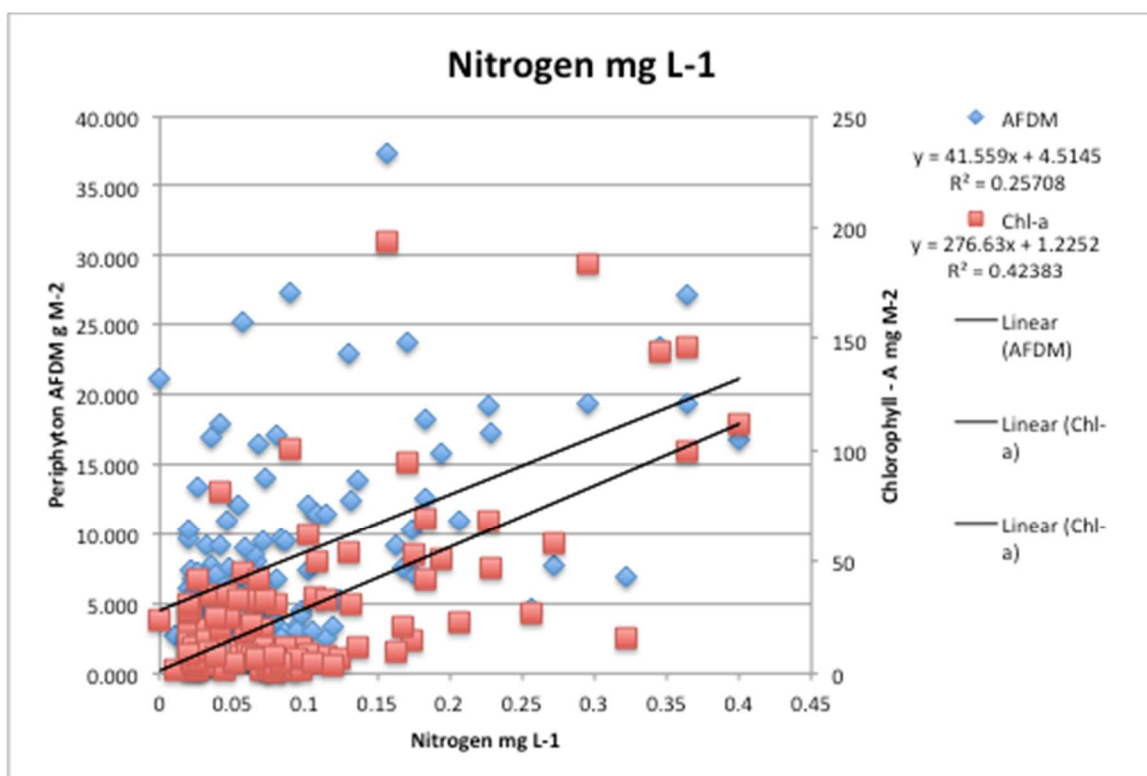
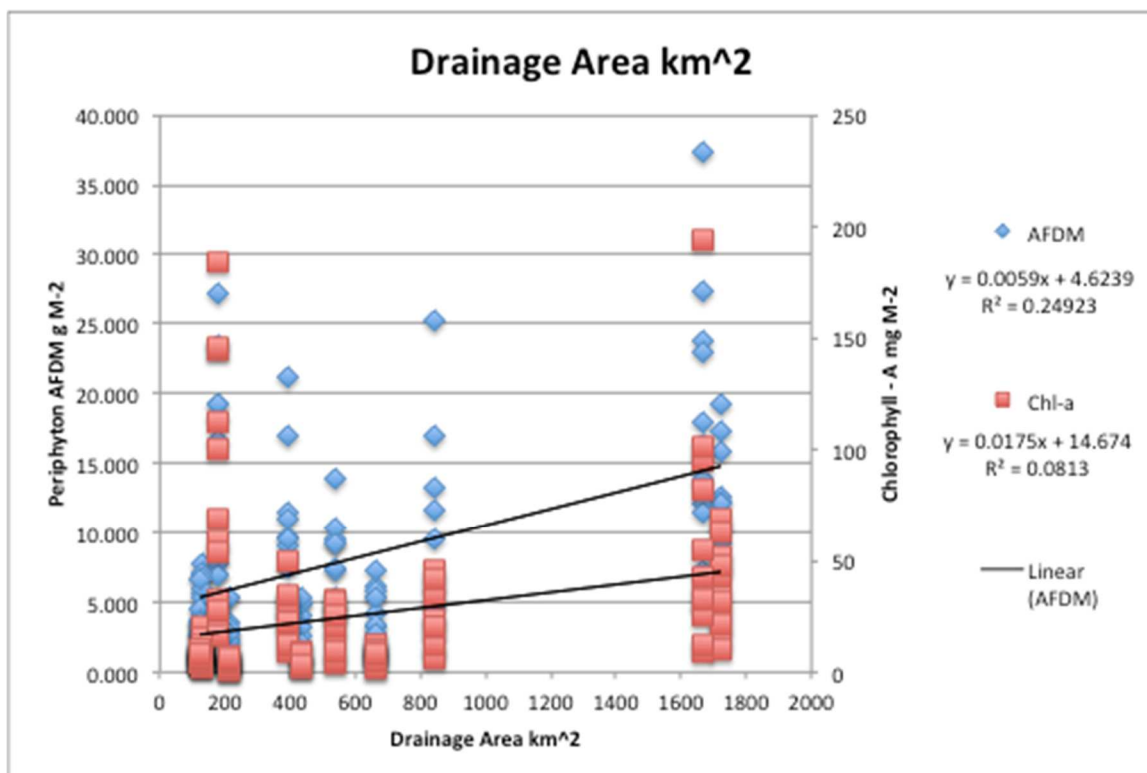
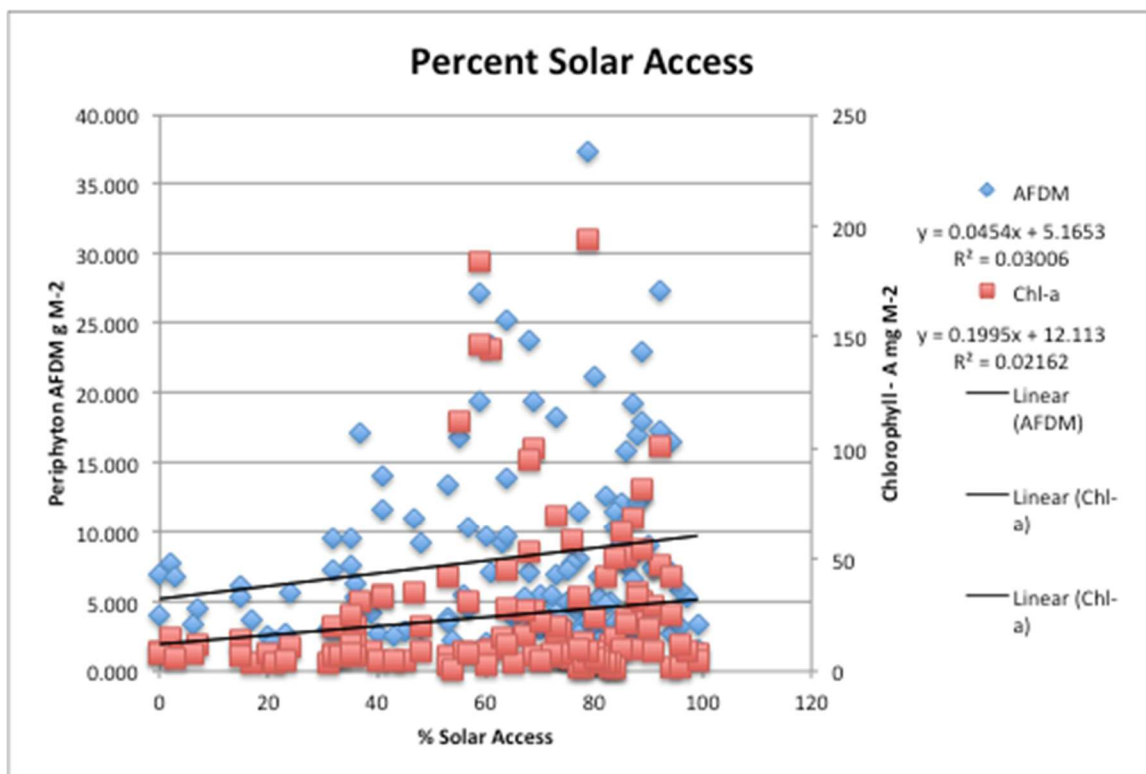
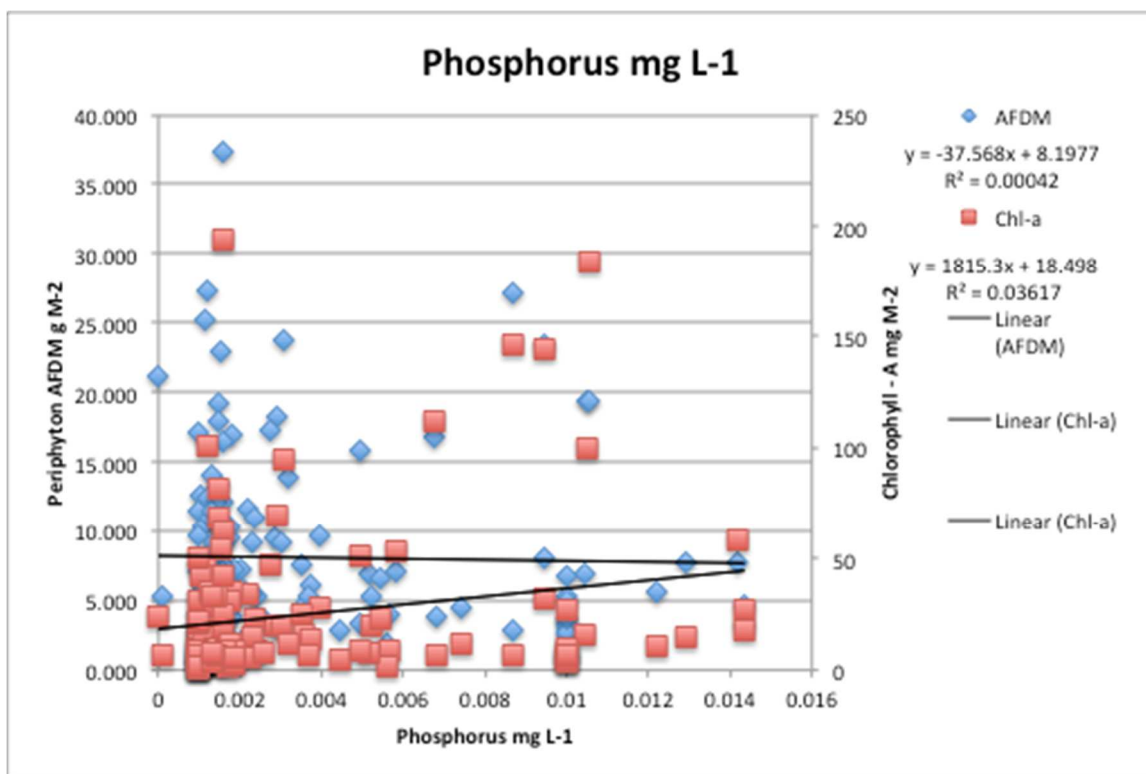


Figure 3: Site Map of Methow Basin





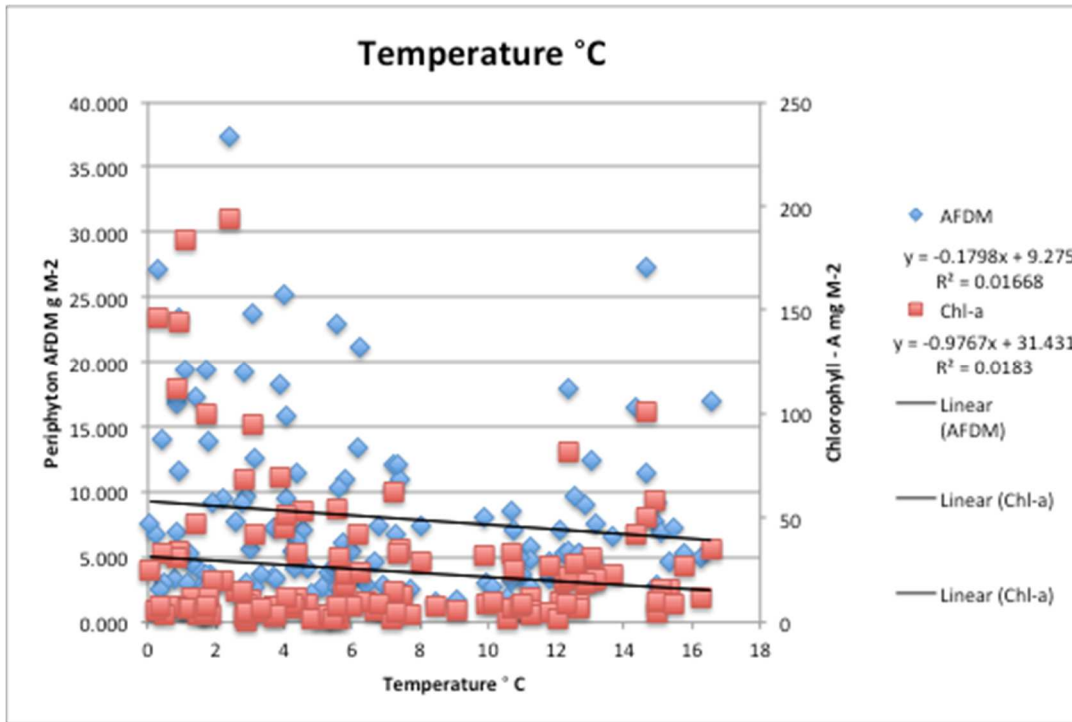


Figure 4: Testing H1-H4 with correlations between environmental drivers and AFDM using Simple Linear Regression. Annual AFDM data in are shown in Blue and Chl-a values are in red. Nitrogen has the strongest relationship on AFDM in the basin over the year. Nitrogen concentration has the strongest correlation with AFDM and Chl-a.

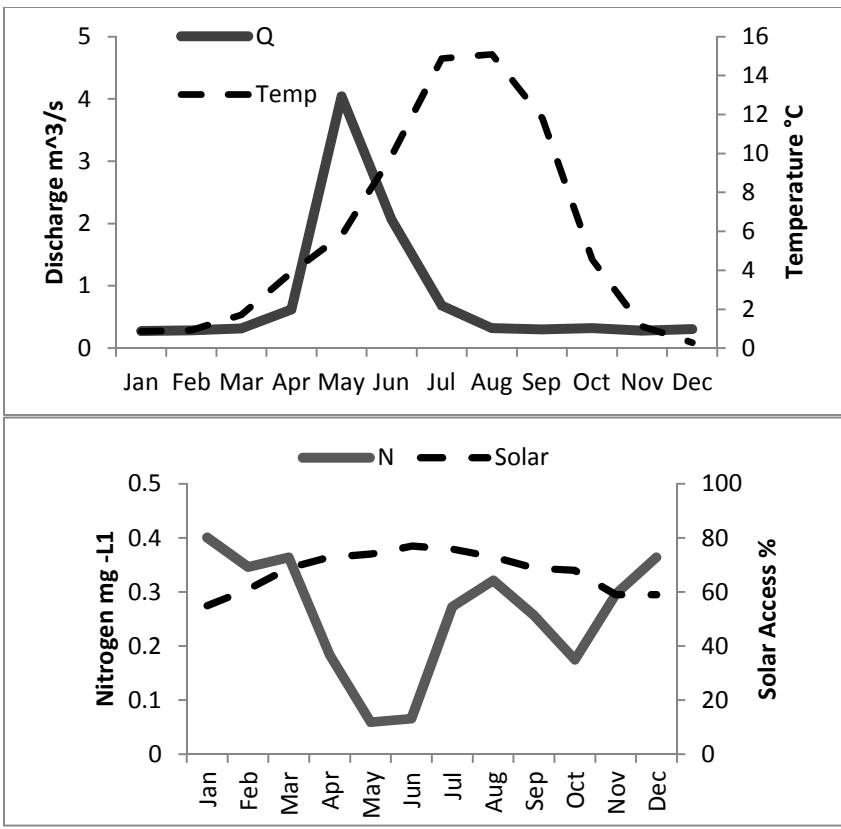


Figure 5: Seasonal Dynamics of Beaver Creek (above) – a small, high biomass stream

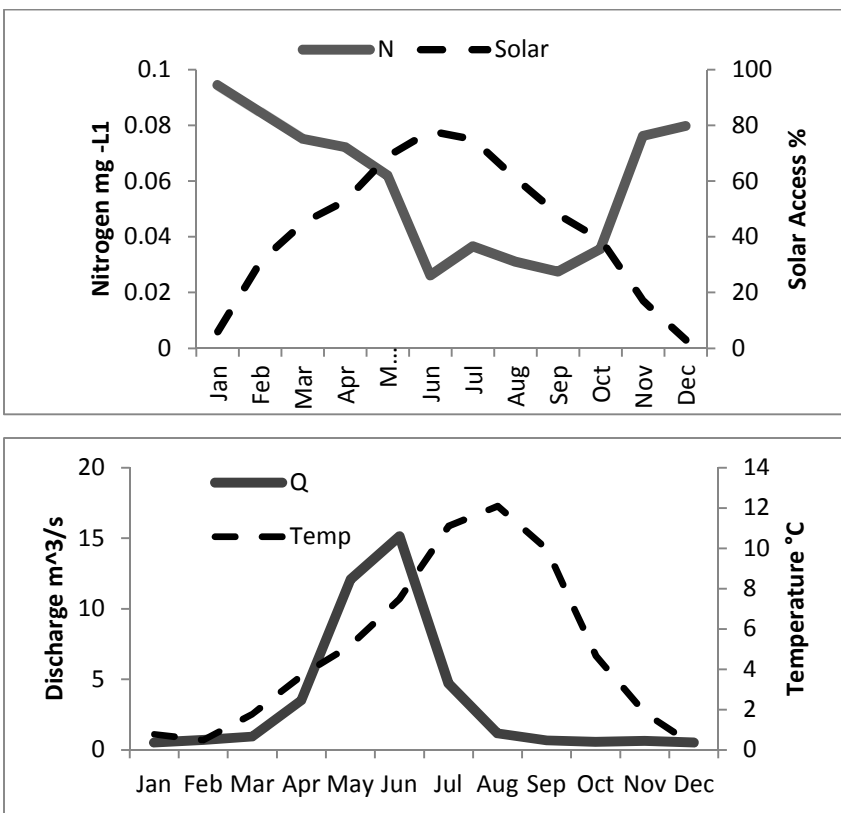


Figure 6: Seasonal Dynamics of Early Winters creek (above) a small low biomass stream

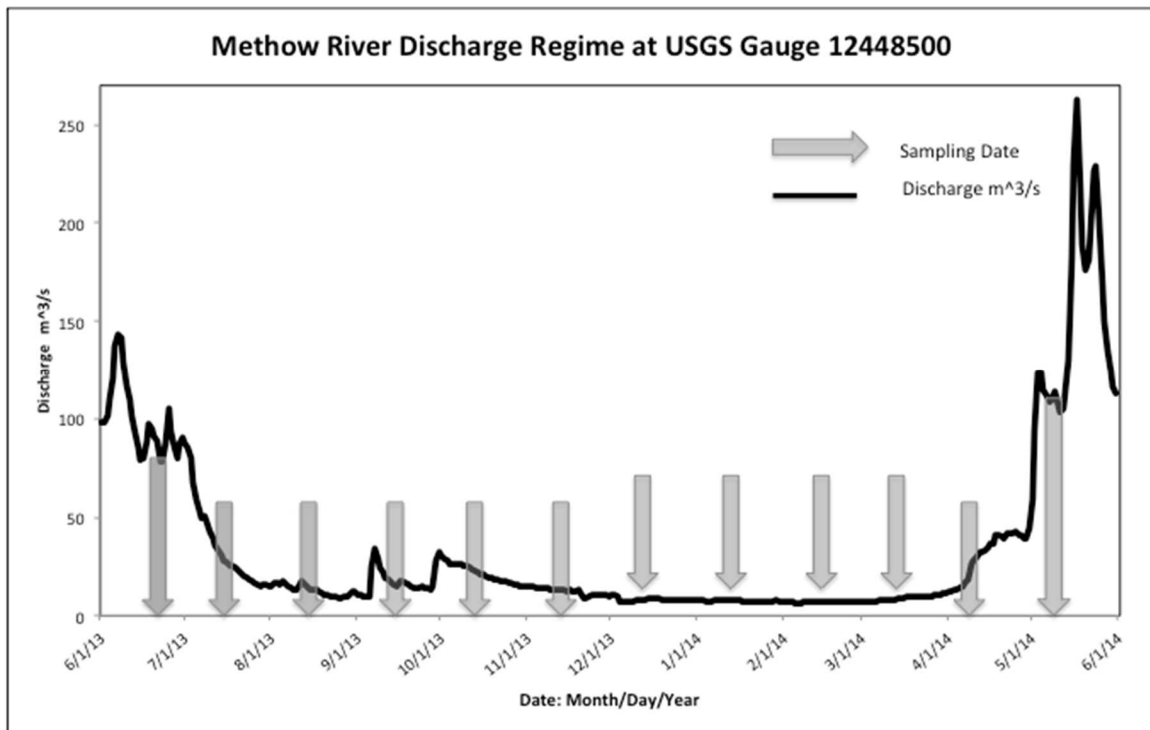


Figure 7: Sampling periods and mainstem Methow Discharge

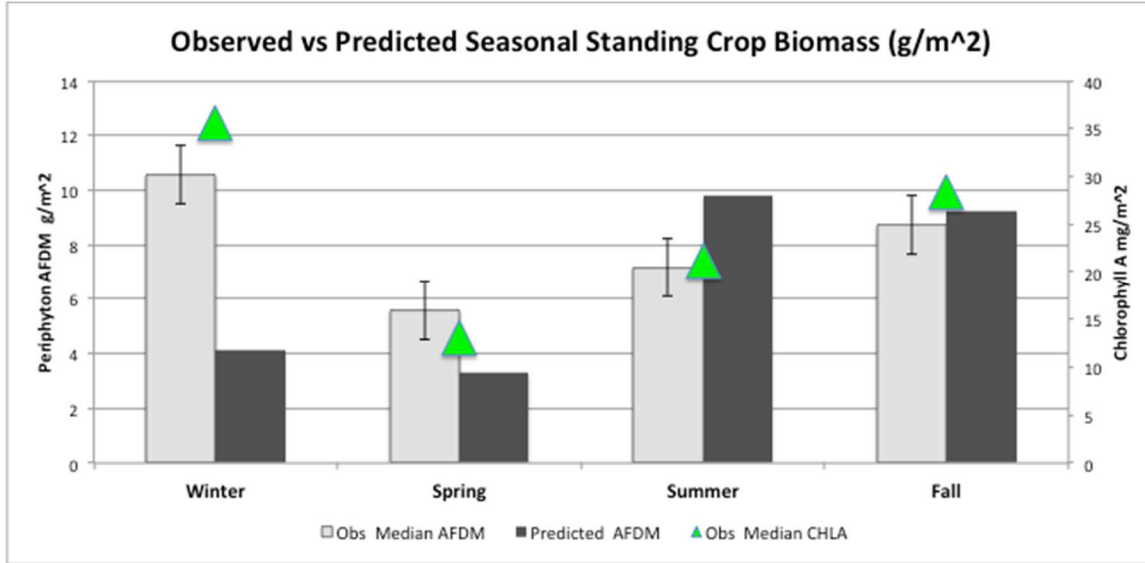


Figure 8: Field collected standing crop AFDM compared to Mechanistically Predicted AFDM and Chl-a by season. Model performance is best in worst in winter (Jan, Feb, Mar), and best in fall (Oct, Nov, Dec). Seasons were adjusted to group May and June together, when the seasonal high flows and annual disturbance occurs.

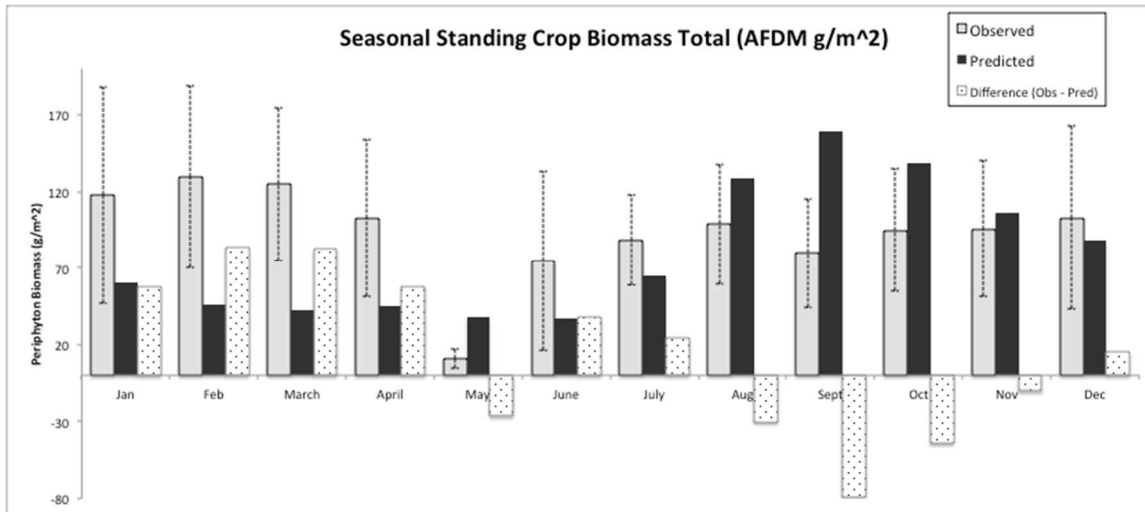


Figure 9: Field collected standing crop AFDM compared to mechanistically predicted AFDM over one year. The difference between the observed and predicted values is high in the early spring, but decreases through the summer and increases again in the fall. This pattern indicates model predictions are best in the summer and not as accurate in the early spring and early fall. The model was most accurate in November and December (fall).

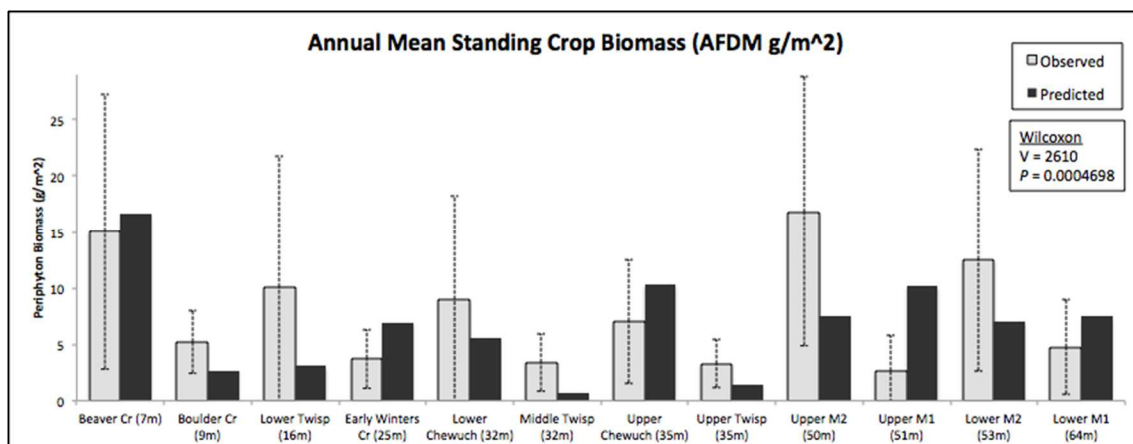


Figure 10: Site-wise comparison of field collected observed versus AFDM biomass predicted by the mechanistic ATP model.

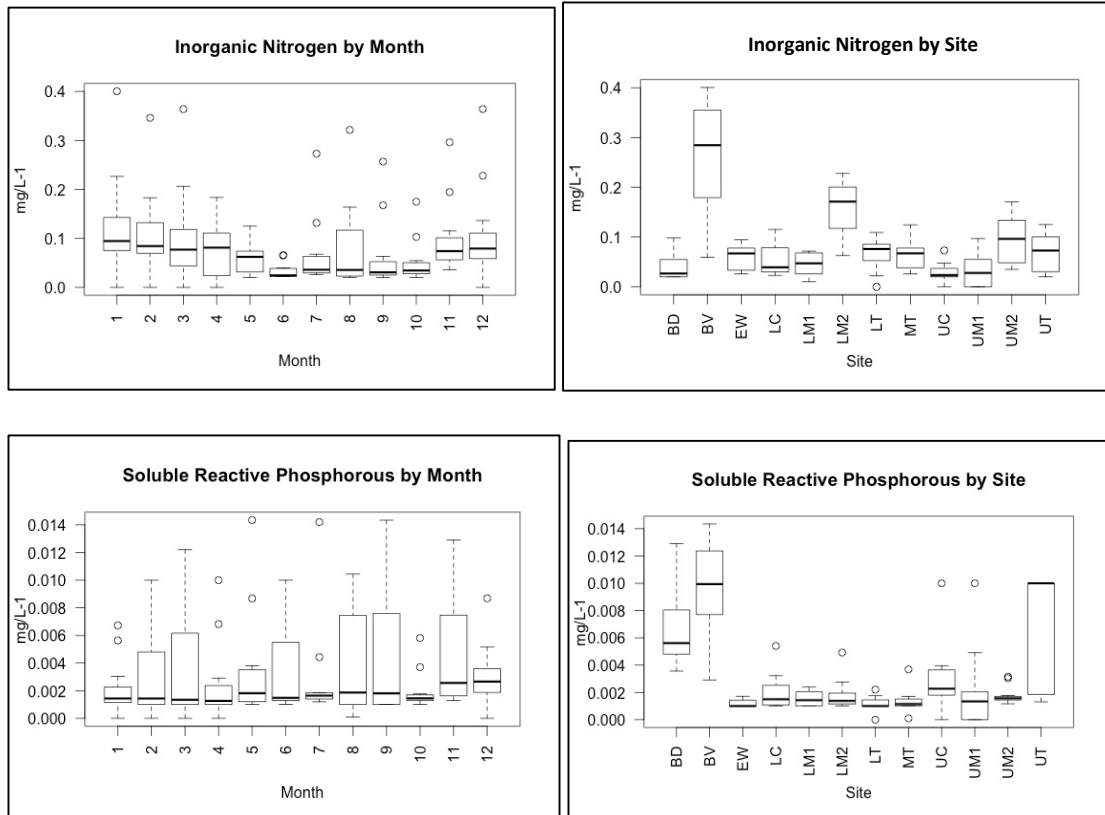


Figure 11: Variation in nutrient levels shown by month and by site, the general pattern is higher N levels in winter. In the site comparison, BV is a consistent outlier due to adjacent

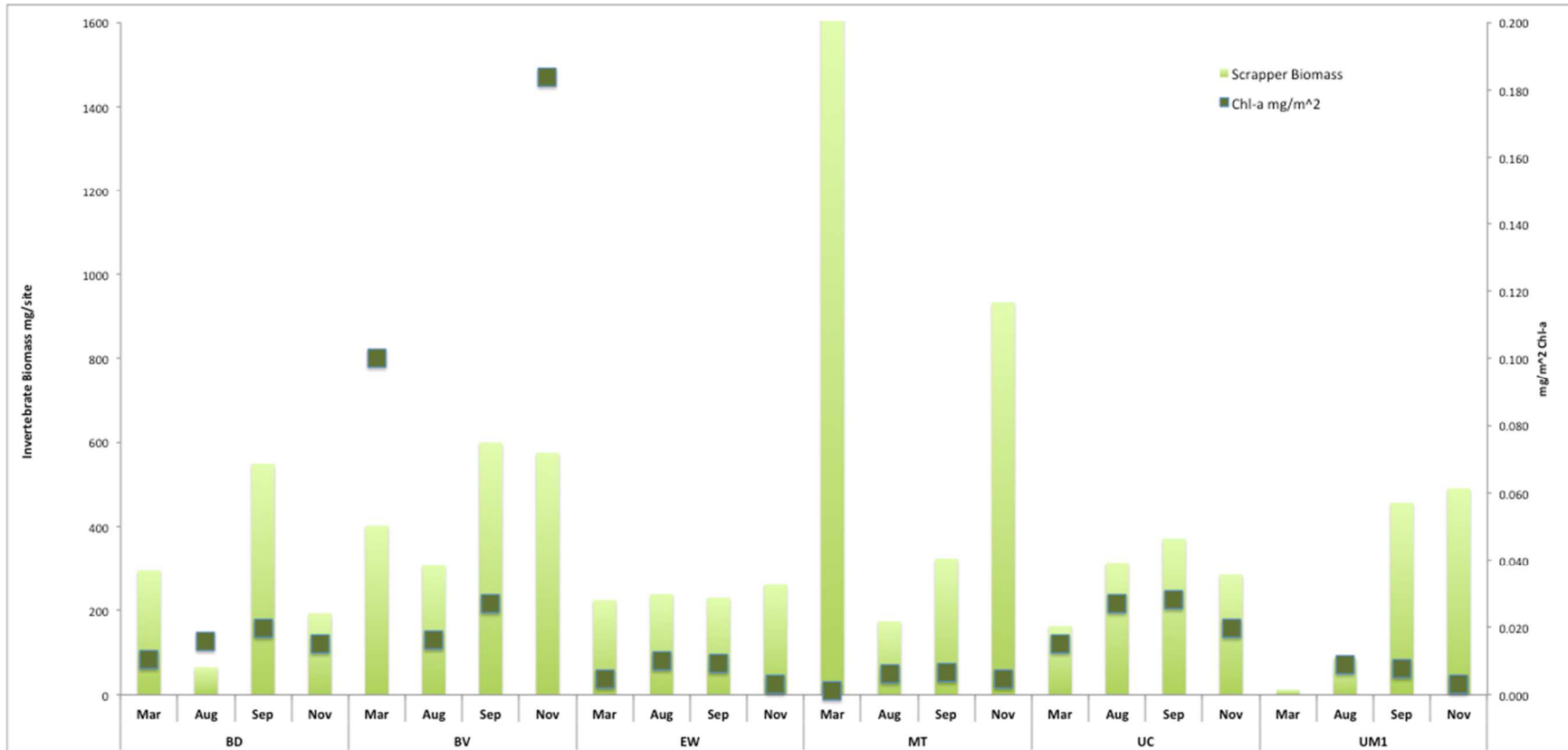


Figure 12: Biomass of invertebrates classified as part of the functional feeding group scappers at all sample sites over all dates in comparison with Chlorophyll-a values. The site with the highest invertebrate biomass (Middle Twisp) consistently had the lowest AFDM and Chl-a biomass in empirical samples. This graph indicates efficiency of invertebrates at MT.

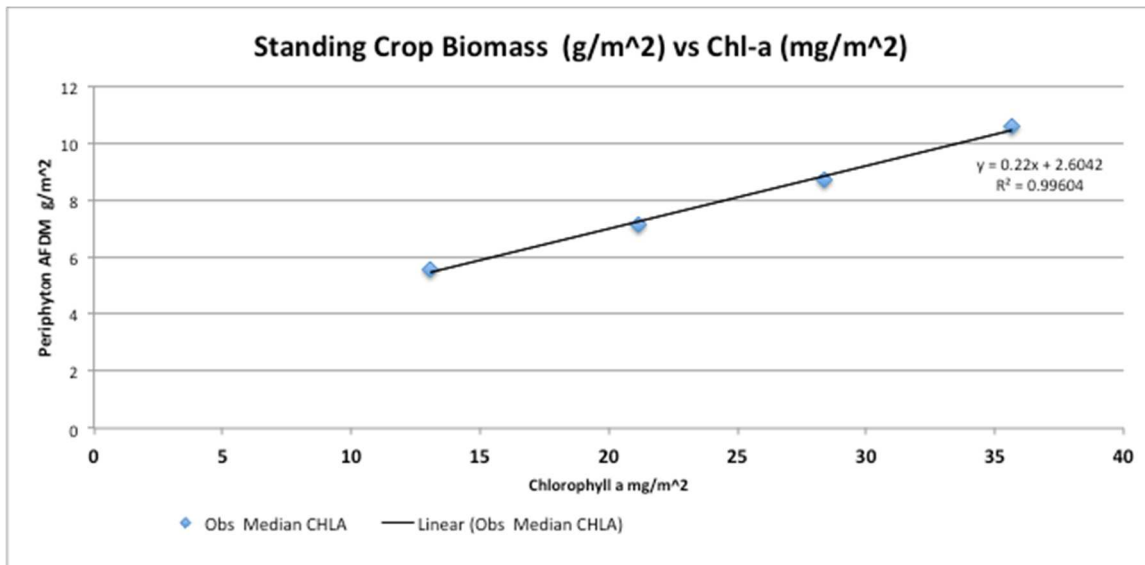


Figure 13: There was a strong correlation between biomass and chlorophyll a. I used AFDM and Chl-a in simple linear regression evaluations and AFDM only in the multiple linear regression evaluations by season due to this strong correlation. Multiple R^2 : 0.7103, F-statistic: 306.4 on 1 and 125 DF, p-value: $< 2.2e-16$

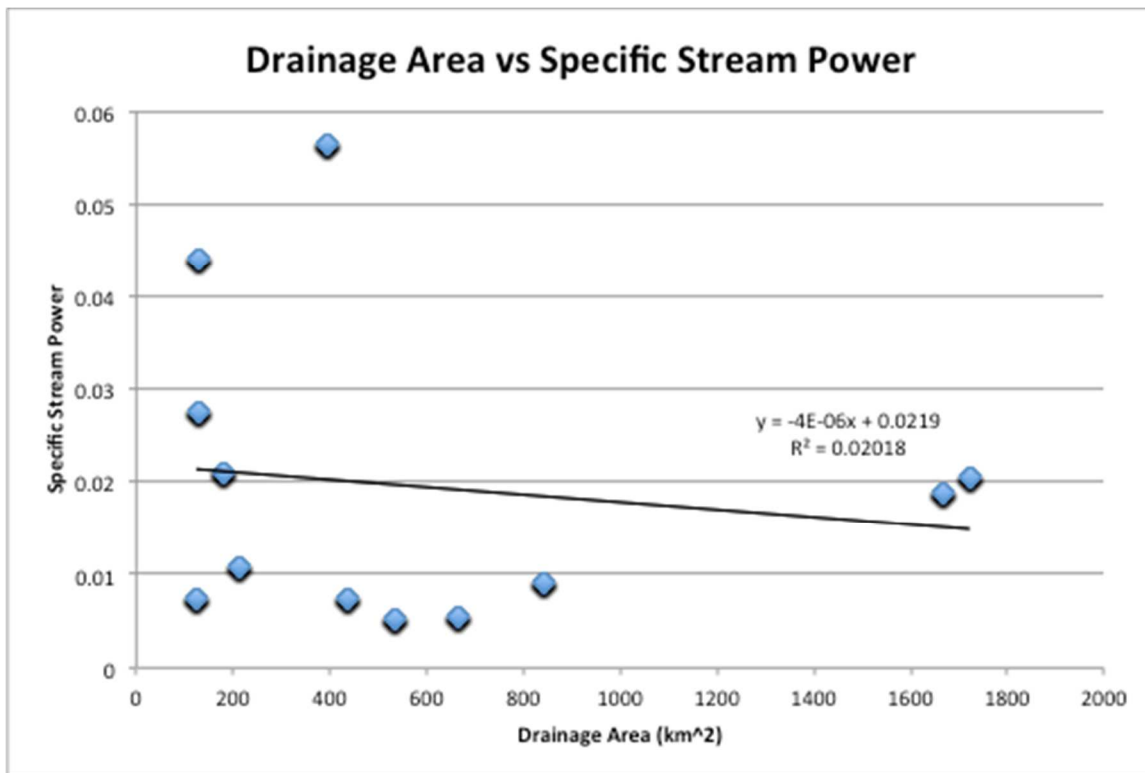


Figure 14: Showing the non inear relationship between Drainage Area and Stream Power. The RCC predicts stream power will peak in mid-size streams, which was observed in this data. ((Label these points with the site name?))

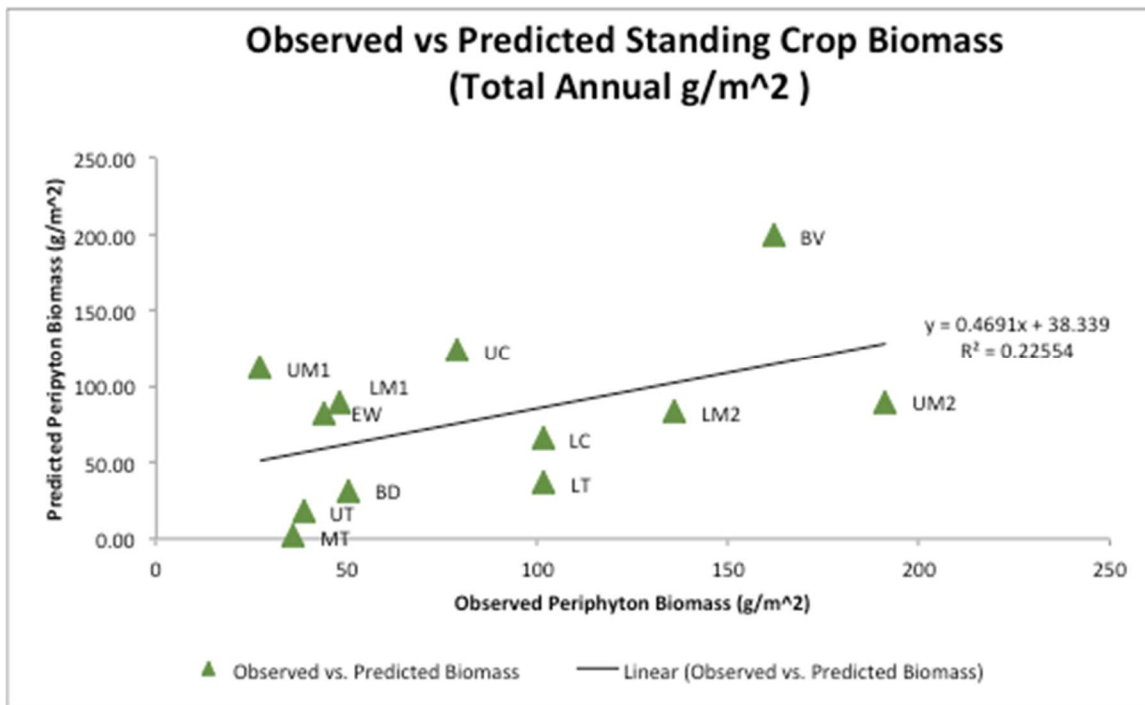


Figure 15: Observed vs Predicted Biomass values, correlation = 0.475

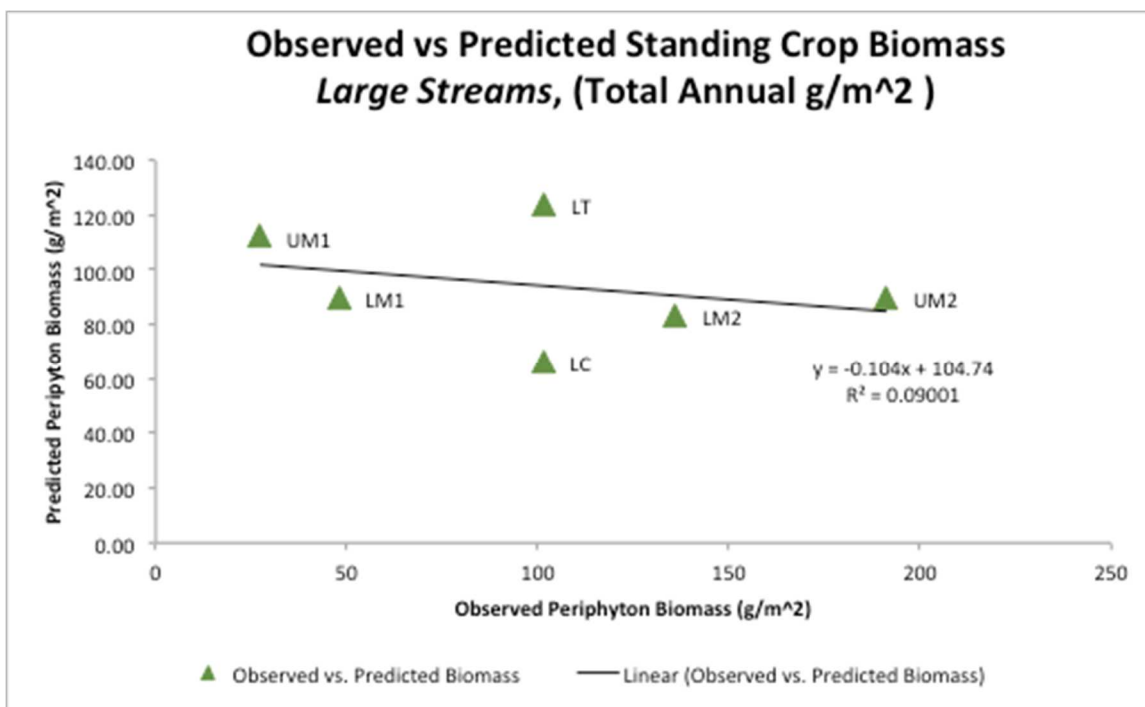
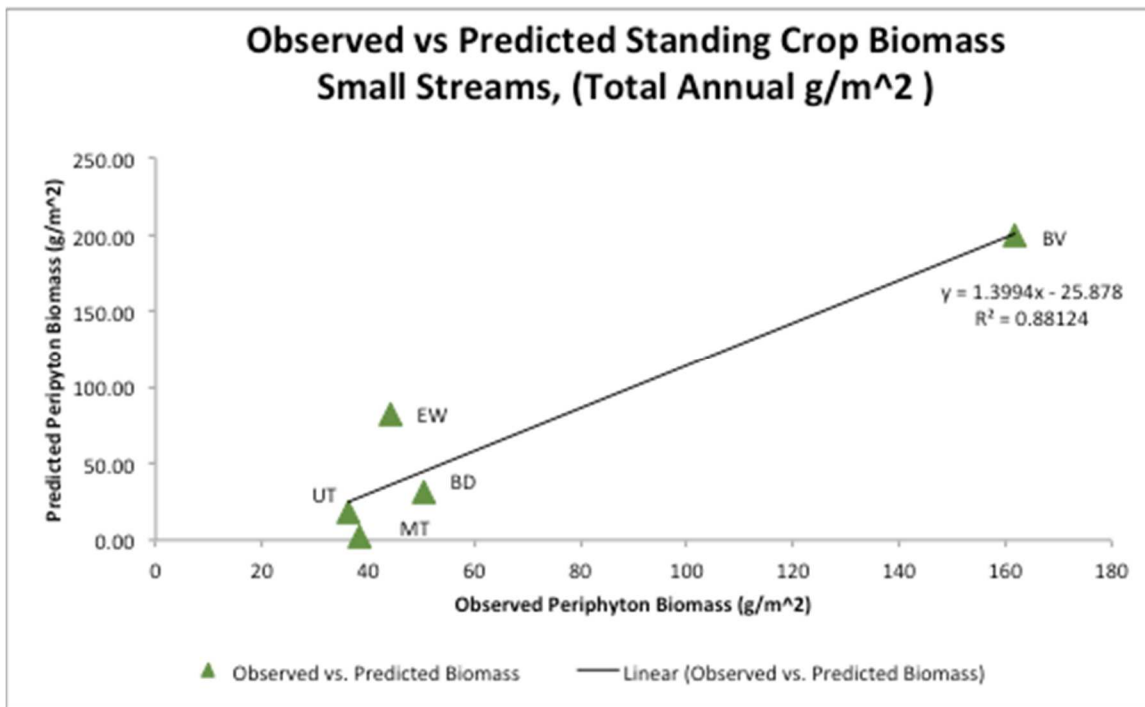


Figure 16: Comparison between model accuracy at small streams vs large streams.

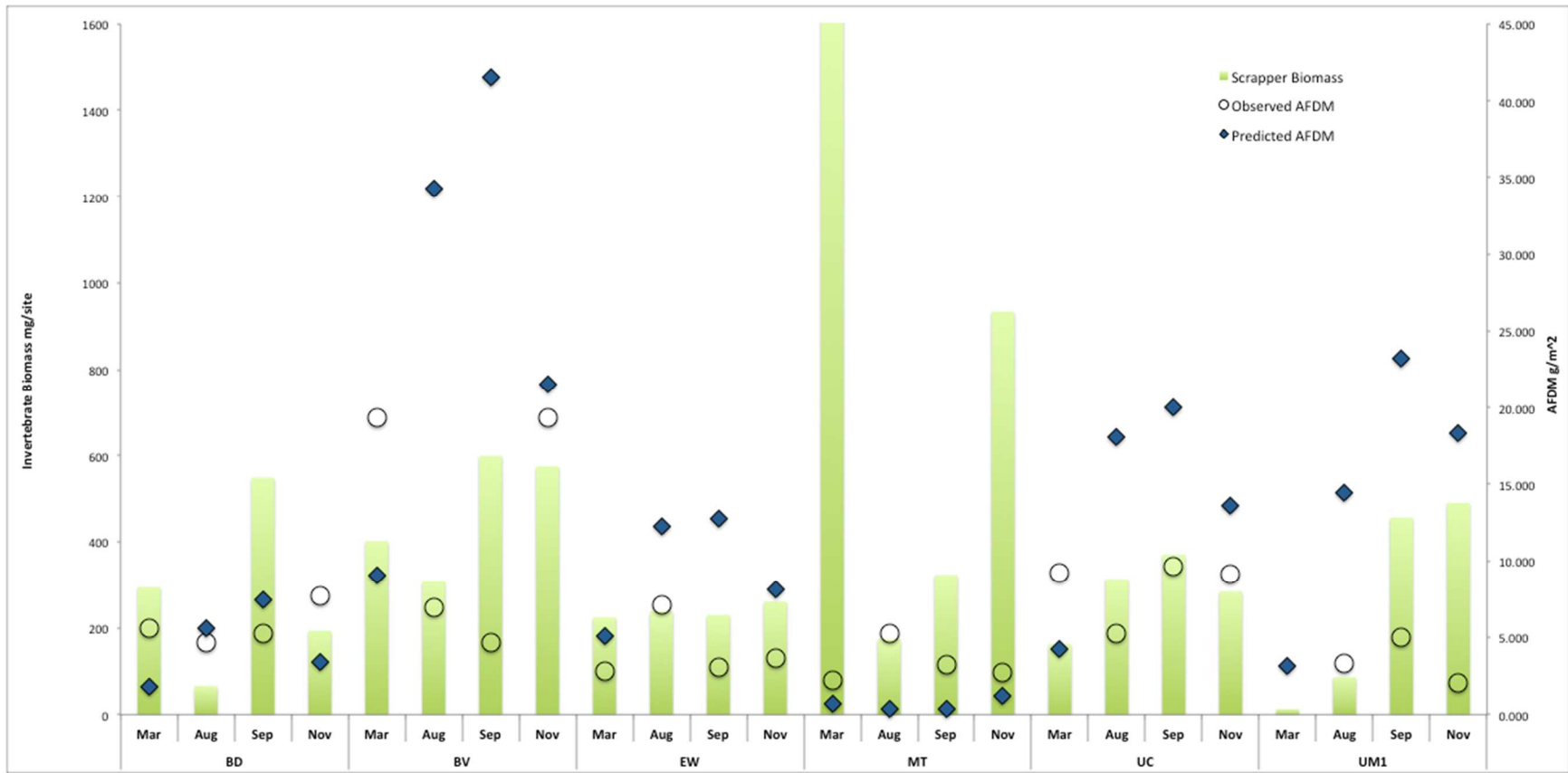


Figure 17: Frequently, but not always, the mechanism-based model (diamonds) over predicts periphyton biomass compared to observed biomass (circles). Invertebrate consumption can help explain this over prediction. Though not all feeding types directly consume biomass, all invertebrates benefit from higher biomass (though filtering consumption or as predators feeding on direct consumers). This important finding demonstrates model the needs to be calibrated using modifiers that account for the affect of grazing.

APPENDIX A: RAW DATA

1. AFDM & Chlorophyll-a
 - a. Seasonal dataset (with environmental variables by season)
 - b. Full dataset
2. Model input data sheet
3. Riparian data
4. Invertebrate data

Table 11: Response and Independent Variable means by Season

Site	Season	MedObs				Solar	Temp C	Q
		AFDM g/m ²	MedObs CHLAmg	N mg/L	P mg/L			
BD	Winter	4.68	10.18	0.0770	0.0084	10	2.0	1.09
BD	Spring	2.87	4.97	0.0210	0.0070	70	7.7	1.83
BD	Summer	4.28	13.26	0.0235	0.0044	62	14.2	0.66
BD	Fall	6.86	12.20	0.0370	0.0073	6	3.0	0.99
BV	Winter	19.84	118.98	0.3701	0.0089	62	1.2	0.29
BV	Spring	9.81	39.74	0.1029	0.0089	75	6.5	2.24
BV	Summer	6.44	33.77	0.2838	0.0130	73	13.9	0.43
BV	Fall	17.84	127.65	0.2783	0.0083	62	2.0	0.30
EW	Winter	3.04	5.61	0.0848	0.0013	27	1.0	0.72
EW	Spring	2.90	5.11	0.0535	0.0010	67	5.5	10.24
EW	Summer	4.36	8.57	0.0317	0.0011	61	11.1	2.19
EW	Fall	4.86	5.80	0.0639	0.0014	20	2.2	0.57
LC	Winter	13.09	29.25	0.0929	0.0014	42	1.8	2.53
LC	Spring	5.61	9.53	0.0303	0.0034	84	10.2	44.83
LC	Summer	8.87	22.17	0.0354	0.0015	81	15.3	7.47
LC	Fall	11.38	20.73	0.0612	0.0018	34	3.1	2.80
LM1	Winter	4.40	6.90	0.0511	0.0012	68	4.6	8.54
LM1	Spring	2.38	3.20	0.0528	0.0014	98	6.8	101.54
LM1	Summer	4.82	8.62	0.0284	0.0020	97	11.9	20.69
LM1	Fall	5.15	8.88	0.0524	0.0018	58	4.8	7.85
LM2	Winter	14.30	44.64	0.2053	0.0016	85	3.9	13.80
LM2	Spring	9.39	15.91	0.1008	0.0012	86	8.8	118.23
LM2	Summer	9.69	21.02	0.1544	0.0012	87	13.7	30.73
LM2	Fall	15.09	53.82	0.1752	0.0031	88	4.2	14.23
LT	Winter	13.37	13.36	0.0888	0.0010	41	1.5	2.41
LT	Spring	14.31	17.66	0.0317	0.0008	86	7.0	19.79
LT	Summer	8.62	30.35	0.0772	0.0012	81	13.3	4.50
LT	Fall	10.25	15.59	0.0708	0.0017	34	4.0	2.86
MT	Winter	2.47	3.83	0.0745	0.0013	36	1.8	1.23
MT	Spring	1.94	2.50	0.0637	0.0010	81	5.8	15.57
MT	Summer	4.02	5.01	0.0656	0.0009	78	11.8	3.43
MT	Fall	3.61	5.18	0.0499	0.0022	26	3.3	1.03
UC	Winter	11.60	15.91	0.0354	0.0012	50	1.2	5.73
UC	Spring	3.28	3.07	0.0224	0.0026	71	7.9	6.23
UC	Summer	7.37	21.25	0.0222	0.0053	69	14.6	1.46
UC	Fall	9.02	25.42	0.0364	0.0028	47	2.5	1.02
UM1	Winter		0.00	0.0000	0.0000	61	3.4	1.44
UM1	Spring	3.34	1.87	0.0695	0.0015	80	6.4	52.64
UM1	Summer	4.37	6.61	0.0288	0.0054	79	11.5	13.99
UM1	Fall	3.72	3.74	0.0364	0.0012	58	3.2	3.79
UM2	Winter	28.03	114.57	0.1529	0.0021	79	3.7	12.36
UM2	Spring	7.18	11.17	0.0586	0.0017	92	8.2	104.10
UM2	Summer	20.56	75.10	0.0665	0.0014	92	13.8	21.95
UM2	Fall	12.50	25.97	0.1022	0.0020	76	4.5	11.90
UT	Winter	2.84	5.39	0.0949	0.0071	49	10.1	0.93
UT	Spring	5.01	2.90	0.0891	0.0073	80	4.1	3.78
UT	Summer	2.70	8.36	0.0270	0.0073	79	1.9	1.81
UT	Fall	3.95	7.30	0.0613	0.0046	43	5.3	1.24

Table 12: Periphyton data set, 12 sites, 12 months. Note: columns are labeled on the first page only.

Site	Month	Rep	Dry Mass + filter (g) + crucible	ASHED DM + filter + crucible	Final AFDM (g)	Sample Rock Planer area (cm ²)	Corrected Area for subsample fraction (m ²)	Biomass (g/m ²)	CHLA mg/m ²	CHLA g/m ²	Autotrophic Index (AI) AFDM/Chl-a
BD	1	1	1.4005	1.3974	0.0062	189.624	0.00104	5.945	16.216	0.01622	366.61
BD	1	2	1.3863	1.3842	0.0042	136.156	0.00129	3.247	7.898	0.00790	411.13
BD	1	3	1.3856	1.3834	0.0044	115.354	0.00127	3.468	8.430	0.00843	411.33
BD	1	4	1.3754	1.3741	0.0026	55.356	0.00066	3.914	14.973	0.01497	261.41
BD	1	5	1.3784	1.3752	0.0064	263.406	0.00158	4.050	8.041	0.00804	503.60
BD	2	1	1.3954	1.3944	0.002	107.754	0.00075	2.652	13.363	0.01336	198.42
BD	2	2	1.3977	1.3948	0.0058	203.26	0.00136	4.280	10.659	0.01066	401.56
BD	2	3	1.3891	1.3849	0.0084	198.543	0.00132	6.346	11.674	0.01167	543.62
BD	2	4	1.3829	1.3805	0.0048	84.902	0.00061	7.915	14.905	0.01491	531.03
BD	2	5	1.3843	1.3819	0.0048	147.986	0.00106	4.541	11.511	0.01151	394.49
BD	3	1	1.4014	1.3981	0.0066	119.304	0.00085	7.745	17.960	0.01796	431.23
BD	3	2	1.3928	1.3901	0.0054	207.215	0.00166	3.257	6.440	0.00644	505.83
BD	3	3	1.3827	1.3804	0.0046	146.228	0.00083	5.577	10.437	0.01044	534.31
BD	3	4	1.3815	1.3787	0.0056	198.517	0.00155	3.614	8.574	0.00857	421.53
BD	3	5	1.3796	1.3771	0.005	118.444	0.00071	7.036	12.640	0.01264	556.61
BD	4	1	1.3965	1.3942	0.0046	186.144	0.00121	3.802	7.440	0.00744	510.98
BD	4	2	1.4138	1.4075	0.0126	153.687	0.00108	11.712	8.110	0.00811	1444.21
BD	4	3	1.3876	1.3858	0.0036	154.147	0.00108	3.336	6.404	0.00640	520.99
BD	4	4	1.3776	1.3752	0.0048	132.79	0.00093	5.164	5.820	0.00582	887.25
BD	4	5	1.3781	1.3765	0.0032	176.764	0.00124	2.586	4.787	0.00479	540.23
BD	5	1	2.6674	2.6647	0.0054	230.178	0.00184	2.933	13.251	0.01325	221.31
BD	5	2	2.6571	2.6547	0.0048	176.457	0.00194	2.473	6.915	0.00692	357.62
BD	5	3	2.685	2.6813	0.0074	129.441	0.00129	5.717	9.439	0.00944	605.67
BD	5	4	2.7168	2.7148	0.004	163.208	0.00196	2.042	3.720	0.00372	549.03
BD	5	5	2.6226	2.6206	0.004	85.593	0.00090	4.451	5.941	0.00594	749.16
BD	6	1	2.581	2.58	0.002	90.143	0.00113	1.775	1.581	0.00158	1122.56
BD	6	2	2.616	2.612	0.008	176.814	0.00265	3.016	0.262	0.00026	11532.70
BD	6	3	2.633	2.629	0.008	249.839	0.00200	4.003	6.020	0.00602	664.90
BD	6	4	2.607	2.605	0.004	223.532	0.00212	1.884	2.558	0.00256	736.24

BD	6	5	2.616	2.615	0.002	211.605	0.00233	0.859	1.390	0.00139	618.22
BD	7	1	1.401	1.399	0.004	226.913	0.00136	2.938	5.306	0.00531	553.76
BD	7	2	1.383	1.38	0.006	123.319	0.00092	6.487	4.842	0.00484	1339.86
BD	7	3	1.371	1.37	0.002	147.49	0.00125	1.595	4.399	0.00440	362.63
BD	7	4	1.371	1.368	0.006	167.233	0.00184	3.262	2.946	0.00295	1107.02
BD	7	5	1.371	1.368	0.006	195.788	0.00215	2.786	2.446	0.00245	1139.15
BD	8	1	1.419	1.414	0.01	213.481	0.00136	7.345	17.981	0.01798	408.48
BD	8	2	1.392	1.39	0.004	160.367	0.00092	4.325	11.966	0.01197	361.43
BD	8	3	1.397	1.392	0.01	158.124	0.00125	7.977	15.674	0.01567	508.91
BD	8	4	1.381	1.377	0.008	235.239	0.00184	4.349	11.516	0.01152	377.64
BD	8	5	1.391	1.386	0.01	232.455	0.00215	4.643	24.056	0.02406	193.02
BD	9	1	1.397	1.395	0.004	112.677	0.00079	5.071	21.908	0.02191	231.49
BD	9	2	1.39	1.386	0.008	160.014	0.00136	5.882	19.706	0.01971	298.48
BD	9	3	1.381	1.378	0.006	113.804	0.00097	6.203	11.208	0.01121	553.43
BD	9	4	1.378	1.376	0.004	112.587	0.00107	3.740	21.583	0.02158	173.27
BD	9	5	1.375	1.373	0.004	94.943	0.00076	5.266	8.967	0.00897	587.27
BD	10	1	1.395	1.391	0.008	163.944	0.00082	9.759	13.375	0.01338	729.67
BD	10	2	1.395	1.391	0.008	299.85	0.00225	3.557	6.039	0.00604	589.03
BD	10	3	1.4	1.393	0.014	247.027	0.00111	12.594	47.956	0.04796	262.62
BD	10	4	1.385	1.38	0.01	302.01	0.00166	6.020	10.296	0.01030	584.71
BD	10	5	1.383	1.379	0.008	195.53	0.00137	5.845	14.165	0.01417	412.62
BD	11	1	1.402	1.399	0.006	244.738	0.00208	2.884	8.197	0.00820	351.88
BD	11	2	1.398	1.394	0.008	189.142	0.00170	4.700	0.000	0.00000	0.00
BD	11	3	1.426	1.419	0.014	202.043	0.00182	7.699	18.544	0.01854	415.18
BD	11	4	1.382	1.375	0.014	154.086	0.00116	12.114	21.399	0.02140	566.13
BD	11	5	1.411	1.403	0.016	204.814	0.00164	9.765	14.978	0.01498	651.96
BD	12	1	1.396	1.392	0.008	172.625	0.00164	4.878	8.235	0.00823	592.39
BD	12	2	1.385	1.383	0.004	142.159	0.00142	2.814	4.890	0.00489	575.41
BD	12	3	1.384	1.379	0.01	94.101	0.00080	12.502	9.954	0.00995	1256.02
BD	12	4	1.374	1.37	0.008	87.38	0.00087	9.155	7.572	0.00757	1209.08
BD	12	5	1.378	1.374	0.008	145.499	0.00116	6.873	10.336	0.01034	664.92
BV	1	1	1.4024	1.3985	0.0078	148.166	0.00086	9.111	48.264	0.04826	188.78
BV	1	2	1.3926	1.3889	0.0074	110.647	0.00044	16.720	112.390	0.11239	148.77
BV	1	3	1.3921	1.3903	0.0036	108.026	0.00039	9.164	72.372	0.07237	126.63
BV	1	4	1.407	1.4001	0.0138	188.773	0.00051	26.805	282.336	0.28234	94.94
BV	1	5	1.3992	1.3946	0.0092	95.346	0.00014	64.327	546.094	0.54609	117.79

BV	2	1	1.3906	1.3818	0.0176	170.402	0.00111	15.890	144.588	0.14459	109.90
BV	2	2	1.4098	1.3996	0.0204	133.62	0.00087	23.488	191.443	0.19144	122.69
BV	2	3	1.4455	1.4307	0.0296	105.765	0.00079	37.315	218.111	0.21811	171.08
BV	2	4	1.4211	1.4121	0.018	167.801	0.00109	16.503	119.430	0.11943	138.18
BV	2	5	1.4428	1.4288	0.028	183.285	0.00110	25.461	136.456	0.13646	186.59
BV	3	1	1.402	1.3951	0.0138	140.277	0.00091	15.135	63.326	0.06333	239.00
BV	3	2	1.4137	1.4053	0.0168	134.983	0.00108	15.558	101.758	0.10176	152.89
BV	3	3	1.4151	1.4048	0.0206	144.828	0.00087	23.706	99.958	0.09996	237.16
BV	3	4	1.4126	1.4046	0.016	138.063	0.00083	19.315	84.479	0.08448	228.63
BV	3	5	1.4025	1.3957	0.0136	166.775	0.00067	20.387	120.502	0.12050	169.18
BV	4	1	1.4009	1.3958	0.0102	171.608	0.00056	18.256	68.980	0.06898	264.65
BV	4	2	1.3992	1.3959	0.0066	113.784	0.00035	18.644	78.876	0.07888	236.37
BV	4	3	1.4421	1.4311	0.022	154.004	0.00066	33.116	114.218	0.11422	289.94
BV	4	4	1.4021	1.3981	0.008	148.195	0.00052	15.520	49.075	0.04908	316.25
BV	4	5	1.3996	1.3942	0.0108	167.622	0.00061	17.718	57.729	0.05773	306.92
BV	5	1	2.644	2.6392	0.0096	130.55	0.00098	9.805	17.865	0.01787	548.82
BV	5	2	2.5828	2.5815	0.0026	180.916	0.00181	1.437	3.548	0.00355	405.05
BV	5	3	2.7046	2.6972	0.0148	221.365	0.00166	8.914	21.166	0.02117	421.17
BV	5	4	2.6246	2.6223	0.0046	192.669	0.00145	3.183	26.515	0.02652	120.06
BV	5	5	2.5784	2.5767	0.0034	118.275	0.00112	3.026	12.494	0.01249	242.19
BV	6	1	2.647	2.642	0.01	186.93	0.00122	8.230	23.247	0.02325	354.03
BV	6	2	2.638	2.634	0.008	199.897	0.00100	8.004	34.284	0.03428	233.46
BV	6	3	2.638	2.631	0.014	234.234	0.00176	7.969	32.386	0.03239	246.07
BV	6	4	2.605	2.604	0.002	216.078	0.00130	1.543	28.902	0.02890	53.38
BV	6	5	2.613	2.608	0.01	188.022	0.00122	8.182	38.816	0.03882	210.80
BV	7	1	1.416	1.412	0.008	119.241	0.00072	11.182	71.128	0.07113	157.21
BV	7	2	1.39	1.386	0.008	138.236	0.00104	7.716	41.085	0.04108	187.81
BV	7	3	1.405	1.399	0.012	179.957	0.00144	8.335	58.575	0.05857	142.30
BV	7	4	1.392	1.388	0.008	199.935	0.00180	4.446	20.927	0.02093	212.44
BV	7	5	1.406	1.399	0.014	211.22	0.00201	6.977	58.261	0.05826	119.75
BV	8	1	1.395	1.392	0.006	72.387	0.00072	8.386	19.913	0.01991	421.16
BV	8	2	1.391	1.387	0.008	202.558	0.00104	7.716	16.216	0.01622	475.84
BV	8	3	1.394	1.391	0.006	130.303	0.00144	4.168	14.158	0.01416	294.38
BV	8	4	1.405	1.401	0.008	131.577	0.00180	4.446	-3.842	-0.00384	-1157.26
BV	8	5	1.415	1.408	0.014	168.642	0.00201	6.977	69.543	0.06954	100.33

BV	9	1	1.414	1.408	0.012	111.681	0.00084	14.327	67.063	0.06706	213.63
BV	9	2	1.405	1.401	0.008	91.51	0.00078	10.285	58.398	0.05840	176.12
BV	9	3	1.394	1.392	0.004	120.404	0.00114	3.497	26.840	0.02684	130.29
BV	9	4	1.407	1.403	0.008	173.103	0.00173	4.622	24.358	0.02436	189.73
BV	9	5	1.397	1.393	0.008	205.791	0.00257	3.110	8.791	0.00879	353.77
BV	10	1	1.403	1.398	0.01	265.756	0.00159	6.271	42.270	0.04227	148.37
BV	10	2	1.401	1.397	0.008	190.245	0.00114	7.009	53.237	0.05324	131.65
BV	10	3	1.408	1.401	0.014	178.877	0.00107	13.044	70.601	0.07060	184.76
BV	10	4	1.418	1.412	0.012	215.315	0.00140	8.574	70.974	0.07097	120.81
BV	10	5	1.406	1.402	0.008	195.857	0.00147	5.446	35.016	0.03502	155.53
BV	11	1	1.397	1.392	0.01	115.032	0.00052	19.318	183.758	0.18376	105.13
BV	11	2	1.405	1.401	0.008	147.807	0.00074	10.825	128.013	0.12801	84.56
BV	11	3	1.419	1.412	0.014	104.115	0.00068	20.687	188.705	0.18870	109.63
BV	11	4	1.403	1.397	0.012	142.697	0.00071	16.819	174.787	0.17479	96.22
BV	11	5	1.407	1.398	0.018	242.527	0.00061	29.687	258.836	0.25884	114.70
BV	12	1	1.413	1.401	0.024	102.629	0.00041	58.463	511.408	0.51141	114.32
BV	12	2	1.404	1.394	0.02	89.483	0.00058	34.386	58.011	0.05801	592.74
BV	12	3	1.409	1.402	0.014	209.035	0.00105	13.395	55.449	0.05545	241.57
BV	12	4	1.426	1.418	0.016	143.349	0.00072	22.323	197.468	0.19747	113.05
BV	12	5	1.416	1.402	0.028	205.845	0.00103	27.205	145.962	0.14596	186.38
EW	1	1	1.3876	1.3842	0.0068	213.076	0.00205	3.324	7.263	0.00726	457.69
EW	1	2	1.3805	1.3777	0.0056	113.218	0.00134	4.185	12.566	0.01257	333.07
EW	1	3	1.3867	1.3822	0.009	133.312	0.00182	4.951	16.841	0.01684	293.98
EW	1	4	1.3859	1.3843	0.0032	270.394	0.00212	1.506	4.553	0.00455	330.79
EW	1	5	1.3907	1.3893	0.0028	152.612	0.00084	3.336	8.228	0.00823	405.42
EW	2	1	1.3754	1.3743	0.0022	91.578	0.00073	3.003	2.487	0.00249	1207.44
EW	2	2	1.3918	1.3899	0.0038	208.921	0.00188	2.021	3.759	0.00376	537.63
EW	2	3	1.3892	1.386	0.0064	169.836	0.00116	5.542	10.938	0.01094	506.64
EW	2	4	1.3728	1.3712	0.0032	134.61	0.00092	3.481	3.903	0.00390	891.87
EW	2	5	1.3769	1.3755	0.0028	181.231	0.00136	2.060	4.803	0.00480	428.90
EW	3	1	1.3823	1.3807	0.0032	165.07	0.00115	2.787	3.892	0.00389	715.94
EW	3	2	1.3771	1.3765	0.0012	108.705	0.00065	1.840	1.611	0.00161	1142.25
EW	3	3	1.3901	1.38881	0.0026	189.093	0.00153	1.685	4.690	0.00469	359.40
EW	3	4	1.3781	1.3758	0.0046	189.639	0.00121	3.812	8.747	0.00875	435.78
EW	3	5	1.3814	1.3789	0.005	140.646	0.00118	4.246	7.093	0.00709	598.69
EW	4	1	1.3741	1.3723	0.0036	165.996	0.00166	2.169	1.670	0.00167	1298.51

EW	4	2	1.3863	1.3831	0.0064	153.695	0.00154	4.164	5.991	0.00599	695.11
EW	4	3	1.3835	1.3826	0.0018	109.93	0.00110	1.637	1.390	0.00139	1178.10
EW	4	4	1.3931	1.3844	0.0174	236.18	0.00236	7.367	5.511	0.00551	1336.78
EW	4	5	1.3827	1.3801	0.0052	148.966	0.00149	3.491	2.777	0.00278	1257.00
EW	5	1	0	0	0	0	0.00000	0.000	0.000	0.00000	0.00
EW	5	2	0	0	0	0	0.00000	0.000	0.000	0.00000	0.00
EW	5	3	0	0	0	0	0.00000	0.000	0.000	0.00000	0.00
EW	5	4	0	0	0	0	0.00000	0.000	0.000	0.00000	0.00
EW	5	5	0	0	0	0	0.00000	0.000	0.000	0.00000	0.00
EW	6	1	2.705	2.704	0.002	251.581	0.00277	0.723	4.027	0.00403	179.46
EW	6	2	2.634	2.628	0.012	261.117	0.00209	5.745	30.675	0.03068	187.27
EW	6	3	2.714	2.712	0.004	267.083	0.00174	2.304	16.540	0.01654	139.30
EW	6	4	2.705	2.701	0.008	241.231	0.00181	4.422	12.547	0.01255	352.41
EW	6	5	2.623	2.622	0.002	125.219	0.00094	2.130	7.971	0.00797	267.16
EW	7	1	1.369	1.368	0.002	160.922	0.00113	1.775	5.997	0.00600	296.04
EW	7	2	1.376	1.375	0.002	128.387	0.00135	1.484	3.988	0.00399	372.00
EW	7	3	1.391	1.387	0.008	173.42	0.00139	5.766	18.597	0.01860	310.07
EW	7	4	1.374	1.371	0.006	226.73	0.00204	2.940	6.496	0.00650	452.63
EW	7	5	1.398	1.388	0.02	236.595	0.00154	13.005	26.043	0.02604	499.37
EW	8	1	1.379	1.375	0.008	179.905	0.00113	7.102	11.824	0.01182	600.66
EW	8	2	1.39	1.384	0.012	64.376	0.00135	8.902	37.911	0.03791	234.81
EW	8	3	1.397	1.391	0.012	275.257	0.00139	8.650	10.056	0.01006	860.17
EW	8	4	1.372	1.369	0.006	154.001	0.00204	2.940	6.259	0.00626	469.78
EW	8	5	1.383	1.381	0.004	230.025	0.00154	2.601	6.753	0.00675	385.16
EW	9	1	1.384	1.382	0.004	146.464	0.00132	3.034	6.293	0.00629	482.22
EW	9	2	1.394	1.392	0.004	197.076	0.00187	2.136	9.151	0.00915	233.47
EW	9	3	1.383	1.381	0.004	239.038	0.00215	1.859	4.794	0.00479	387.85
EW	9	4	1.379	1.376	0.006	137.222	0.00123	4.858	17.236	0.01724	281.88
EW	9	5	1.384	1.381	0.006	199.141	0.00184	3.257	11.249	0.01125	289.55
EW	10	1	1.381	1.377	0.008	256.77	0.00193	4.154	8.541	0.00854	486.38
EW	10	2	1.423	1.417	0.012	191.962	0.00154	7.814	14.513	0.01451	538.42
EW	10	3	1.394	1.389	0.01	249.853	0.00200	5.003	9.163	0.00916	546.01
EW	10	4	1.372	1.369	0.006	173.926	0.00148	4.059	5.006	0.00501	810.78
EW	10	5	1.376	1.373	0.006	346.933	0.00347	1.729	3.389	0.00339	510.30
EW	11	1	1.374	1.373	0.002	175.462	0.00132	1.520	3.320	0.00332	457.82
EW	11	2	1.382	1.379	0.006	164.755	0.00165	3.642	3.456	0.00346	1053.86

EW	11	3	1.417	1.412	0.01	243.456	0.00146	6.846	8.018	0.00802	853.86
EW	11	4	1.372	1.369	0.006	193.803	0.00155	3.870	3.034	0.00303	1275.64
EW	11	5	1.376	1.375	0.002	196.461	0.00196	1.018	1.093	0.00109	931.05
EW	12	1	1.384	1.382	0.004	190.832	0.00143	2.795	5.526	0.00553	505.71
EW	12	2	1.381	1.377	0.008	114.039	0.00103	7.795	5.965	0.00596	1306.74
EW	12	3	1.381	1.378	0.006	117.856	0.00088	6.788	5.812	0.00581	1168.01
EW	12	4	1.378	1.376	0.004	68.272	0.00075	5.326	2.818	0.00282	1890.04
EW	12	5	1.378	1.373	0.01	144.138	0.00115	8.672	5.456	0.00546	1589.37
LC	1	1	1.3962	1.3937	0.005	215.542	0.00108	4.639	-3.081	-0.00308	-1505.93
LC	1	2	1.3959	1.3911	0.0096	220.51	0.00055	17.414	65.228	0.06523	266.97
LC	1	3	1.3842	1.3829	0.0026	188.708	0.00132	1.968	4.721	0.00472	416.95
LC	1	4	1.3859	1.3849	0.002	170.214	0.00081	2.467	7.789	0.00779	316.78
LC	1	5	1.3757	1.3743	0.0028	128.476	0.00128	2.179	7.929	0.00793	274.87
LC	2	1	1.3989	1.3955	0.0068	87.435	0.00058	11.666	18.887	0.01889	617.66
LC	2	2	1.4293	1.4232	0.0122	165.146	0.00103	11.873	40.892	0.04089	290.34
LC	2	3	1.4005	1.3941	0.0128	293.318	0.00117	10.910	34.316	0.03432	317.92
LC	2	4	1.4358	1.4254	0.0208	150.446	0.00079	26.394	49.801	0.04980	529.99
LC	2	5	1.3769	1.3742	0.0054	139.406	0.00113	4.785	10.636	0.01064	449.89
LC	3	1	1.4459	1.4268	0.0382	288.495	0.00141	27.084	45.650	0.04565	593.31
LC	3	2	1.4117	1.4052	0.013	151.167	0.00078	16.585	38.227	0.03823	433.86
LC	3	3	1.3913	1.3875	0.0076	199.299	0.00127	5.992	11.627	0.01163	515.40
LC	3	4	1.4174	1.4042	0.0264	110.321	0.00053	49.570	67.965	0.06797	729.34
LC	3	5	1.4091	1.3991	0.02	135.188	0.00080	25.150	46.666	0.04667	538.94
LC	4	1	1.3971	1.3944	0.0054	151.877	0.00152	3.556	5.160	0.00516	689.06
LC	4	2	1.3907	1.3875	0.0064	218.496	0.00164	3.905	4.889	0.00489	798.85
LC	4	3	1.3902	1.3872	0.006	129.09	0.00129	4.648	5.655	0.00565	821.92
LC	4	4	1.4044	1.3953	0.0182	87.787	0.00079	23.036	56.026	0.05603	411.16
LC	4	5	1.3801	1.3771	0.006	100.102	0.00100	5.994	7.048	0.00705	850.47
LC	5	1	0	0	0	0	0.00000	0.000	0.000	0.00000	0.00
LC	5	2	0	0	0	0	0.00000	0.000	0.000	0.00000	0.00
LC	5	3	0	0	0	0	0.00000	0.000	0.000	0.00000	0.00
LC	5	4	0	0	0	0	0.00000	0.000	0.000	0.00000	0.00
LC	5	5	0	0	0	0	0.00000	0.000	0.000	0.00000	0.00
LC	6	1	2.627	2.624	0.006	140.301	0.00091	6.579	22.946	0.02295	286.73
LC	6	2	2.675	2.667	0.016	202.116	0.00152	10.555	20.520	0.02052	514.36

LC	6	3	2.707	2.701	0.012	266.045	0.00186	6.444	23.531	0.02353	273.84
LC	7	1	1.408	1.401	0.014	291.195	0.00160	8.741	36.180	0.03618	241.61
LC	7	2	1.392	1.386	0.012	227.36	0.00136	8.797	14.857	0.01486	592.10
LC	7	3	1.405	1.395	0.02	214.582	0.00118	16.946	44.552	0.04455	380.37
LC	7	4	1.429	1.416	0.026	276.55	0.00152	17.094	35.236	0.03524	485.12
LC	7	5	1.399	1.387	0.024	204.342	0.00112	21.355	34.842	0.03484	612.89
LC	8	1	1.396	1.392	0.008	132.48	0.00160	4.995	4.781	0.00478	1044.84
LC	8	2	1.392	1.39	0.004	177.391	0.00136	2.932	9.120	0.00912	321.52
LC	8	3	1.391	1.387	0.008	156.012	0.00118	6.779	11.885	0.01189	570.32
LC	8	4	1.395	1.392	0.006	222.831	0.00152	3.945	10.008	0.01001	394.14
LC	8	5	1.396	1.388	0.016	171.192	0.00112	14.236	35.358	0.03536	402.64
LC	9	1	1.389	1.387	0.004	106.994	0.00118	3.399	6.420	0.00642	529.41
LC	9	2	1.408	1.403	0.01	176.489	0.00185	5.396	21.823	0.02182	247.28
LC	9	3	1.39	1.387	0.006	140.731	0.00155	3.876	16.761	0.01676	231.25
LC	9	4	1.4	1.394	0.012	245.729	0.00172	6.976	33.768	0.03377	206.60
LC	9	5	1.373	1.371	0.004	114.512	0.00086	4.657	12.941	0.01294	359.90
LC	10	1	1.403	1.4	0.006	281.217	0.00169	3.556	19.783	0.01978	179.75
LC	10	2	1.389	1.386	0.006	178.706	0.00107	5.596	22.685	0.02269	246.67
LC	10	3	1.4	1.389	0.022	275.608	0.00165	13.304	41.804	0.04180	318.24
LC	10	4	1.397	1.386	0.022	263.128	0.00145	15.202	54.689	0.05469	277.97
LC	10	5	1.379	1.372	0.014	101.141	0.00061	23.070	78.800	0.07880	292.77
LC	11	1	1.391	1.389	0.004	194.635	0.00097	4.110	9.610	0.00961	427.72
LC	11	2	1.39	1.388	0.004	159.253	0.00135	2.955	11.479	0.01148	257.42
LC	11	3	1.392	1.385	0.014	223.308	0.00123	11.399	29.006	0.02901	392.98
LC	11	4	1.4	1.393	0.014	184.978	0.00148	9.461	20.379	0.02038	464.23
LC	11	5	1.387	1.379	0.016	169.095	0.00101	15.770	39.647	0.03965	397.76
LC	12	0	0	0	0	0	0.00000	0.000	0.000	0.00000	0.00
LC	12	0	0	0	0	0	0.00000	0.000	0.000	0.00000	0.00
LC	12	0	0	0	0	0	0.00000	0.000	0.000	0.00000	0.00
LC	12	0	0	0	0	0	0.00000	0.000	0.000	0.00000	0.00
LC	12	0	0	0	0	0	0.00000	0.000	0.000	0.00000	0.00
LM1	1	1	1.3834	1.3812	0.0044	206.562	0.00258	1.704	3.975	0.00397	428.74
LM1	1	2	1.381	1.3786	0.0048	182.409	0.00137	3.509	8.621	0.00862	406.98
LM1	1	3	1.3871	1.3841	0.006	149.051	0.00093	6.441	14.498	0.01450	444.24
LM1	1	4	1.3794	1.3772	0.0044	266.62	0.00071	6.189	11.942	0.01194	518.21
LM1	1	5	1.3871	1.3815	0.0112	276.153	0.00069	16.223	38.339	0.03834	423.15

LM1	2	1	1.3942	1.3917	0.005	162.463	0.00118	4.232	6.593	0.00659	641.85
LM1	2	2	1.3853	1.3838	0.003	236.677	0.00178	1.690	4.360	0.00436	387.63
LM1	2	3	1.3852	1.3831	0.0042	213.798	0.00139	3.012	4.617	0.00462	652.41
LM1	2	4	1.3936	1.3851	0.017	158.224	0.00096	17.769	26.310	0.02631	675.38
LM1	2	5	1.4081	1.3956	0.025	258.877	0.00124	20.119	18.631	0.01863	1079.86
LM1	3	1	1.3853	1.3843	0.002	260.595	0.00209	0.959	2.169	0.00217	442.37
LM1	3	2	1.3833	1.3801	0.0064	160.085	0.00167	3.831	3.135	0.00313	1222.16
LM1	3	3	1.3841	1.3826	0.003	210.786	0.00165	1.819	1.815	0.00182	1001.86
LM1	3	4	1.3778	1.3765	0.0026	125.302	0.00094	2.767	1.529	0.00153	1808.97
LM1	3	5	1.3893	1.3856	0.0074	156.538	0.00100	7.429	7.912	0.00791	938.91
LM1	4	1	1.3801	1.3788	0.0026	181.329	0.00136	1.912	2.393	0.00239	799.07
LM1	4	2	1.3847	1.3817	0.006	247.236	0.00185	3.236	1.751	0.00175	1848.25
LM1	4	3	1.3869	1.3849	0.004	182.895	0.00137	2.916	2.009	0.00201	1451.59
LM1	4	4	1.3862	1.3837	0.005	172.029	0.00129	3.875	3.244	0.00324	1194.45
LM1	4	5	1.3914	1.3882	0.0064	203.83	0.00153	4.186	1.618	0.00162	2587.74
LM1	5	1	0	0	0	0	0.00000	0.000	0.000	0.00000	0.00
LM1	5	2	0	0	0	0	0.00000	0.000	0.000	0.00000	0.00
LM1	5	3	0	0	0	0	0.00000	0.000	0.000	0.00000	0.00
LM1	5	4	0	0	0	0	0.00000	0.000	0.000	0.00000	0.00
LM1	5	5	0	0	0	0	0.00000	0.000	0.000	0.00000	0.00
LM1	6	1	2.636	2.635	0.002	265.628	0.00226	0.886	9.452	0.00945	93.72
LM1	6	2	2.617	2.616	0.002	198.961	0.00109	1.828	8.815	0.00881	207.34
LM1	6	3	2.653	2.652	0.002	161.385	0.00121	1.652	1.885	0.00189	876.55
LM1	6	4	2.641	2.64	0.002	187.519	0.00131	1.524	5.875	0.00587	259.35
LM1	6	5	2.668	2.667	0.002	215.706	0.00151	1.325	7.578	0.00758	174.79
LM1	7	1	1.377	1.376	0.002	178.398	0.00152	1.319	3.501	0.00350	376.69
LM1	7	2	1.377	1.375	0.004	129.91	0.00117	3.421	6.965	0.00696	491.23
LM1	7	3	1.381	1.378	0.006	132.549	0.00119	5.030	4.478	0.00448	1123.28
LM1	7	4	1.379	1.376	0.006	170.286	0.00153	3.915	5.172	0.00517	756.90
LM1	7	5	1.379	1.377	0.004	164.384	0.00164	2.433	7.554	0.00755	322.11
LM1	8	1	1.383	1.379	0.008	147.479	0.00152	5.276	10.875	0.01087	485.12
LM1	8	2	1.383	1.378	0.01	131.218	0.00117	8.553	8.789	0.00879	973.17
LM1	8	3	1.391	1.387	0.008	229.722	0.00119	6.706	6.493	0.00649	1032.86
LM1	8	4	1.381	1.377	0.008	189.161	0.00153	5.220	7.971	0.00797	654.89
LM1	8	5	1.385	1.381	0.008	134.386	0.00164	4.867	12.681	0.01268	383.78
LM1	9	1	1.385	1.382	0.006	115.488	0.00104	5.773	11.893	0.01189	485.36

LM1	9	2	1.383	1.38	0.006	154.451	0.00124	4.856	11.701	0.01170	415.00
LM1	9	3	1.394	1.389	0.01	199.618	0.00140	7.157	20.487	0.02049	349.32
LM1	9	4	1.398	1.395	0.006	172.168	0.00121	4.979	10.724	0.01072	464.24
LM1	9	5	1.398	1.394	0.008	84.19	0.00055	14.619	28.450	0.02845	513.85
LM1	10	1	1.39	1.388	0.004	149.777	0.00135	2.967	9.832	0.00983	301.80
LM1	10	2	1.387	1.385	0.004	178.585	0.00161	2.489	12.455	0.01245	199.82
LM1	10	3	1.393	1.39	0.006	236.555	0.00213	2.818	10.544	0.01054	267.29
LM1	10	4	1.389	1.386	0.006	353.103	0.00265	2.266	7.989	0.00799	283.58
LM1	10	5	1.388	1.384	0.008	248.29	0.00186	4.296	7.862	0.00786	546.41
LM1	11	1	1.382	1.378	0.008	227.537	0.00148	5.409	3.169	0.00317	1707.07
LM1	11	2	1.383	1.379	0.008	194.532	0.00146	5.483	5.735	0.00573	956.16
LM1	11	3	1.391	1.386	0.01	184.29	0.00111	9.044	12.415	0.01241	728.47
LM1	11	4	1.387	1.385	0.004	248.414	0.00161	2.477	9.448	0.00945	262.19
LM1	11	5	1.381	1.379	0.004	194.904	0.00107	3.731	8.819	0.00882	423.10
LM1	12	1	1.386	1.382	0.008	108.236	0.00114	7.039	22.717	0.02272	309.86
LM1	12	2	1.38	1.376	0.008	138.205	0.00111	7.236	7.978	0.00798	906.95
LM1	12	3	1.4	1.392	0.016	175.005	0.00140	11.428	6.492	0.00649	1760.26
LM1	12	4	1.383	1.38	0.006	149.295	0.00090	6.698	26.471	0.02647	253.04
LM1	12	5	1.385	1.379	0.012	231.582	0.00162	7.402	6.343	0.00634	1167.08
LM2	1	1	1.3893	1.384	0.0106	173.305	0.00061	17.475	46.386	0.04639	376.74
LM2	1	2	1.3997	1.3864	0.0266	183.912	0.00096	27.722	68.568	0.06857	404.29
LM2	1	3	1.3919	1.3847	0.0144	167.12	0.00080	17.951	36.665	0.03666	489.60
LM2	1	4	1.3961	1.3881	0.016	134.199	0.00083	19.260	99.853	0.09985	192.88
LM2	1	5	1.3994	1.3912	0.0164	70.179	0.00033	50.243	160.211	0.16021	313.61
LM2	2	1	1.3885	1.3837	0.0096	345.467	0.00086	11.115	52.391	0.05239	212.16
LM2	2	2	1.3931	1.3862	0.0138	218.093	0.00087	15.819	42.496	0.04250	372.25
LM2	2	3	1.3936	1.3895	0.0082	199.099	0.00100	8.237	27.325	0.02733	301.45
LM2	2	4	1.3867	1.3842	0.005	118.763	0.00040	12.630	20.880	0.02088	604.89
LM2	2	5	1.4006	1.3902	0.0208	84.973	0.00045	46.509	78.551	0.07855	592.09
LM2	3	1	1.4026	1.3909	0.0234	206.926	0.00090	26.096	98.916	0.09892	263.82
LM2	3	2	1.3995	1.3898	0.0194	133.208	0.00093	20.805	35.505	0.03550	585.98
LM2	3	3	1.3913	1.3846	0.0134	159.681	0.00136	9.873	22.870	0.02287	431.69
LM2	3	4	1.3925	1.3863	0.0124	132.602	0.00113	11.002	14.503	0.01450	758.57
LM2	3	5	1.4033	1.3949	0.0168	193.146	0.00155	10.873	10.776	0.01078	1008.97
LM2	4	1	1.3914	1.3841	0.0146	205.431	0.00082	17.768	19.005	0.01901	934.88
LM2	4	2	1.3842	1.3806	0.0072	255.628	0.00070	10.328	14.571	0.01457	708.78

LM2	4	3	1.3912	1.3866	0.0092	259.184	0.00084	10.902	30.489	0.03049	357.58
LM2	4	4	1.3875	1.3852	0.0046	183.067	0.00125	3.679	6.765	0.00676	543.90
LM2	4	5	1.3917	1.3874	0.0086	114.254	0.00097	8.855	11.627	0.01163	761.64
LM2	5	1	0	0	0	0	0.00000	0.000	0.000	0.00000	0.00
LM2	5	2	0	0	0	0	0.00000	0.000	0.000	0.00000	0.00
LM2	5	3	0	0	0	0	0.00000	0.000	0.000	0.00000	0.00
LM2	5	4	0	0	0	0	0.00000	0.000	0.000	0.00000	0.00
LM2	5	5	0	0	0	0	0.00000	0.000	0.000	0.00000	0.00
LM2	6	1	2.643	2.64	0.006	148.89	0.00097	6.200	33.675	0.03368	184.10
LM2	6	2	2.665	2.663	0.004	154.3	0.00108	3.703	33.155	0.03316	111.70
LM2	6	3	2.653	2.65	0.006	83.118	0.00054	11.106	16.239	0.01624	683.89
LM2	6	4	2.657	2.653	0.008	146.252	0.00073	10.940	41.759	0.04176	261.98
LM2	6	5	2.656	2.652	0.008	189.08	0.00095	8.462	30.265	0.03026	279.60
LM2	7	1	1.398	1.388	0.02	268.62	0.00161	12.409	31.455	0.03146	394.50
LM2	7	2	1.384	1.38	0.008	117.097	0.00064	12.422	31.376	0.03138	395.89
LM2	7	3	1.387	1.383	0.008	108.527	0.00065	12.286	39.472	0.03947	311.25
LM2	7	4	1.397	1.388	0.018	265.101	0.00146	12.345	40.449	0.04045	305.21
LM2	7	5	1.384	1.38	0.008	177.041	0.00115	6.952	17.896	0.01790	388.47
LM2	8	1	1.392	1.387	0.01	195.727	0.00161	6.205	8.783	0.00878	706.43
LM2	8	2	1.379	1.376	0.006	78.445	0.00064	9.316	27.715	0.02772	336.14
LM2	8	3	1.382	1.379	0.006	136.553	0.00065	9.214	10.228	0.01023	900.90
LM2	8	4	1.389	1.383	0.012	154.436	0.00146	8.230	14.406	0.01441	571.29
LM2	8	5	1.39	1.384	0.012	242.838	0.00115	10.428	8.605	0.00861	1211.79
LM2	9	1	1.387	1.38	0.014	243.159	0.00134	10.468	44.167	0.04417	237.01
LM2	9	2	1.383	1.38	0.006	209.446	0.00157	3.820	10.936	0.01094	349.28
LM2	9	3	1.393	1.385	0.016	149.855	0.00105	15.253	55.222	0.05522	276.21
LM2	9	4	1.378	1.377	0.002	113.312	0.00085	2.353	13.370	0.01337	176.02
LM2	9	5	1.394	1.388	0.012	188.202	0.00160	7.501	21.371	0.02137	351.00
LM2	10	1	1.395	1.387	0.016	140.359	0.00098	16.285	83.792	0.08379	194.35
LM2	10	2	1.388	1.383	0.01	164.906	0.00082	12.128	62.439	0.06244	194.24
LM2	10	3	1.397	1.393	0.008	230.17	0.00115	6.951	70.426	0.07043	98.70
LM2	10	4	1.383	1.382	0.002	198.012	0.00109	1.836	14.529	0.01453	126.40
LM2	10	5	1.395	1.389	0.012	107.534	0.00075	15.942	44.653	0.04465	357.02
LM2	11	1	1.398	1.389	0.018	245.549	0.00110	16.290	51.375	0.05138	317.08
LM2	11	2	1.399	1.39	0.018	244.81	0.00135	13.368	51.724	0.05172	258.46
LM2	11	3	1.383	1.381	0.004	146.519	0.00154	2.600	8.470	0.00847	306.95

LM2	11	4	1.415	1.403	0.024	179.907	0.00108	22.234	42.944	0.04294	517.74
LM2	11	5	1.398	1.391	0.014	88.368	0.00088	15.843	55.096	0.05510	287.55
LM2	12	1	1.392	1.383	0.018	142.546	0.00093	19.427	55.223	0.05522	351.79
LM2	12	2	1.421	1.401	0.04	143.224	0.00107	37.238	47.633	0.04763	781.76
LM2	12	3	1.404	1.397	0.014	147.136	0.00081	17.300	110.996	0.11100	155.86
LM2	12	4	1.383	1.379	0.008	306.385	0.00184	4.352	27.497	0.02750	158.27
LM2	12	5	1.38	1.375	0.01	128.231	0.00096	10.398	6.455	0.00645	1610.89
LT	1	1	0	0	0	0	0.00000	0.000	0.000	0.00000	0.00
LT	1	2	0	0	0	0	0.00000	0.000	0.000	0.00000	0.00
LT	1	3	0	0	0	0	0.00000	0.000	0.000	0.00000	0.00
LT	1	4	0	0	0	0	0.00000	0.000	0.000	0.00000	0.00
LT	1	5	0	0	0	0	0.00000	0.000	0.000	0.00000	0.00
LT	2	1	1.3981	1.3912	0.0138	130.336	0.00091	15.126	29.917	0.02992	505.59
LT	2	2	1.4102	1.4036	0.0132	130.551	0.00104	12.639	30.103	0.03010	419.85
LT	2	3	1.4422	1.43	0.0244	169.105	0.00118	20.613	65.938	0.06594	312.61
LT	2	4	1.4026	1.395	0.0152	127.407	0.00089	17.043	37.048	0.03705	460.03
LT	2	5	1.4093	1.4001	0.0184	144.779	0.00101	18.156	31.011	0.03101	585.46
LT	3	1	1.3887	1.3842	0.009	189.248	0.00104	8.647	-4.427	-0.00443	-1953.14
LT	3	2	1.3995	1.3957	0.0076	191.37	0.00078	9.748	7.538	0.00754	1293.09
LT	3	3	1.4002	1.3959	0.0086	203.148	0.00104	8.274	11.398	0.01140	725.92
LT	3	4	1.3772	1.3723	0.0098	150.205	0.00056	17.534	13.650	0.01365	1284.53
LT	3	5	1.3859	1.3826	0.0066	151.212	0.00068	9.699	9.078	0.00908	1068.49
LT	4	1	1.4024	1.3973	0.0102	109.945	0.00063	16.235	12.450	0.01245	1304.03
LT	4	2	1.4212	1.4134	0.0156	185.148	0.00072	21.591	31.797	0.03180	679.02
LT	4	3	1.434	1.4272	0.0136	230.281	0.00064	21.163	23.694	0.02369	893.18
LT	4	4	1.4255	1.4191	0.0128	180.661	0.00063	20.370	16.218	0.01622	1256.00
LT	4	5	1.397	1.3931	0.0078	107.435	0.00036	21.781	24.554	0.02455	887.04
LT	5	1	0	0	0	0	0.00000	0.000	0.000	0.00000	0.00
LT	5	2	0	0	0	0	0.00000	0.000	0.000	0.00000	0.00
LT	5	3	0	0	0	0	0.00000	0.000	0.000	0.00000	0.00
LT	5	4	0	0	0	0	0.00000	0.000	0.000	0.00000	0.00
LT	5	5	0	0	0	0	0.00000	0.000	0.000	0.00000	0.00
LT	6	1	2.671	2.599	0.144	183.658	0.00174	82.533	57.901	0.05790	1425.42
LT	6	2	2.704	2.696	0.016	293.103	0.00147	10.918	29.275	0.02927	372.94
LT	6	3	2.642	2.637	0.01	270.252	0.00149	6.728	11.727	0.01173	573.69

LT	6	4	2.608	2.604	0.008	214.601	0.00107	7.456	15.979	0.01598	466.59
LT	6	5	2.619	2.618	0.002	89.289	0.00054	3.733	37.961	0.03796	98.34
LT	7	1	1.382	1.378	0.008	144.608	0.00094	8.511	22.171	0.02217	383.89
LT	7	2	1.392	1.389	0.006	102.443	0.00067	9.011	8.814	0.00881	1022.33
LT	7	3	1.402	1.396	0.012	164.471	0.00123	9.728	19.039	0.01904	510.96
LT	7	4	1.381	1.375	0.012	125.119	0.00088	13.701	46.678	0.04668	293.53
LT	7	5	1.392	1.387	0.01	158.667	0.00127	7.878	15.280	0.01528	515.59
LT	8	1	1.403	1.395	0.016	171.284	0.00094	17.022	34.116	0.03412	498.94
LT	8	2	1.409	1.402	0.014	109.528	0.00067	21.025	61.355	0.06135	342.68
LT	8	3	1.395	1.391	0.008	157.924	0.00123	6.485	42.887	0.04289	151.22
LT	8	4	1.385	1.38	0.01	121.381	0.00088	11.418	49.779	0.04978	229.37
LT	8	5	1.401	1.395	0.012	86.998	0.00127	9.454	82.820	0.08282	114.15
LT	9	1	1.396	1.391	0.01	252.08	0.00164	6.103	27.014	0.02701	225.92
LT	9	2	1.402	1.396	0.012	118.247	0.00089	13.531	63.308	0.06331	213.73
LT	9	3	1.407	1.404	0.006	177.881	0.00142	4.216	19.879	0.01988	212.10
LT	9	4	1.376	1.373	0.006	157.833	0.00134	4.472	14.331	0.01433	312.08
LT	9	5	1.397	1.392	0.01	229.572	0.00184	5.445	22.224	0.02222	245.00
LT	10	1	1.388	1.379	0.018	197.55	0.00099	18.223	61.386	0.06139	296.86
LT	10	2	1.397	1.391	0.012	165.133	0.00099	12.111	25.621	0.02562	472.72
LT	10	3	1.39	1.387	0.006	153.215	0.00092	6.527	14.734	0.01473	442.99
LT	10	4	1.372	1.369	0.006	110.43	0.00055	10.867	36.771	0.03677	295.52
LT	10	5	1.395	1.39	0.01	152.166	0.00091	10.953	34.724	0.03472	315.42
LT	11	1	1.383	1.381	0.004	136.606	0.00116	3.445	11.824	0.01182	291.34
LT	11	2	1.409	1.402	0.014	207.978	0.00135	10.356	26.773	0.02677	386.81
LT	11	3	1.392	1.388	0.008	119.65	0.00084	9.552	0.046	0.00005	207684.3 2
LT	11	4	1.385	1.377	0.016	125.741	0.00101	15.906	21.028	0.02103	756.41
LT	11	5	1.408	1.402	0.012	245.385	0.00172	6.986	12.060	0.01206	579.28
LT	12	1	0	0	0	0	0.00000	0.000	0.000	0.00000	0.00
LT	12	2	0	0	0	0	0.00000	0.000	0.000	0.00000	0.00
LT	12	3	0	0	0	0	0.00000	0.000	0.000	0.00000	0.00
LT	12	4	0	0	0	0	0.00000	0.000	0.000	0.00000	0.00
LT	12	5	0	0	0	0	0.00000	0.000	0.000	0.00000	0.00
MT	1	1	1.4052	1.4034	0.0036	149.331	0.00161	2.239	4.003	0.00400	559.27
MT	1	2	1.3995	1.3983	0.0024	106.047	0.00193	1.245	1.588	0.00159	783.88
MT	1	3	1.406	1.4005	0.011	188.674	0.00189	5.830	6.142	0.00614	949.29

MT	1	4	1.407	1.404	0.006	152.582	0.00145	4.139	5.783	0.00578	715.74
MT	1	5	1.3952	1.3941	0.0022	113.673	0.00136	1.613	1.904	0.00190	847.20
MT	2	1	1.391	1.3892	0.0036	128.795	0.00110	3.288	8.529	0.00853	385.56
MT	2	2	1.389	1.3876	0.0028	142.55	0.00143	1.964	6.333	0.00633	310.16
MT	2	3	1.3939	1.3922	0.0034	159.642	0.00160	2.130	3.424	0.00342	622.01
MT	2	4	1.396	1.3936	0.0048	159.757	0.00160	3.005	6.285	0.00629	478.05
MT	2	5	1.4014	1.3996	0.0036	115.216	0.00121	2.976	9.944	0.00994	299.25
MT	3	1	1.3874	1.3865	0.0018	178.311	0.00104	1.725	1.153	0.00115	1495.71
MT	3	2	1.3951	1.3932	0.0038	219.426	0.00115	3.306	3.502	0.00350	944.16
MT	3	3	1.3908	1.3902	0.0012	189.989	0.00141	0.849	1.097	0.00110	773.73
MT	3	4	1.3816	1.3806	0.002	127.503	0.00091	2.196	0.981	0.00098	2239.64
MT	3	5	1.4046	1.4012	0.0068	236.307	0.00177	3.837	5.196	0.00520	738.43
MT	4	1	1.3947	1.3897	0.01	186.727	0.00087	11.514	2.898	0.00290	3973.80
MT	4	2	1.3879	1.3865	0.0028	209.658	0.00133	2.106	1.580	0.00158	1333.03
MT	4	3	1.3941	1.3915	0.0052	223.936	0.00139	3.732	6.220	0.00622	599.99
MT	4	4	1.3936	1.3925	0.0022	145.243	0.00101	2.171	1.992	0.00199	1090.04
MT	4	5	1.4016	1.4003	0.0026	182.063	0.00127	2.047	2.126	0.00213	962.79
MT	5	1	2.6175	2.6152	0.0046	191.36	0.00201	2.289	3.869	0.00387	591.72
MT	5	2	2.6261	2.6239	0.0044	107.842	0.00173	2.550	2.953	0.00295	863.54
MT	5	3	2.6366	2.6361	0.001	121.118	0.00145	0.688	6.143	0.00614	112.00
MT	5	4	2.6407	2.6391	0.0032	120.044	0.00162	1.975	2.159	0.00216	914.58
MT	5	5	2.6454	2.6428	0.0052	129.009	0.00136	3.839	5.187	0.00519	740.08
MT	6	1	2.641	2.64	0.002	192.32	0.00192	1.040	2.036	0.00204	510.83
MT	6	2	2.588	2.585	0.006	142.432	0.00285	2.106	0.860	0.00086	2449.14
MT	6	3	2.568	2.567	0.002	170.129	0.00170	1.176	1.494	0.00149	786.78
MT	6	4	2.591	2.59	0.002	154.97	0.00147	1.358	0.704	0.00070	1928.34
MT	6	5	2.618	2.616	0.004	210.649	0.00200	1.999	5.219	0.00522	383.01
MT	7	1	1.39	1.388	0.004	111.581	0.00112	3.585	2.463	0.00246	1455.20
MT	7	2	1.388	1.386	0.004	112.87	0.00113	3.544	3.845	0.00384	921.76
MT	7	3	1.383	1.378	0.01	163.774	0.00147	6.784	1.424	0.00142	4764.36
MT	7	4	1.388	1.386	0.004	90.788	0.00113	3.525	1.942	0.00194	1814.75
MT	7	5	1.388	1.386	0.004	149.161	0.00149	2.682	1.086	0.00109	2468.59
MT	8	1	1.397	1.395	0.004	126.579	0.00112	3.585	5.993	0.00599	598.14
MT	8	2	1.396	1.393	0.006	137.747	0.00113	5.316	8.561	0.00856	620.92
MT	8	3	1.394	1.391	0.006	167.883	0.00147	4.071	6.406	0.00641	635.48
MT	8	4	1.398	1.395	0.006	169.411	0.00113	5.287	6.067	0.00607	871.40

MT	8	5	1.401	1.397	0.008	199.704	0.00149	5.363	14.020	0.01402	382.56
MT	9	1	1.41	1.407	0.006	156.43	0.00156	3.836	6.596	0.00660	581.52
MT	9	2	1.395	1.391	0.008	274.921	0.00275	2.910	5.721	0.00572	508.68
MT	9	3	1.404	1.401	0.006	182.643	0.00183	3.285	6.688	0.00669	491.20
MT	9	4	1.407	1.404	0.006	186.469	0.00186	3.218	9.145	0.00914	351.87
MT	9	5	1.409	1.406	0.006	204.021	0.00204	2.941	7.021	0.00702	418.85
MT	10	1	1.394	1.391	0.006	116.67	0.00123	4.898	5.053	0.00505	969.21
MT	10	2	1.425	1.421	0.008	188.251	0.00198	4.047	6.801	0.00680	595.07
MT	10	3	1.395	1.393	0.004	177.036	0.00195	2.054	1.901	0.00190	1080.28
MT	10	4	1.404	1.401	0.006	206.431	0.00217	2.768	2.345	0.00234	1180.68
MT	10	5	1.415	1.413	0.004	182.249	0.00228	1.756	4.362	0.00436	402.53
MT	11	1	1.395	1.393	0.004	156.264	0.00148	2.694	6.077	0.00608	443.38
MT	11	2	1.398	1.395	0.006	194.778	0.00146	4.107	7.237	0.00724	567.56
MT	11	3	1.387	1.385	0.004	211.735	0.00212	1.889	2.531	0.00253	746.37
MT	11	4	1.395	1.392	0.006	197.757	0.00218	2.758	4.717	0.00472	584.72
MT	11	5	1.404	1.403	0.002	236.594	0.00248	0.805	3.055	0.00305	263.56
MT	12	1	1.392	1.388	0.008	114.145	0.00097	8.245	30.651	0.03065	269.01
MT	12	2	1.403	1.401	0.004	133.944	0.00107	3.733	5.372	0.00537	694.86
MT	12	3	1.391	1.39	0.002	170.289	0.00187	1.068	7.293	0.00729	146.40
MT	12	4	1.417	1.407	0.02	150.25	0.00120	16.639	5.639	0.00564	2950.50
MT	12	5	1.401	1.398	0.006	124.429	0.00112	5.358	6.462	0.00646	829.09
UC	1	1	1.3855	1.384	0.003	165.337	0.00141	2.135	1.826	0.00183	1169.28
UC	1	2	1.3828	1.377	0.0116	208.685	0.00076	15.286	45.907	0.04591	332.98
UC	1	3	1.4005	1.3963	0.0084	139.022	0.00042	20.141	48.276	0.04828	417.20
UC	1	4	1.4009	1.3951	0.0116	118.717	0.00083	13.959	30.192	0.03019	462.34
UC	1	5	1.3965	1.3927	0.0076	119.347	0.00057	13.373	32.713	0.03271	408.79
UC	2	1	0	0	0	0	0.00000	0.000	0.000	0.00000	0.00
UC	2	2	0	0	0	0	0.00000	0.000	0.000	0.00000	0.00
UC	2	3	0	0	0	0	0.00000	0.000	0.000	0.00000	0.00
UC	2	4	0	0	0	0	0.00000	0.000	0.000	0.00000	0.00
UC	2	5	0	0	0	0	0.00000	0.000	0.000	0.00000	0.00
UC	3	1	1.3896	1.3859	0.0074	156.553	0.00080	9.239	15.015	0.01501	615.32
UC	3	2	1.3847	1.3801	0.0092	155.726	0.00082	11.279	22.308	0.02231	505.58
UC	3	3	1.3957	1.393	0.0054	160.393	0.00076	7.070	11.764	0.01176	601.02
UC	3	4	1.3948	1.3898	0.01	168.622	0.00084	11.861	21.809	0.02181	543.86
UC	3	5	1.3906	1.3881	0.005	146.303	0.00071	7.006	10.402	0.01040	673.55

UC	4	1	1.3882	1.3854	0.0056	186.696	0.00187	3.000	4.609	0.00461	650.84
UC	4	2	1.3901	1.3818	0.0166	178.573	0.00098	16.902	19.757	0.01976	855.48
UC	4	3	1.3946	1.3921	0.005	154.539	0.00155	3.235	3.688	0.00369	877.35
UC	4	4	1.392	1.3805	0.023	132.553	0.00133	17.352	2.122	0.00212	8175.74
UC	4	5	1.3938	1.3912	0.0052	134.93	0.00135	3.854	2.671	0.00267	1442.94
UC	5	1	0	0	0	0	0.00000	0.000	0.000	0.00000	0.00
UC	5	2	0	0	0	0	0.00000	0.000	0.000	0.00000	0.00
UC	5	3	0	0	0	0	0.00000	0.000	0.000	0.00000	0.00
UC	5	4	0	0	0	0	0.00000	0.000	0.000	0.00000	0.00
UC	5	5	0	0	0	0	0.00000	0.000	0.000	0.00000	0.00
UC	6	1	2.632	2.628	0.008	315.35	0.00347	2.306	5.527	0.00553	417.27
UC	6	2	2.572	2.569	0.006	126.506	0.00158	3.794	9.920	0.00992	382.48
UC	6	3	2.699	2.695	0.008	117.013	0.00146	5.469	14.822	0.01482	369.00
UC	6	4	2.616	2.613	0.006	195.198	0.00283	2.120	2.967	0.00297	714.36
UC	6	5	2.571	2.569	0.004	164.778	0.00148	2.697	0.865	0.00086	3118.86
UC	7	1	1.383	1.379	0.008	149.328	0.00112	7.143	8.693	0.00869	821.68
UC	7	2	1.38	1.375	0.01	163.197	0.00139	7.209	8.554	0.00855	842.75
UC	7	3	1.392	1.388	0.008	153.355	0.00107	7.452	22.240	0.02224	335.09
UC	7	4	1.385	1.383	0.004	202.213	0.00152	2.637	8.635	0.00863	305.46
UC	7	5	1.406	1.397	0.018	239.24	0.00179	10.032	30.424	0.03042	329.73
UC	8	1	1.383	1.381	0.004	152.528	0.00112	3.572	10.621	0.01062	336.27
UC	8	2	1.386	1.381	0.01	228.665	0.00139	7.209	17.845	0.01785	403.97
UC	8	3	1.398	1.392	0.012	169.718	0.00107	11.179	27.039	0.02704	413.42
UC	8	4	1.395	1.391	0.008	106.463	0.00152	5.275	35.837	0.03584	147.19
UC	8	5	1.396	1.392	0.008	164.387	0.00179	4.459	28.456	0.02846	156.68
UC	9	1	1.398	1.393	0.01	134.971	0.00081	12.348	44.068	0.04407	280.21
UC	9	2	1.384	1.379	0.01	138.64	0.00104	9.617	26.821	0.02682	358.57
UC	9	3	1.403	1.397	0.012	202.591	0.00152	7.898	12.747	0.01275	619.59
UC	9	4	1.392	1.389	0.006	168.686	0.00127	4.743	28.023	0.02802	169.24
UC	9	5	1.398	1.391	0.014	130.167	0.00104	13.444	47.311	0.04731	284.17
UC	10	1	1.389	1.384	0.01	191.976	0.00096	10.418	29.256	0.02926	356.10
UC	10	2	1.377	1.375	0.004	116.066	0.00064	6.266	27.778	0.02778	225.57
UC	10	3	1.394	1.391	0.006	151.685	0.00076	7.911	31.354	0.03135	252.32
UC	10	4	1.398	1.392	0.012	134.276	0.00067	17.874	60.988	0.06099	293.07
UC	10	5	1.393	1.389	0.008	140.051	0.00077	10.386	47.588	0.04759	218.24
UC	11	1	1.385	1.383	0.004	181.826	0.00118	3.384	6.650	0.00665	508.96

UC	11	2	1.383	1.378	0.01	142.699	0.00100	10.011	19.750	0.01975	506.89
UC	11	3	1.4	1.397	0.006	240.292	0.00168	3.567	10.889	0.01089	327.58
UC	11	4	1.397	1.393	0.008	103.641	0.00067	11.875	28.745	0.02875	413.12
UC	11	5	1.397	1.392	0.01	155.874	0.00109	9.165	20.265	0.02026	452.26
UC	12	1	1.385	1.383	0.004	180.88	0.00163	2.457	4.480	0.00448	548.43
UC	12	2	1.383	1.381	0.004	148.393	0.00148	2.696	9.026	0.00903	298.63
UC	12	3	1.401	1.395	0.012	144.684	0.00087	13.823	32.017	0.03202	431.75
UC	12	4	1.396	1.392	0.008	163.769	0.00106	7.515	25.163	0.02516	298.66
UC	12	5	1.4	1.393	0.014	116.086	0.00075	18.554	58.397	0.05840	317.72
UM1	1	1	0	0	0	0	0.00000	0.000	0.000	0.00000	0.00
UM1	1	2	0	0	0	0	0.00000	0.000	0.000	0.00000	0.00
UM1	1	3	0	0	0	0	0.00000	0.000	0.000	0.00000	0.00
UM1	1	4	0	0	0	0	0.00000	0.000	0.000	0.00000	0.00
UM1	1	5	0	0	0	0	0.00000	0.000	0.000	0.00000	0.00
UM1	2	1	0	0	0	0	0.00000	0.000	0.000	0.00000	0.00
UM1	2	2	0	0	0	0	0.00000	0.000	0.000	0.00000	0.00
UM1	2	3	0	0	0	0	0.00000	0.000	0.000	0.00000	0.00
UM1	2	4	0	0	0	0	0.00000	0.000	0.000	0.00000	0.00
UM1	2	5	0	0	0	0	0.00000	0.000	0.000	0.00000	0.00
UM1	3	1	0	0	0	0	0.00000	0.000	0.000	0.00000	0.00
UM1	3	2	0	0	0	0	0.00000	0.000	0.000	0.00000	0.00
UM1	3	3	0	0	0	0	0.00000	0.000	0.000	0.00000	0.00
UM1	3	4	0	0	0	0	0.00000	0.000	0.000	0.00000	0.00
UM1	3	5	0	0	0	0	0.00000	0.000	0.000	0.00000	0.00
UM1	4	1	1.3975	1.3843	0.0264	167.177	0.00163	16.197	1.725	0.00173	9388.47
UM1	4	2	1.3987	1.3951	0.0072	169.1	0.00169	4.258	1.668	0.00167	2552.58
UM1	4	3	1.3982	1.3944	0.0076	194.49	0.00185	4.113	2.324	0.00232	1770.14
UM1	4	4	1.3862	1.3835	0.0054	153.776	0.00146	3.696	2.005	0.00200	1843.81
UM1	4	5	1.3808	1.3787	0.0042	105.51	0.00103	4.083	1.809	0.00181	2256.80
UM1	5	1	0	0	0	0	0.00000	0.000	0.000	0.00000	0.00
UM1	5	2	0	0	0	0	0.00000	0.000	0.000	0.00000	0.00
UM1	5	3	0	0	0	0	0.00000	0.000	0.000	0.00000	0.00
UM1	5	4	0	0	0	0	0.00000	0.000	0.000	0.00000	0.00
UM1	5	5	0	0	0	0	0.00000	0.000	0.000	0.00000	0.00
UM1	6	1	2.661	2.658	0.006	210.969	0.00137	4.375	6.917	0.00692	632.55
UM1	6	2	2.603	2.602	0.002	290.721	0.00204	0.983	5.647	0.00565	174.04

UM1	6	3	2.568	2.566	0.004	239.028	0.00155	2.575	2.301	0.00230	1118.76
UM1	6	4	2.59	2.589	0.002	190.717	0.00124	1.613	2.812	0.00281	573.66
UM1	6	5	2.599	2.588	0.022	208.01	0.00156	14.102	3.813	0.00381	3698.32
UM1	7	1	1.394	1.393	0.002	160.1	0.00128	1.562	4.104	0.00410	380.45
UM1	7	2	1.392	1.388	0.008	170.876	0.00145	5.508	2.070	0.00207	2660.57
UM1	7	3	1.392	1.389	0.006	195.085	0.00185	3.237	3.357	0.00336	964.36
UM1	7	4	1.377	1.374	0.006	173.906	0.00122	4.929	2.720	0.00272	1812.08
UM1	7	5	1.379	1.375	0.008	193.496	0.00164	4.864	5.412	0.00541	898.74
UM1	8	1	1.383	1.38	0.006	119.526	0.00128	4.685	8.799	0.00880	532.38
UM1	8	2	1.387	1.385	0.004	199.274	0.00145	2.754	12.266	0.01227	224.51
UM1	8	3	1.383	1.382	0.002	226.394	0.00185	1.079	7.911	0.00791	136.42
UM1	8	4	1.374	1.372	0.004	161.45	0.00122	3.286	5.314	0.00531	618.33
UM1	8	5	1.372	1.368	0.008	145.882	0.00164	4.864	9.314	0.00931	522.21
UM1	9	1	1.405	1.399	0.012	177.773	0.00151	7.941	19.539	0.01954	406.43
UM1	9	2	1.384	1.382	0.004	107.315	0.00080	4.970	7.661	0.00766	648.72
UM1	9	3	1.389	1.387	0.004	162.49	0.00162	2.462	3.142	0.00314	783.48
UM1	9	4	1.382	1.379	0.006	251.242	0.00176	3.412	5.377	0.00538	634.49
UM1	9	5	1.378	1.376	0.004	100.704	0.00076	5.296	13.032	0.01303	406.39
UM1	10	1	1.394	1.389	0.01	222.948	0.00156	6.408	9.114	0.00911	703.03
UM1	10	2	1.413	1.41	0.006	186.317	0.00168	3.578	8.032	0.00803	445.46
UM1	10	3	1.392	1.386	0.012	262.375	0.00210	5.717	12.229	0.01223	467.50
UM1	10	4	1.376	1.373	0.006	137.341	0.00144	4.161	4.513	0.00451	921.92
UM1	10	5	1.377	1.372	0.01	265.21	0.00186	5.387	8.017	0.00802	671.91
UM1	11	1	1.386	1.382	0.008	175.349	0.00184	4.345	4.012	0.00401	1083.14
UM1	11	2	1.38	1.378	0.004	249.871	0.00250	1.601	1.696	0.00170	943.70
UM1	11	3	1.387	1.384	0.006	256.73	0.00128	4.674	3.175	0.00317	1472.22
UM1	11	4	1.378	1.377	0.002	272.656	0.00177	1.129	2.306	0.00231	489.28
UM1	11	5	1.372	1.37	0.004	229.296	0.00195	2.052	5.111	0.00511	401.54
UM1	12	0	0	0	0	0	0.00000	0.000	0.000	0.00000	0.00
UM1	12	0	0	0	0	0	0.00000	0.000	0.000	0.00000	0.00
UM1	12	0	0	0	0	0	0.00000	0.000	0.000	0.00000	0.00
UM1	12	0	0	0	0	0	0.00000	0.000	0.000	0.00000	0.00
UM1	12	0	0	0	0	0	0.00000	0.000	0.000	0.00000	0.00
UM2	1	1	1.3989	1.3932	0.0114	107.831	0.00027	42.288	277.776	0.27778	152.24
UM2	1	2	1.4001	1.3944	0.0114	134.479	0.00067	16.954	94.986	0.09499	178.49
UM2	1	3	1.3998	1.3932	0.0132	155.278	0.00047	28.336	120.043	0.12004	236.05

UM2	1	4	1.4061	1.3993	0.0136	114.571	0.00057	23.741	85.108	0.08511	278.95
UM2	1	5	1.4049	1.3957	0.0184	181.628	0.00082	22.512	62.448	0.06245	360.50
UM2	2	1	1.4525	1.4288	0.0474	142.079	0.00100	47.660	296.526	0.29653	160.73
UM2	2	2	1.438	1.4139	0.0482	176.498	0.00124	39.013	191.416	0.19142	203.81
UM2	2	3	1.4227	1.4082	0.029	181.131	0.00118	24.632	194.343	0.19434	126.74
UM2	2	4	1.4058	1.3976	0.0164	98.416	0.00074	22.219	135.867	0.13587	163.53
UM2	2	5	1.4122	1.4	0.0244	100.478	0.00065	37.360	217.361	0.21736	171.88
UM2	3	1	1.403	1.394	0.018	146.02	0.00095	18.965	49.696	0.04970	381.61
UM2	3	2	1.4306	1.4175	0.0262	110.875	0.00067	39.384	119.838	0.11984	328.64
UM2	3	3	1.4196	1.4092	0.0208	246.821	0.00091	22.983	54.384	0.05438	422.61
UM2	3	4	1.41	1.3998	0.0204	249.303	0.00091	22.317	41.219	0.04122	541.42
UM2	3	5	1.3988	1.3901	0.0174	117.168	0.00047	37.126	83.059	0.08306	446.99
UM2	4	1	1.3964	1.3933	0.0062	151.18	0.00084	7.348	12.560	0.01256	585.03
UM2	4	2	1.3901	1.3884	0.0034	115.105	0.00056	6.055	8.718	0.00872	694.59
UM2	4	3	1.3945	1.3902	0.0086	189.353	0.00090	9.538	8.278	0.00828	1152.14
UM2	4	4	1.3938	1.3916	0.0044	157.33	0.00115	3.822	5.955	0.00596	641.80
UM2	4	5	1.3976	1.393	0.0092	132.315	0.00086	10.697	15.867	0.01587	674.16
UM2	5	1	0	0	0	0	0.00000	0.000	0.000	0.00000	0.00
UM2	5	2	0	0	0	0	0.00000	0.000	0.000	0.00000	0.00
UM2	5	3	0	0	0	0	0.00000	0.000	0.000	0.00000	0.00
UM2	5	4	0	0	0	0	0.00000	0.000	0.000	0.00000	0.00
UM2	5	5	0	0	0	0	0.00000	0.000	0.000	0.00000	0.00
UM2	6	1	2.774	2.769	0.01	193.168	0.00106	9.412	25.552	0.02555	368.36
UM2	6	2	2.621	2.618	0.006	155.51	0.00086	7.015	43.779	0.04378	160.24
UM2	6	3	2.622	2.618	0.008	123.669	0.00093	8.625	24.786	0.02479	347.98
UM2	6	4	2.583	2.581	0.004	181.595	0.00145	2.753	23.486	0.02349	117.23
UM2	6	5	2.605	2.604	0.002	121.47	0.00067	2.994	21.159	0.02116	141.48
UM2	7	1	1.405	1.396	0.018	176.999	0.00115	15.645	35.340	0.03534	442.71
UM2	7	2	1.404	1.397	0.014	162.434	0.00106	13.260	42.469	0.04247	312.22
UM2	7	3	1.399	1.393	0.012	121.942	0.00073	16.401	43.430	0.04343	377.64
UM2	7	4	1.415	1.409	0.012	119.797	0.00066	18.213	54.366	0.05437	335.00
UM2	7	5	1.412	1.402	0.02	178.479	0.00098	20.374	21.577	0.02158	944.25
UM2	8	1	1.407	1.398	0.018	127.25	0.00115	15.645	114.797	0.11480	136.29
UM2	8	2	1.432	1.416	0.032	241.223	0.00106	30.308	106.800	0.10680	283.78
UM2	8	3	1.412	1.402	0.02	127.419	0.00073	27.335	71.356	0.07136	383.09
UM2	8	4	1.425	1.409	0.032	219.337	0.00066	48.567	81.644	0.08164	594.86

UM2	8	5	1.404	1.394	0.02	143.493	0.00098	20.374	100.759	0.10076	202.21
UM2	9	1	1.395	1.391	0.008	141.695	0.00085	9.410	82.072	0.08207	114.65
UM2	9	2	1.417	1.409	0.016	88.131	0.00062	25.935	106.810	0.10681	242.82
UM2	9	3	1.417	1.406	0.022	307.891	0.00200	10.993	43.009	0.04301	255.60
UM2	9	4	1.424	1.411	0.026	177.462	0.00133	19.535	39.238	0.03924	497.85
UM2	9	5	1.398	1.39	0.016	148.502	0.00089	17.957	101.917	0.10192	176.19
UM2	10	1	1.391	1.385	0.012	155.199	0.00078	15.464	41.273	0.04127	374.68
UM2	10	2	1.396	1.39	0.012	157.464	0.00071	16.935	61.217	0.06122	276.64
UM2	10	3	1.397	1.391	0.012	197.602	0.00099	12.146	33.438	0.03344	363.23
UM2	10	4	1.393	1.388	0.01	214.806	0.00107	9.311	26.792	0.02679	347.52
UM2	10	5	1.399	1.392	0.014	258.274	0.00129	10.841	27.890	0.02789	388.72
UM2	11	1	1.395	1.391	0.008	214.148	0.00128	6.226	14.547	0.01455	428.00
UM2	11	2	1.399	1.392	0.014	204.053	0.00122	11.435	35.289	0.03529	324.03
UM2	11	3	1.397	1.39	0.014	126.408	0.00095	14.767	32.627	0.03263	452.60
UM2	11	4	1.409	1.401	0.016	155.112	0.00093	17.192	59.639	0.05964	288.26
UM2	11	5	1.395	1.388	0.014	261.759	0.00131	10.697	19.708	0.01971	542.76
UM2	12	1	1.403	1.392	0.022	204.119	0.00112	19.596	49.754	0.04975	393.86
UM2	12	2	1.395	1.391	0.008	95.869	0.00058	13.908	16.908	0.01691	822.57
UM2	12	3	1.402	1.394	0.016	149.183	0.00090	17.875	7.067	0.00707	2529.34
UM2	12	4	1.396	1.393	0.006	155.864	0.00101	5.922	11.850	0.01185	499.77
UM2	12	5	1.392	1.39	0.004	134.682	0.00108	3.712	11.005	0.01101	337.33
UT	1	1	1.3781	1.3768	0.0026	144.849	0.00138	1.885	5.461	0.00546	345.11
UT	1	2	1.3979	1.3954	0.005	193.496	0.00168	2.972	6.565	0.00657	452.63
UT	1	3	1.4088	1.4063	0.005	188.007	0.00145	3.442	8.366	0.00837	411.41
UT	1	4	1.3957	1.3947	0.002	114.619	0.00115	1.745	3.626	0.00363	481.29
UT	1	5	1.3956	1.3938	0.0036	189.254	0.00101	3.567	8.468	0.00847	421.21
UT	2	1	1.3903	1.3884	0.0038	166.498	0.00106	3.599	9.540	0.00954	377.26
UT	2	2	1.3852	1.3831	0.0042	202.928	0.00193	2.173	4.684	0.00468	463.96
UT	2	3	1.3973	1.3963	0.002	252.075	0.00164	1.218	1.471	0.00147	828.32
UT	2	4	1.3876	1.3857	0.0038	204.335	0.00149	2.557	3.695	0.00370	692.04
UT	2	5	1.3983	1.3967	0.0032	207.355	0.00124	2.572	5.152	0.00515	499.24
UT	3	1	1.3847	1.383	0.0034	179.48	0.00114	2.977	5.291	0.00529	562.63
UT	3	2	1.406	1.4039	0.0042	218.181	0.00128	3.289	4.630	0.00463	710.20
UT	3	3	1.4089	1.4072	0.0034	178.884	0.00134	2.534	3.404	0.00340	744.40
UT	3	4	1.3867	1.3854	0.0026	136.247	0.00065	4.007	4.910	0.00491	816.25
UT	3	5	1.3868	1.3856	0.0024	184.019	0.00096	2.490	5.211	0.00521	477.78

UT	4	1	1.3769	1.3762	0.0014	103.91	0.00104	1.347	2.330	0.00233	578.30
UT	4	2	1.3885	1.3864	0.0042	83.346	0.00125	3.359	3.896	0.00390	862.35
UT	4	3	1.3988	1.3967	0.0042	93.727	0.00112	3.734	4.100	0.00410	910.79
UT	4	4	1.4119	1.4085	0.0068	114.005	0.00114	5.965	9.109	0.00911	654.83
UT	4	5	1.3906	1.3882	0.0048	174.293	0.00166	2.899	3.814	0.00381	760.11
UT	5	1	0	0	0	0	0.00000	0.000	0.000	0.00000	0.00
UT	5	2	0	0	0	0	0.00000	0.000	0.000	0.00000	0.00
UT	5	3	0	0	0	0	0.00000	0.000	0.000	0.00000	0.00
UT	5	4	0	0	0	0	0.00000	0.000	0.000	0.00000	0.00
UT	5	5	0	0	0	0	0.00000	0.000	0.000	0.00000	0.00
UT	6	1	2.631	2.622	0.018	317.793	0.00270	6.664	4.890	0.00489	1362.72
UT	6	2	2.608	2.602	0.012	200.6	0.00181	6.647	3.870	0.00387	1717.30
UT	6	3	2.619	2.612	0.014	175.489	0.00140	9.972	4.796	0.00480	2079.13
UT	6	4	2.621	2.614	0.014	200.236	0.00170	8.226	2.519	0.00252	3265.53
UT	6	5	2.635	2.632	0.006	208.771	0.00177	3.381	5.461	0.00546	619.17
UT	7	1	1.387	1.385	0.004	259.086	0.00233	1.715	3.092	0.00309	554.81
UT	7	2	1.384	1.383	0.002	115.667	0.00104	1.921	7.034	0.00703	273.14
UT	7	3	1.401	1.399	0.004	165.795	0.00166	2.413	7.779	0.00778	310.15
UT	7	4	1.398	1.397	0.002	200.675	0.00151	1.329	6.177	0.00618	215.13
UT	7	5	1.382	1.381	0.002	153.655	0.00123	1.627	1.077	0.00108	1510.71
UT	8	1	1.372	1.368	0.008	103.844	0.00233	3.431	17.425	0.01743	196.89
UT	8	2	1.393	1.391	0.004	142.671	0.00104	3.842	11.394	0.01139	337.23
UT	8	3	1.398	1.395	0.006	196.002	0.00166	3.619	8.868	0.00887	408.08
UT	8	4	1.39	1.387	0.006	152.848	0.00151	3.987	4.645	0.00464	858.29
UT	8	5	1.383	1.382	0.002	119.76	0.00123	1.627	5.877	0.00588	276.83
UT	9	1	1.383	1.38	0.006	150.336	0.00120	4.989	12.422	0.01242	401.62
UT	9	2	1.397	1.394	0.006	186.833	0.00187	3.211	7.138	0.00714	449.93
UT	9	3	1.418	1.415	0.006	288.829	0.00217	2.770	13.781	0.01378	200.99
UT	9	4	1.39	1.389	0.002	118.14	0.00118	1.693	10.050	0.01005	168.45
UT	9	5	1.396	1.394	0.004	247.761	0.00248	1.614	9.107	0.00911	177.27
UT	10	1	1.378	1.376	0.004	172.948	0.00130	3.084	7.667	0.00767	402.22
UT	10	2	1.386	1.382	0.008	234.094	0.00176	4.557	6.590	0.00659	691.42
UT	10	3	1.395	1.389	0.012	204.207	0.00153	7.835	11.319	0.01132	692.19
UT	10	4	1.4	1.395	0.01	143.065	0.00129	7.766	11.141	0.01114	697.08
UT	10	5	1.393	1.388	0.01	273.128	0.00259	3.854	0.000	0.00000	0.00
UT	11	1	1.402	1.4	0.004	253.178	0.00215	1.859	4.065	0.00406	457.29

UT	11	2	1.402	1.398	0.008	215.933	0.00205	3.900	6.307	0.00631	618.34
UT	11	3	1.417	1.413	0.008	180.755	0.00181	4.426	9.343	0.00934	473.70
UT	11	4	1.406	1.403	0.006	231.936	0.00313	1.916	6.554	0.00655	292.37
UT	11	5	1.42	1.415	0.01	269.712	0.00270	3.708	6.871	0.00687	539.58
UT	12	1	1.378	1.374	0.008	169.762	0.00102	7.854	7.684	0.00768	1022.08
UT	12	2	1.395	1.392	0.006	185.311	0.00167	3.598	2.549	0.00255	1411.19
UT	12	3	1.414	1.412	0.004	168.889	0.00186	2.153	9.180	0.00918	234.55
UT	12	4	1.408	1.405	0.006	211.623	0.00201	2.984	10.265	0.01026	290.74
UT	12	5	1.402	1.399	0.006	139.788	0.00124	4.850	5.579	0.00558	869.26

General Reach Characteristics	
Reach Length (meters)	326
Gradient (meters/meters)	0.010

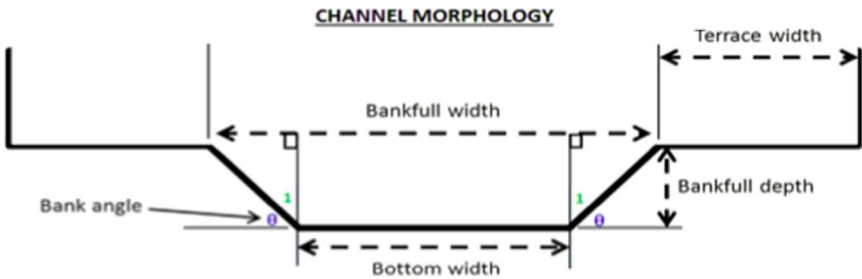
Channel Morphology	
Bankfull Width (meters)	32.09
Bankfull Width to Depth Ratio	32.20
Bankfull Depth (meters)*2	1.78
Wetted Width (meters)	28.79
Wetted Width to Depth Ratio	31.93
Wetted Depth (meters)	1.11
Floodplain Terrace Width (meters)	64.18

Bank Angle Calculations	
Bank Angle $\theta = \arctan\left(\frac{[BF\ Width - WW]/2}{[BF\ Depth - Surface\ D]}\right)$	
Bankfull width - wetted width	1.6500
Bankfull depth - wetted depth	0.671
Step 1) $\theta = \arctan(\text{opposite/adjacent})$	1.185
Convert θ from radians to degrees	67.870
Step 2) Bank angle $\theta = 90 - \text{Angle } 1$	22.13
Right Bank Angle (degrees)	22
Left Bank Angle (degrees)	22

Nutrients & Turbidity			
Month	Water Turbidity (NTU)	Nitrogen concentration (mg/L)	Phosphorus concentration (mg/L)
January	3.0	0.0770654	0.0012946
February	3.0	0.0674831	0.0015184
March	3.0	0.0789286	0.0010000
April	3.0	0.0901127	0.0010000
May	5.0	0.0748964	0.0010000
June	6.0	0.0260000	0.0010000
July	5.6	0.0451941	0.0017007
August	5.1	0.1245656	0.0001000
September	4.9	0.0268940	0.0010000
October	5.9	0.0310451	0.0013405
November	6.6	0.0514678	0.0015203
December	8.9	0.0670684	0.0036878
Av	5.000000	0.063393	0.001347

Discharge, Temperature and Light Regimes				
Day	Discharge (m ³ /sec)	Water Temperature (°C)	Total Incoming PAR (mol/m ² /day*1)	Proportion of PAR lost to shading
1-Jan	0.93	1.134	10.41018	0.82857
2-Jan	0.96	1.891	4.21368	0.82857
3-Jan	0.96	1.451	13.32318	0.82857
4-Jan	0.96	0.449	13.46718	0.82857
5-Jan	0.93	0.402	12.77868	0.80877
6-Jan	0.93	0.613	8.21118	0.80877
7-Jan	0.88	0.970	5.96718	0.80877
8-Jan	1.05	0.931	3.49818	0.80877
9-Jan	1.08	0.994	3.23118	0.7963
10-Jan	1.02	1.677	13.70268	0.7963
11-Jan	1.02	1.900	7.01568	0.7963
12-Jan	1.08	2.189	7.78218	0.7963
13-Jan	1.05	2.822	11.82468	0.80943
14-Jan	1.05	2.540	7.75968	0.80943
15-Jan	0.91	2.099	13.78368	0.80943
16-Jan	0.93	1.438	14.37018	0.80943
17-Jan	0.96	1.042	13.14018	0.79867
18-Jan	0.96	1.197	4.73718	0.79867
19-Jan	0.99	1.259	4.44618	0.79867
20-Jan	0.99	0.729	6.03018	0.79867
21-Jan	0.99	0.956	5.21268	0.8006
22-Jan	0.99	0.855	6.19068	0.8006
23-Jan	0.96	0.925	17.31018	0.8006
24-Jan	1.02	1.324	4.12518	0.8006
25-Jan	0.99	1.740	4.66818	0.74077
26-Jan	1.02	1.739	4.66368	0.74077
27-Jan	1.08	1.626	5.43168	0.74077
28-Jan	1.05	2.079	6.86268	0.74077
29-Jan	1.02	1.591	12.00318	0.74077
30-Jan	1.02	1.862	14.02968	0.74077
31-Jan	1.08	2.245	17.05068	0.74077
1-Feb	1.02	1.824	7.06668	0.75813
2-Feb	1.02	1.387	8.42118	0.75813
3-Feb	1.02	0.768	20.83818	0.75813
4-Feb	1.02	0.617	14.05218	0.75813
5-Feb	1.02	0.178	16.77018	0.75343
6-Feb	0.99	0.200	17.60868	0.75343
7-Feb	0.93	0.378	20.42718	0.75343
8-Feb	0.96	0.351	17.61918	0.75343

Size Distribution	
Substrate size (meters)	Proportion of stream bed with substrates less than listed size
0	0
0.01	0.06
0.02	0.09
0.03	0.13
0.04	0.18
0.05	0.27
0.06	0.34
0.07	0.45
0.08	0.56
0.09	0.63
0.1	0.7
0.11	0.75
0.12	0.78
0.13	0.83
0.14	0.91
0.15	0.95
0.16	0.95
0.17	0.97
0.18	0.97
0.19	0.97
0.2	0.97
0.21	0.97
0.22	0.97
0.23	0.98
0.24	0.98
0.25	0.98
0.26	0.99
0.27	0.99
0.28	0.99
0.29	0.99
0.3	0.99
0.31	0.99
0.32	0.99
0.33	0.99
0.34	1
0.35	1
0.36	1
0.37	1
0.38	1



Empirical Data		
Month	Julian Day	AFOM (g/m ²)
January	7	3.01311
February	36	2.67255
March	66	2.38245
April	97	4.31401
May	126	2.26816
June	175	1.53582
July	205	4.0239
August	239	4.72434
September	268	3.23783
October	297	3.10462
November	324	2.45083
December	343	7.00856
Total		40.74
Average		3.39

Figure 18: Example of ATP Model inputs organized for each study site in order to run the ATP Model in Stella software. Data includes channel topography from CHaMP surveys and daily or monthly environmental variables collected in the field (only a portion of the data are shown above).

Table 13: Riparian Tree Size Classes and Types at 12 Sites

Sites	BD	BV	EW	LC	LM1	LM2	LT	LT	MT	UC	UM1	UM2	Total
Conifer Size Class DBH (cm)	7	2	18	9	4		2		4	13	11	3	
L (40-60+)		1	2	4					2	10	2	2	23
M (23-39)	1	1	9	2	3				1		3	1	21
S (13-22)	3		5	3	1		2		1	3	6		24
VS (0-12 cm)	3		2										5
Deciduous Size Class DBH (cm)	29	15	11	18	27	8	18	4	30	10	19	14	
L (40-60+)		2	2	5	2	3	1		1		4	7	27
M (23-39)	2	2	1	8	9	3	1	1	4		1	4	36
S (13-22)	8	5	3	5	16	2	16	3	15	9	13		95
VS (0-12 cm)	19	6	5						10	1	1	3	45
Species													
Alder (<i>Alnus incana</i>)	24		2				3		19	8		1	57
Big Leaf Maple (<i>Acer macrophyllum</i>)			1										1
Water Birch (<i>Betula occidentalis</i>)										1	1		2
Bitter Cherry (<i>Prunus emarginata</i>)		4	1										5
Black Cottonwood (<i>Populus trichocarpa</i>)	3	9	5	18	26	8	13	4	11		16	11	124
Douglas Fir (<i>Pseudotsuga menziesii</i>)	6		6								8		20
Douglas Maple (<i>Acer glabrum</i>)											2		2
Ponderosa Pine (<i>Pinus ponderosa</i>)	1	2	1	9	3		2		1	5		3	27
Western Red Cedar (<i>Thuja plicata</i>)			12		1						3		16
Red Osier Dogwood (<i>Cornus sericea</i>)	2	1	1		1		2			1		2	10
Engelman Spruce (<i>picea engelmannii</i>)									3	8			11
Willow, peach leaf or Scouler's		1											1
Total	36	17	29	27	31	8	20	4	34	23	30	17	276

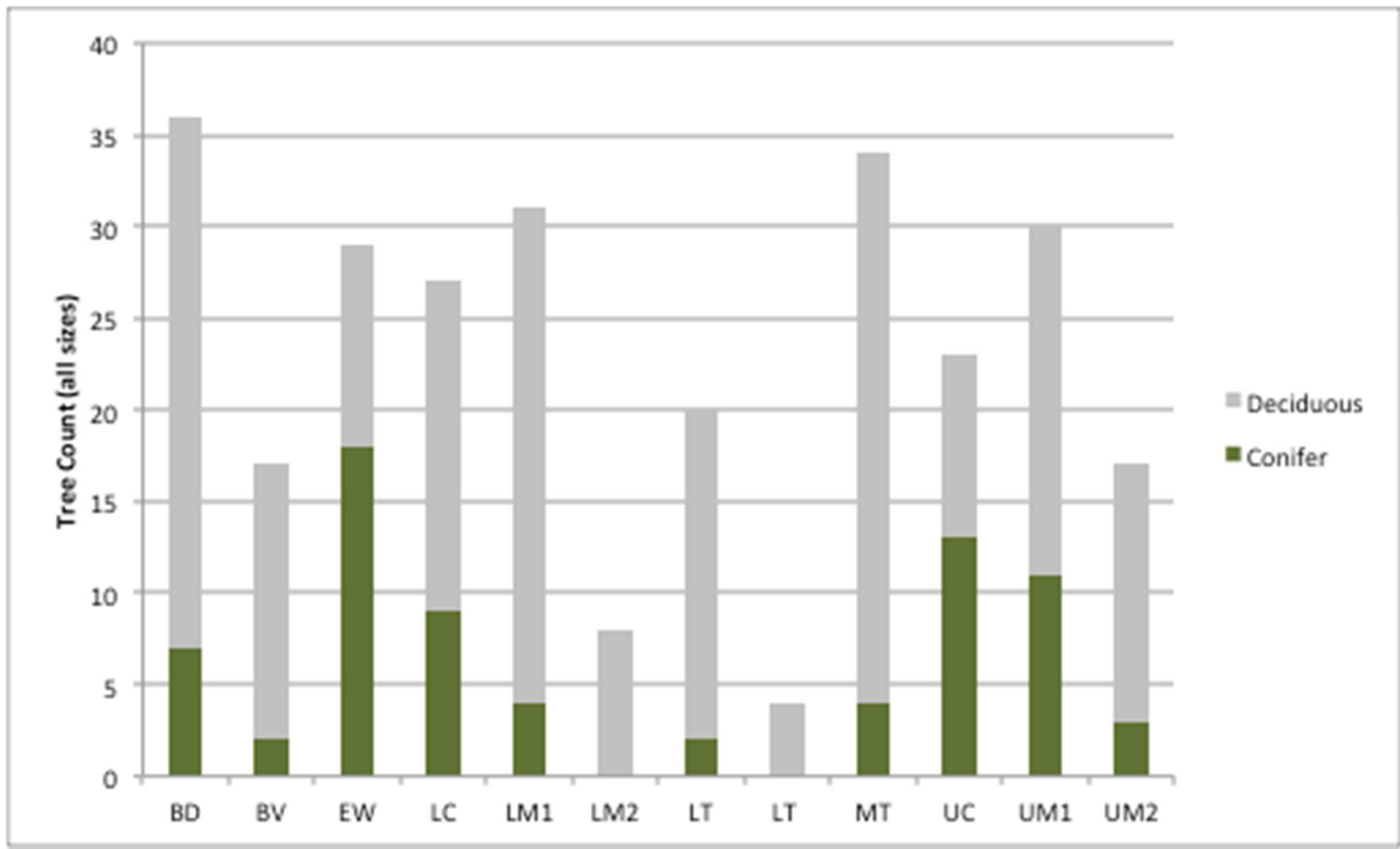


Figure 19: Proportion of deciduous vs coniferous trees along riparian areas at 12 sites

Table 14: Raw drift invertebrate sample data (mg/site/sample)

Drift	Site	Month	Type	Terrestrial	Filtering Collectors	Gathering Collectors	Predators	Scraping Collectors	Shredders	Other Terrest.	Grand Total
BD	BD	Mar	Drift	0.18	3.47	9.25	12.58	3.79	2.74		32.02
	BD	Aug	Drift	19.21	3.36	13.14	3.64	8.55	0.13		48.04
	BD	Sep	Drift	229.45	3.91	13.23	7.74	1.80	1.03	4.35	261.51
	BD	Nov	Drift	40.09	7.88	31.86	0.39	8.80	0.91	0.37	90.30
BV	BV	Mar	Drift	12.39	67.16	43.94	101.05	9.92	0.62		235.08
	BV	Aug	Drift	37.50	2.01	16.04	3.74	39.40			98.68
	BV	Sep	Drift	2.57	113.94	29.82	5.27	32.46	0.48	4.16	188.71
	BV	Nov	Drift		40.59	70.50	2.69	82.42	4.00		200.21
EW	EW	Mar	Drift	0.15	1.67	44.67	1.37	3.69	2.60		54.15
	EW	Aug	Drift	2.43	1.49	9.54	0.19	23.26	2.44		39.34
	EW	Sep	Drift	35.19	3.35	65.70	1.33	18.62	0.58		124.76
	EW	Nov	Drift	1.33	2.06	29.71	1.88	13.28	4.32		52.58
MT	MT	Mar	Drift	0.91	0.03	12.63	3.75	17.56	2.14		37.02
	MT	Aug	Drift	57.56	11.31	38.03	4.12	16.38			127.39
	MT	Sep	Drift	10.56	0.40	4.75	7.65	18.72	0.60	120.58	163.27
	MT	Nov	Drift	2.43	1.49	9.54	0.19	23.26	2.44		39.34
UC	UC	Mar	Drift	1.33	42.77	56.77	20.95	5.25	4.94		132.00
	UC	Aug	Drift	5.52	0.62	12.87	2.58	32.93			54.51
	UC	Sep	Drift	6.68		6.14	12.00	1.41	26.67	239.78	292.69
	UC	Nov	Drift	58.79	2.92	53.39	0.00	5.84	6.36	0.53	127.84
UM 1	UM1	Mar	Drift	17.00		2.02	0.00	4.78	0.91		24.70
	UM1	Aug	Drift	14.60	0.37	0.38	0.00	1.27			16.62
	UM1	Sep	Drift	1.65		1.46	0.00	0.22		15.29	18.62
	UM1	Nov	Drift	0.59	3.19	18.96	53.81	50.43	12.09		139.06

Table 15: Raw benthic invertebrate sample biomass (mg/site per sample)

	Site	Month	Type	Filtering Collectors	Gathering Collectors	Predators	Scraping Collectors	Shredders	Grand Total
BD	BD	Mar	Benthic	3678.05	673.72	24.85	293.59	41.25	4711.46
	BD	Aug	Benthic	361.89	99.18	78.45	65.54	2.97	608.03
	BD	Sep	Benthic	953.39	553.31	361.47	548.28	115.19	2531.64
	BD	Nov	Benthic	689.42	517.21	6.31	192.78	57.88	1463.61
BV	BV	Mar	Benthic	7687.23	4949.44	22124.76	401.64	78.66	35241.72
	BV	Aug	Benthic	59.32	175.69	136.64	306.83	2.66	681.14
	BV	Sep	Benthic	2947.14	316.31	1943.82	598.85	26.75	5832.87
	BV	Nov	Benthic	5519.97	722.51	173.98	574.49	53.40	7044.34
EW	EW	Mar	Benthic	738.65	419.50	51.23	223.87	32.92	1466.18
	EW	Aug	Benthic	7.45	478.27	510.86	237.75	13.73	1248.05
	EW	Sep	Benthic	1036.43	535.98	110.58	229.36	148.28	2060.62
	EW	Nov	Benthic	802.93	525.36	565.39	260.68	41.40	2195.76
MT	MT	Mar	Benthic	3181.07	184.23	446.10	1627.53	244.00	5682.93
	MT	Aug	Benthic	58.67	161.81	1128.64	173.48	1.12	1523.71
	MT	Sep	Benthic	340.60	65.90	94.39	323.09	10.81	834.79
	MT	Nov	Benthic	6834.39	177.87	516.81	933.40	9190.37	17655.83
UC	UC	Mar	Benthic	168.07	89.05	177.18	162.31	50.88	647.50
	UC	Aug	Benthic	86.03	125.28	1223.41	312.90	41.48	1789.11
	UC	Sep	Benthic	3322.13	343.72	2367.83	370.48	402.41	6806.57
	UC	Nov	Benthic	1137.44	502.53	128.22	284.16	87.04	2139.39
UM 1	UM1	Mar	Benthic	57.45	1.25	7.54	12.33	0.48	79.06
	UM1	Aug	Benthic	3.09	53.09	34.35	86.22	0.66	177.41
	UM1	Sep	Benthic	339.16	381.66	178.78	456.01	24.28	1379.89
	UM1	Nov	Benthic	251.58	43.37	170.68	490.24	44.11	999.98

APPENDIX B: LABORATORY METHODS

Ash Free Dry Mass (AFDM)

To be used with FPOM (BOM or Transport), chlorophyll and leaf litter projects. Adapted from the Cary Institute, Millbrook, NY Updated 26 October 2007 H.A. Bechtold

1. Weigh clean, dry crucibles for samples. Record as 'crucible weight' on data sheet.
2. Place all material from each sample into a crucible, rinse out sample container with DI water to remove any small lingering pieces.
 - a. Record sample site, location, date, time and type and respective crucible numbers on data sheet.
3. Place crucibles on a metal or plastic tray, LABEL the tray with your name, date and project.
4. Move samples into the 'Dry' drying oven (105° C) to dry to a constant mass for 24 hrs.
5. Once dry: record and weigh cooled samples. To ensure samples do not absorb moisture mass, place samples in the desiccators next to the scale before and during weighing. This is Sample Dry Weight (+ crucible).
6. Ash sample (in crucible or tin weigh boat) for >2 hr in Muffle furnace.
 - a. Let muffle furnace heat up to temperature 550° C for most AFDM, and to 400° C for the pre-ashing of peri-filters.
 - b. Use gloves, tongs, and common sense to remove heavy rectangular metal trays from furnace containing samples.
 - c. Be sure to turn OFF furnace at completion
7. Remove samples from furnace and allow to cool completely.
8. Weigh and record as ASHED weight of samples as previously described
9. Dump crucible contents into the trash and wash crucibles in the sink, dry in the wet oven, and return to cabinet below hood.

Chlorophyll A -From Frank Wilhelm and Ritchie, 2006

1. For extraction, roll the filter and place each in a separate 10 mL centrifuge tube. Add 10.0 mL of 95% ethanol (EtOH) (Ritchie, 2006). Macerate the filters, cap the tubes and store in a dark refrigerator for 18-24 hr. Shake the tubes vigorously 1 hr after adding EtOH. Make sure all of the filter paper is in the EtOH solution after shaking.
2. After the extraction period, centrifuge at 5,000 rpm for 10 minutes to separate the chlorophyll *a*/EtOH solution and the glass fibers.
3. Read the optical density (absorbance) in a 1 cm cell against 95% EtOH blanks at 750, 665 and 649 nm (the spectrophotometer in the lab will correct for the EtOH blanks).

4. Chlorophyll *a* is calculated from:

$$\text{Chlorophyll } a = v [13.7 (665 - 750) - 5.76 (649 - 750)] /$$

$(\mu\text{g/L}) \qquad \qquad \qquad (\text{V}) (\text{L})$

Where:

750 is the absorbance value for turbidity (this is a correction for any turbidity remaining in the samples from filter particles or other small particles which can interfere with the spectrophotometer. This reading should be close to zero).

649 is the absorbance value for chlorophyll b

665 is the total chlorophyll

v is the volume of the EtOH extractant in ml (10)

V is the volume of water filtered in liters (**X**) (1L = 1000 mL)

l is the length of the light path through the cell, in cm (1)

Constants "13.7" and "5.76" convert from L to Micrograms/Liter. Output is in $\mu\text{g/L}$.

A variety of Chl a extraction methods exist. We have used EtOH because it is relatively safe in a classroom setting and results are shown to be similar to other methods (Ritchie, 2006).